HISTONE H3 MODIFICATIONS AND THEIR ROLE IN DNA DAMAGE RESPONSE

By

ASMITA SHARDA

LIFE09201304002

Tata Memorial Centre, Mumbai

A thesis submitted to the

Board of Studies in Life Sciences

In partial fulfillment of requirements
for the Degree of

DOCTOR OF PHILOSOPHY

Of

HOMI BHABHA NATIONAL INSTITUTE

November,2020

Homi Bhabha National Institute

Recommendations of the Viva Voce Committee

As members of the Viva Voce Committee, we certify that we have read the dissertation prepared by Ms. Asmita Sharda entitled "**Histone H3 modifications and their role in DNA Damage Response**" and recommend that it may be accepted as fulfilling the thesis requirement for the award of Degree of Doctor of Philosophy.

S.N. Dalal

Chairperson – Dr. Sorab N. Dalal Date: 20/11/2020

Sanjay

Guide/Convener – Dr. Sanjay Gupta Date: 19/11/2020

Co-guide – N.A. Date:

B. Ilgachandhar

External Examiner – Dr. B.J. Rao Date: 10th Nov, 2020

B.N. Pandey 21/11/2020

Member – Dr. B.N. Pandey Date:

Member -Dr. Sanjeev Waghmare Date: 19/11/2020

Final approval and acceptance of this thesis is contingent upon the candidate's submission of the final copies of the thesis to HBNI.

I hereby certify that I have read this thesis prepared under my direction and recommend that it may be accepted as fulfilling the thesis requirement.

Date: 19/11/2020
Place: Navi Mumbai

Sanjay

Dr. Sanjay Gupta 19/11/2020
Guide

CHAPTER 4 RESULTS

LIST OF ABBREVIATIONS

Abbreviation	Full form
53BP1	p53 binding protein 1
ATM	Ataxia Telangiectasia Mutated
ATR	Ataxia Telangiectasia and Rad3 related
AURKB	Aurora Kinase B
bp	Base Pair
BRCA1	Breast Cancer type 1 susceptibility protein
Brd4	Bromodomain-containing 4
CAF1	Chromatin Assembly Factor 1
CDK	Cyclin Dependent Kinase
CDK1	Cyclin Dependent Kinase 1
CEN-H3	CENtromere specific histone H3
ChIP	Chromatin Immuno-Precipitation
CHK1/2	Checkpoint Kinase 1/2
CHX	Cycloheximide
CRB	CREB Binding Protein
CtIP	C-terminal binding protein Interacting Protein
DDR	DNA Damage Response
DMEM	Dulbecco's Modified Eagle Medium
DNA	Deoxyribonucleic acid
DNA-PK	DNA-dependent Protein Kinase
DNA-PKcs	DNA-dependent Protein Kinase Catalytic Subunit
DSBs	Double Strand Breaks
EGF	Epidermal Growth Factor
EYA	Eyes Absent Homolog
FBS	Fetal Bovine Serum
GCN5	General Control Non-Derepressible 5
GFP	Green Fluorescent Protein

HAT	Histone Acetyltransferase
HDAC	Histone Deacetylase
hMOF	Human Males-absent-on-the First
HR	Homologus Recombination
IR	Ionizing Radiation
IRIF	Ionizing Radiation Induced Foci
Kb	Kilo-base
kDa	kilo Dalton
KDM	lysine (K) Demethylase
Mb	Mega-base
MDC1	Mediator DNA damage Checkpoint 1
MKP-1	MAP Kinase Phosphatase-1
MNase	Micrococcal Nuclease
MNU	N-Methyl-N-Nitroso-Urea
MRE11	Meiotic Recombination 11
MSK1	Mitogen Stimulated Kinase-1
NBS1	Nijmegen Breakage Syndrome 1
NCP	Nucleosome Core Particle
NHEJ	Non-Homologus End Joining
PARP	Poly-ADP Ribose Polymerase
PBS	Phosphate Buffered Saline
PCA	Principle Component Analysis
PCR	Polymerase Chain Reaction
PHD	Plant Homeo-Domain
PKCδ	Protein Kinase C δ
PP1α	Protein Phosphatase 1α
pre-RC	pre-Replication Complex
PTMs	Post-Translational Modifications
RNA	Ribonucleic Acid
RPM	Rotations Per Minute
RPMI	Roswell Park Memorial Institute medium

SAGA	Spt-Ada-Gcn5 Acetyltransferase
STK6	Serine/Threonine Kinase 6 (
TRIM66	(Tripartite motif containing 66)
TSA	Trichostatin A
UDR	Ubiquitin-Dependent Recruitment
Vel	Velcade
VPA	Valproic Acid
ZMYND8	[Zinc Finger and MYND (Myeloid, Nervy and DEAF-1) domain containing 8]

Chapter 6

Conclusions and

Summary

Chromatin essentially acts as a barrier for all DNA related processes like replication, transcription and repair. Thus for all these processes to commence or cease, the modulation of chromatin architecture is inevitable. In response to DNA damage, many changes occur in the chromatin that allows access to DNA repair proteins at the site of damage. A major contributor of such changes is histone PTMs. Since histone PTMs are strong determinants of the DDR, this study explores the effect of DDR associated histone PTM alterations in a cell cycle phase specific manner. A noteworthy point is that as cell cycle phases differ in their intrinsic radio-resistance, the pattern of histone PTM alteration during DDR could specific for a particular cell cycle phase.

It is essential to understand the concept of radio-resistance in depth because of its clinical implications in the field of radiotherapy. Unfortunately, tumor recurrence may occur even after successful treatment regime. Radio-resistance is an enigmatic phenomenon and whether radio-resistant cells have different epigenetic profile compared to non-resistant cells is an important question that needs to be addressed. An understanding of the epigenetic alterations in radio-resistant tumors, could be useful to target radio-resistant cells or to decrease the incidence of radio-resistance altogether by using drugs against epigenetic modifiers (epi-drugs).

In this study, we explored the epigenetic determinants of the intrinsically radiosensitive mitotic cells and also that of acquired radio-resistant breast cancer cells. Interestingly in both the scenario, interplay between H3S10ph and histone acetylation was found to be associated with radio sensitivity of mitotic cells as well as radio resistance, as summarized in model 2.

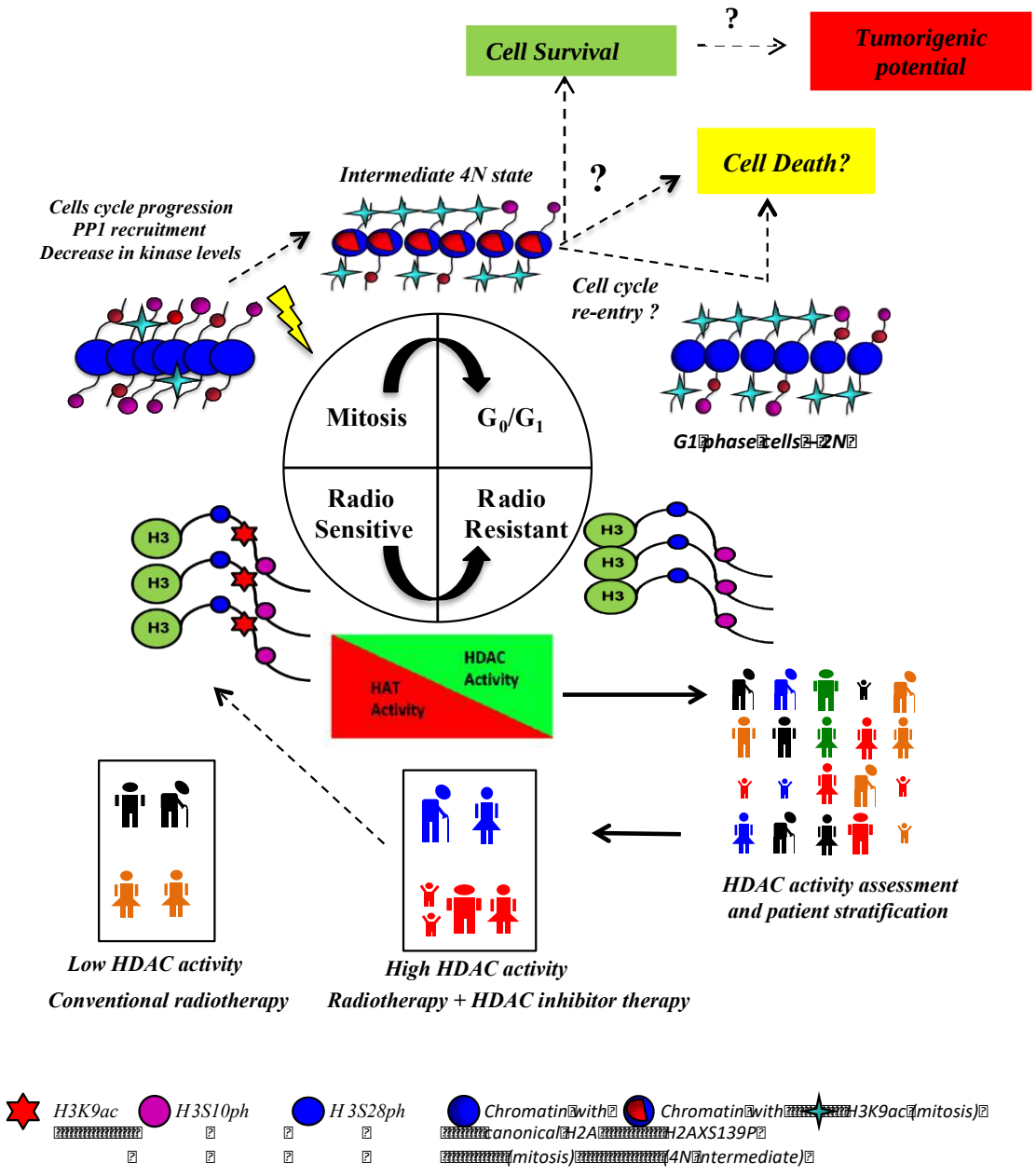

Model 2- *Diagrammatic representation depicting the role of histone H3 PTMs in DNA damage and radio-resistance.*

DNA damage in M-phase of the cell cycle induces a state of cells in which they have de-condensed nuclei with 4N DNA content because of incomplete cell division process. These cells have absence of both cyclin B as well as cyclin D, indicating exit from mitosis but in an intermediate state before G1. There is co-existence of H3 phospho-acetyl marks on same nucleosome as ϒH2AX in mitosis but not after cells have started cycling. Increase of H3K9ac takes place on those nucleosomes on which there is no ϒH2AX but presence of H3S10P. Post DNA damage in M-phase of the cell cycle, there is no recovery of H3S10P/28P. This can be attributed to decreased levels as well as reduced chromatin recruitment of histone kinases Msk1 and AURKB. Decreased levels of MSK1 are influenced by alteration in its translation, while AURKB is influenced by cell cycle dependent progression. Additionally, overall there is stabilization and chromatin recruitment of phosphatase PP1.

Radio-resistant cells developed by fractionated irradiation have compact chromatin architecture and decreased histone phospho-acetylation. This can be attributed to enhanced HDAC activity and reduced HAT activity. Inter-tumoral HDAC activity exists within a single tumor type, hence emphasizing on identifying the right population to be targeted for HDAC inhibitor therapy. Finally, treatment with HDAC inhibitor, Valproic acid is able to retain γH2AX levels up to 24 hours post IR in and increase cell death in acquired radio-resistant cell line.

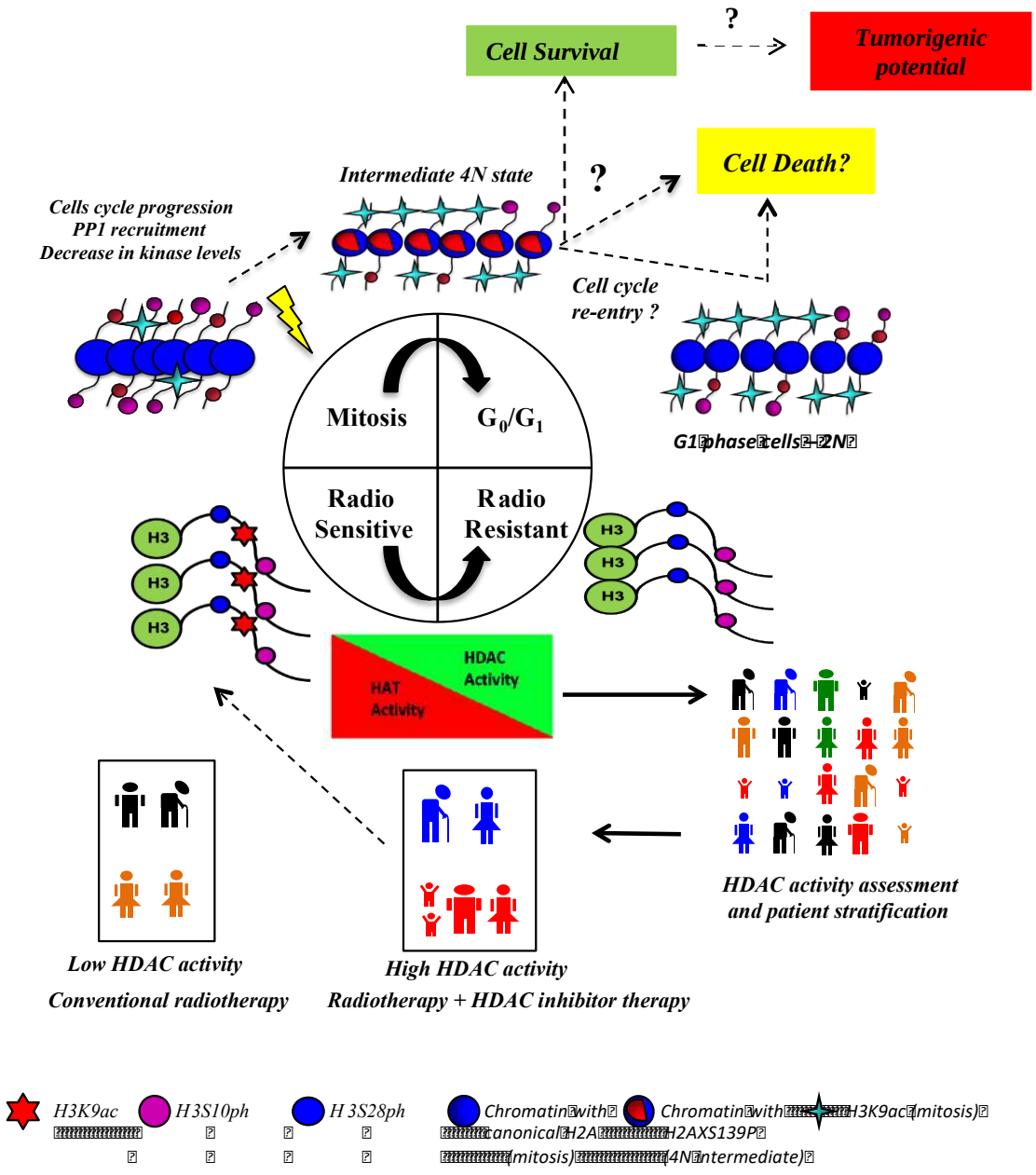

Model 2- *Diagrammatic representation depicting the role of histone H3 PTMs in DNA damage and radio-resistance.*

Chapter 1

Introduction

1. Introduction to Epigenetics

1.1 History of Chromatin Biology

Since the late 19th century, the field of chromatin biology was revolutionized by several significant studies. In 1871, Friedrich Miescher discovered a phosphorus rich material in leukocytes and termed it *nuclein*(1). The first landmark observation was in 1874, when Miescher isolated both *nuclein* and a basic protein from salmon sperm, which he named as *protamin*(1). This led to the idea that nuclear material was a combination of both acidic and basic substances. By 1880, Walther Fleming had coined the term *chromatin* to denote readily stainable nuclear material, while in 1884, Albretch Kossel identified a basic protein (distinct from Miescher's *protamin*) using geese erythrocytes and termed it as *histon*(1). In 1894, Lilienfeld isolated both histones and Deoxyribonucleic Acid (DNA) from calf thymus nuclei and named the complex as *nucleohistone*(1). Rapid progress in the 20th century led to structural and biochemical characterization of both DNA and histones. Taking cues from Micrococcal Nuclease (MNase) digestion pattern and sedimentation equilibration studies, Roger Kornberg suggested the existence of a 200 base pair (bp) repeating unit and a histone $(H3/H4)_2$ tetramer in 1974 (2-8) [2–8]. This breakthrough discovery paved the way for extensive research in field of nucleosome organization. In 1997, a study by Richmond and Luger provided atomic level details for the Nucleosome Core Particle (NCP) through its crystal structure(9).The original definition of the term epigenetics is deeply rooted in developmental biology and embryology. In 1949, Conrad Waddington coined the term "epigenetics" to explain developmental processes involved in formation of an organism from a zygote(1).

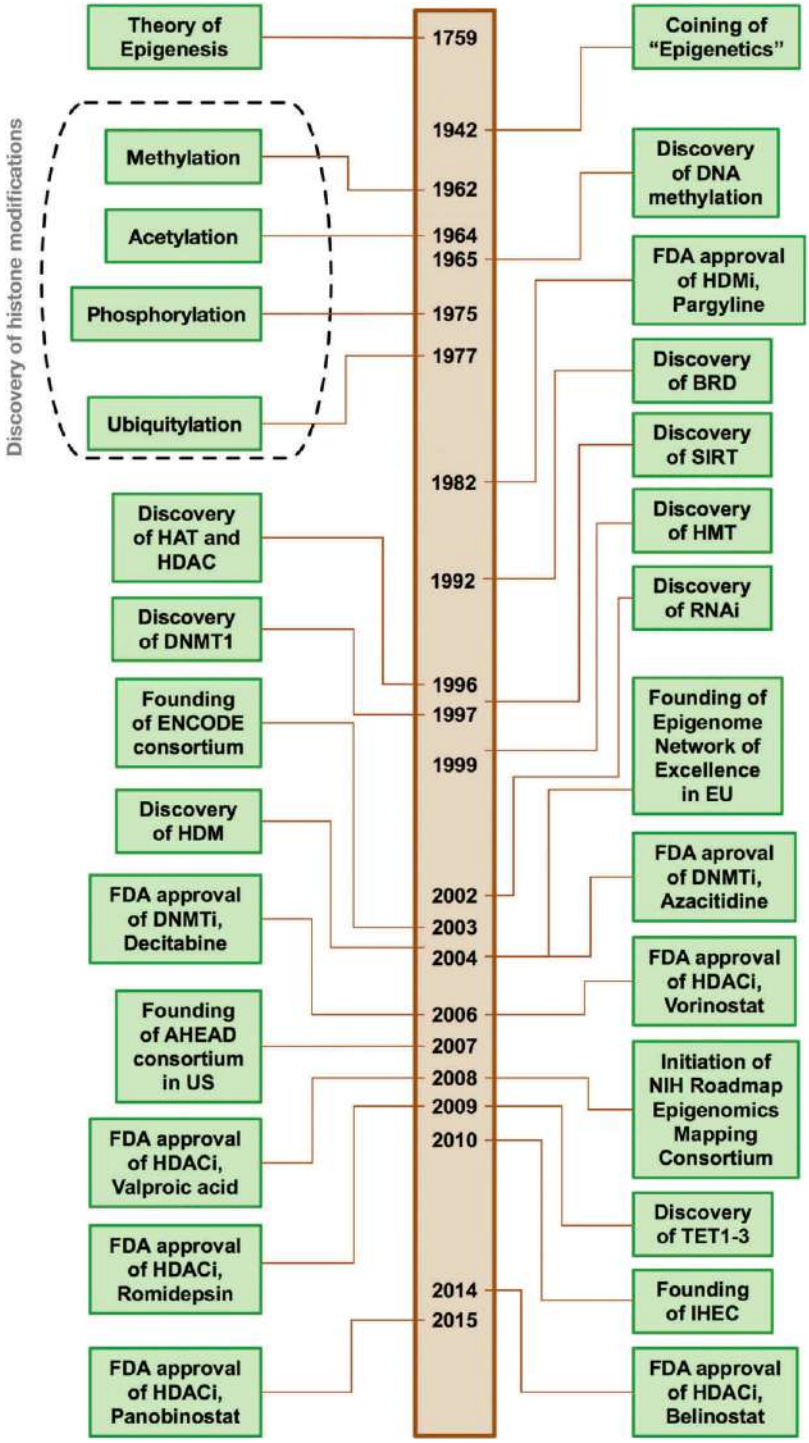

Figure 1.1 *Major milestones in chromatin biology and advancements in the field of epigenetics and epigenome modifying agents. Adapted from Prachayasittikul, V. et al. Exploring the epigenetic drug discovery landscape. Expert Opinion on Drug Discovery(2017)*(10).

The modern day definition of epigenetics describes it as “mitotically or meiotically inherited changes in gene function, which are not a result of alteration in DNA sequence”. This emphasizes that even with an identical genetic component, gene expression patterns are differentially regulated and inherited clonally(11),(12).

Previously, histones were considered to provide only a structural scaffold for DNA compaction. However, in the 1950s, Stedman and Stedman proposed that histones could also repress gene expression(1). Thereafter, scientific advances led to the notion that chromatin is not a static entity but is constantly adapting according to extra/intracellular cues. Therefore, the field of chromatin biology has now grown extensively to encompass histone isoforms, variants, Post-Translational Modifications (PTMs), chromatin remodelers, DNA methylation and Ribonucleic Acid (RNA) interference in regulation of DNA-related processes such as transcription, DNA replication, recombination and repair.

1.2 Nucleosome- The repeating unit of chromatin

To maintain accessibility to the genetic information, the DNA is organized in the form of a nucleo-protein complex called chromatin. Nucleosome is the basic repeating unit of chromatin, comprising of DNA and histones. Histones are small basic proteins, rich in amino acids arginine and lysine, which imparts them a net positive charge at physiological pH. Thus, they act as a scaffold for interaction and compaction of the negatively charged DNA. Histones are of two types- core histones (H2A, H2B, H3 and H4) and linker histones (H1/H5). The NCP comprises of an octamers, consisting of core histones in a ratio of 1:1:1:1.

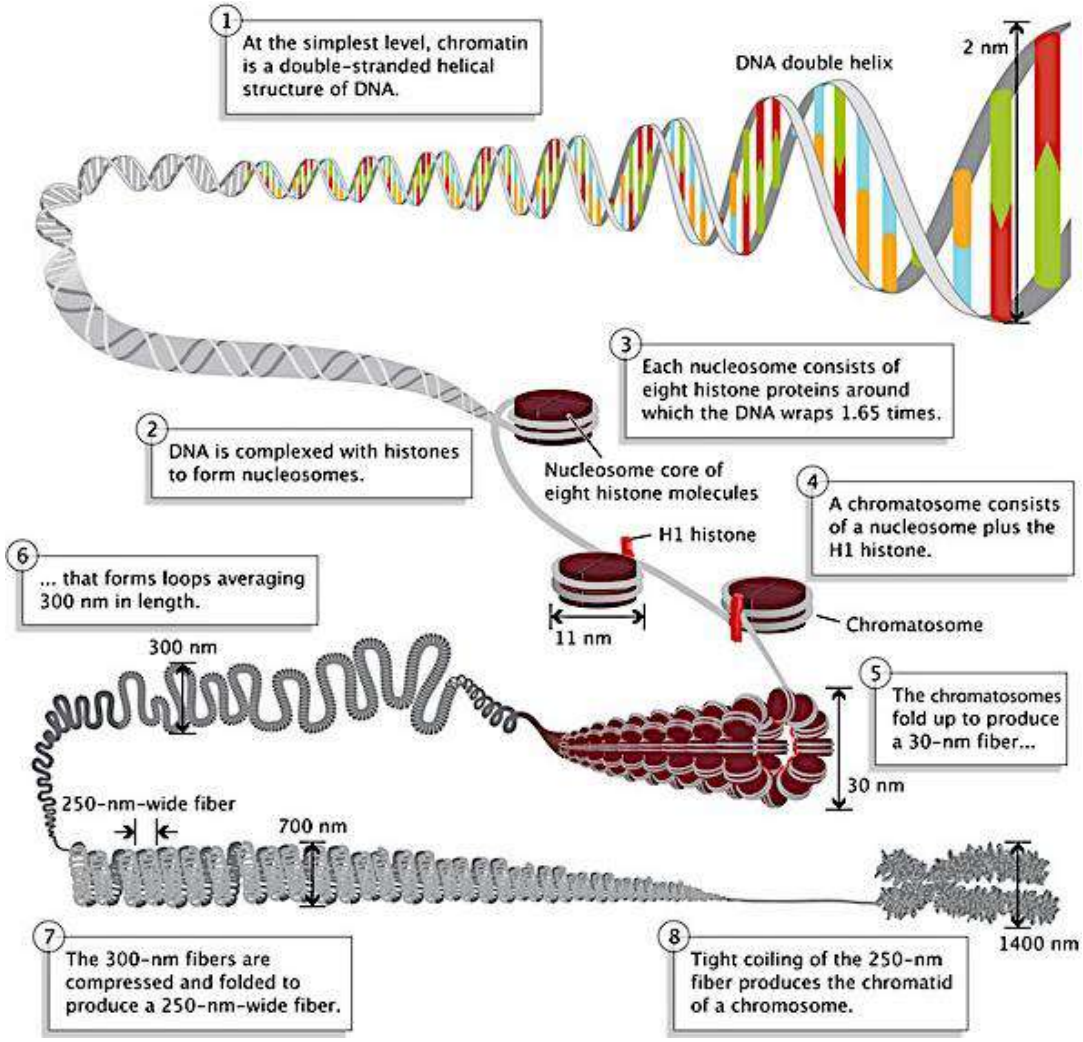

Figure 1.2 Representation of levels of complexity in the formation of a nucleoprotein complex called chromatin.

Adapted from Pierce, Benjamin Genetics- A conceptual approach, 2nd edition.

These core histones exist as two dimers of histones H2A and H2B and one tetramer of histones H3 and H4(1),(13). 146bp of DNA are wrapped around the octamer forming a nucleosome core particle. Addition of linker histone to this structure leads to higher order compaction of DNA. One linker histone binds per nucleosome at the exterior surface of the particle(14),(15). Adjacent nucleosomes are connected to each other through linker DNA, having variable length (160-

240bp) (15). A schematic of these levels of compaction are represented in Figure 1.2

1.3 Structure of Histones

Histones are one of the most evolutionarily conserved proteins and have an excess of basic amino acids over acidic amino acids, with positive and negative charge distributed evenly throughout the globular region of the histone. Histone H1 is considered to be Lysine (K) rich whereas H3 and H4 are considered to be Arginine (R) rich(13). Structurally, histones have a classic Helix-Loop-Helix conformation α1-L1-α2-L2-α3, where α1 to 3 are α-helices joined by inter-connecting loops L1 and L2(14,16). The central and longest α-helix (α2) is involved in the formation of a handshake-like "histone-fold" motif that is critical for dimerization of histones H2A-H2B and H3-H4. Four-helix bundle interactions are responsible for formation of H3-H4 tetramer and also mediate interaction between H2B and H4, thereby assembling a 200 kilo Dalton (kDa) octamer(14). A dyad axis splits the nucleosome into pseudo twofold symmetry, with one base pair centered on the dyad with 72 and 73 base pairs on either side, also depicted in Figure 1.3 (16). An interesting feature of histones is presence of extended N and C-terminal regions that flank the central helices. These unstructured protrusions are called histone tails. 10 flexible histone tails protrude out of the nucleosome at defined locations (eight N-terminal tails contributed by each core histone and two C-terminal tails of H2A) and mediate inter as well as intra-nucleosomal interactions(14,16),(17). Additionally, histone tails have a propensity to attain several Post-Translational Modifications (PTMs) that can influence histone-DNA interaction (Figure 1.4).

1.4 Histone Post Translational Modifications (PTMs)

One of the ways by which chromatin exists in a dynamic state is by covalent addition or removal of chemical moieties from the globular regions of histones as well as their N and C-terminal extensions. The change in the PTMs causes alterations in the overall histone charge. This modulates the histone-DNA affinity to permit or restrict access of cellular machinery to the underlying DNA sequence. The role of histone acetylation and methylation as histone PTMs that may act as an "off and on" switch for *in vivo* transcription in calf thymus nuclei was first reported by Allfrey(18). Indeed, by virtue of their occupancy and positioning, histone PTMs such as methylation, phosphorylation, ubiquitylation, SUMOylation, PARylation, acylation, crotonylation, glycosylation, butyrylation, propionylation and citrullination critically regulate processes such as replication, repair, transcription and recombination(19).

Chemical moieties such as acetylation, methylation, ubiquitylation and crotonylation are added on lysine (K) residues, methylation occurs on both lysine and arginine (R) residue, while phosphorylation occurs on Serine (S), Threonine (T) and Tyrosine (Y) residues. There is also variation in the stoichiometry and arrangement of the moiety added, for example, H3K4 (lysine at 4^{th} position of histone H3) undergoes mono-, di-, or trimethylation with the arrangement of the methyl groups being arranged in a *cis*- or at *trans*- manner(14). It is not only the N and C-terminal regions of histones, but certain residues within the globular domain of the histones also that can undergo PTMs. It is possible that PTMs on histone tails might have a different outcome compared to globular regions of histone, in terms of nucleosome stability(20–24).

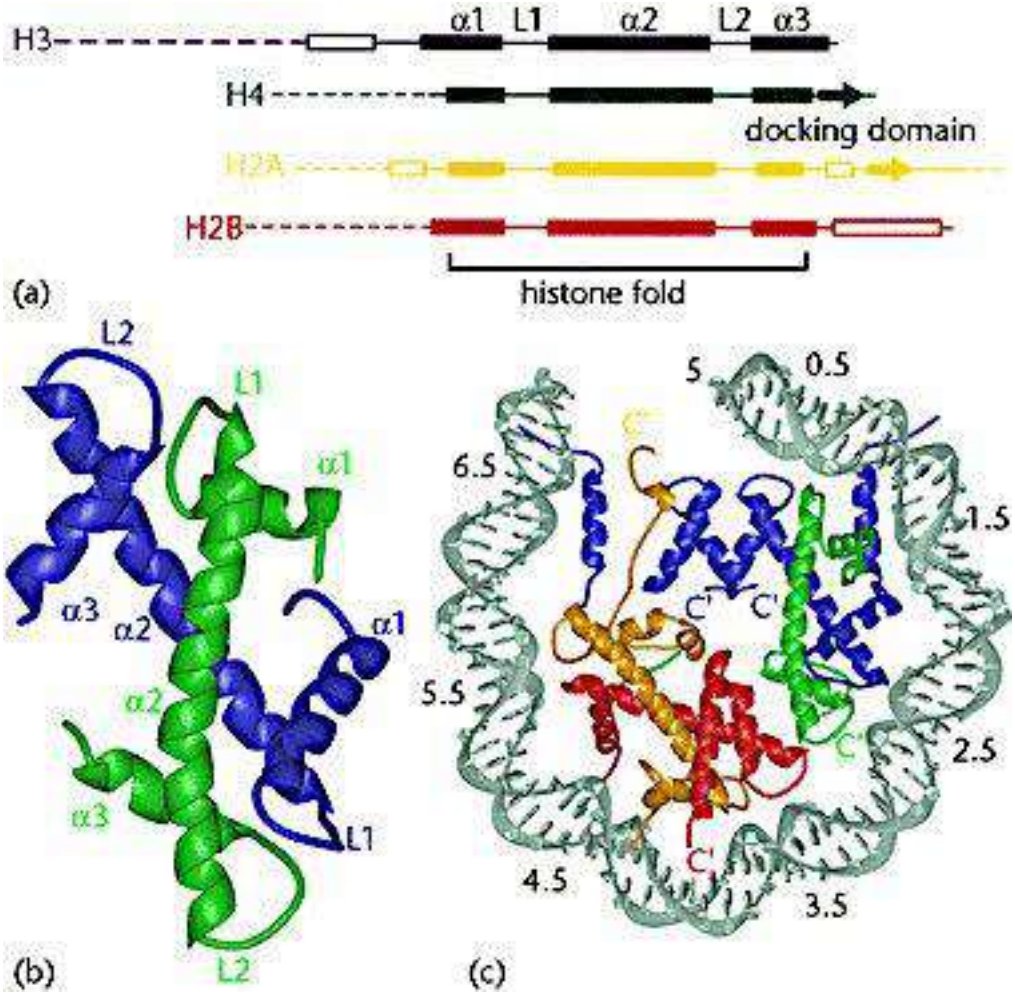

Figure 1.3 Histone secondary structure elements and their interaction within nucleosome core particle. *(a) Representation of the secondary structure elements like α-helices and loops in core histone proteins. (b) Interaction of histone H3 and H4 central α-helices to form a histone fold. (c) Location and interaction of all 4 core histones within half of the nucleosome core particle.*

Adapted from Luger, K. Nucleosomes: Structure and function (2001) (26).

Chromatin modifying enzymes are responsible for addition and removal of these PTMs on histones in a highly regulated and context-dependent manner. Addition of PTMs on histone is mediated by a group of enzymes called "writers", for example, Histone Acetyl Transferase (HAT) adds acetyl group, KMTs (Lysine methyl transferase) adds methyl groups and kinases add phosphate group on histones. Enzymes called "erasers" act to remove these PTMs, for example Histone De-acetylases (HDACs) remove acetyl groups, KDMs (Lysine De-Methylases) remove methyl groups and phosphatases lead to removal of phosphate groups(19),(25).

1.5 Mode of action of histone PTMs

The sole function of histone PTMs is not just to alter the histone charge and influence chromatin organization (also called *cis* mechanism) (25). The histone N-terminal tails contribute to around 25% of the histone mass and act as landing sites for several proteins/complexes on chromatin and mediate specific downstream roles (*trans* mechanism) (25). These proteins possess special domains that recognize and bind to specific histone PTM; hence they are named as "readers". Examples of such domains include bromodomain (recognition of acetylated residues), chromodomain and Plant Homeo-Domain (PHD) domain (recognition of methylated residues) and recognition of phosphorylated residues is specifically by 14-3-3 group of proteins(25). It is very fascinating as to how the dynamic state of chromatin is maintained by the vast repertoire of PTMs that occur on histones. This can be explained by the "histone code" hypothesis, that suggests PTMs act alone or in combination with other PTMs (on the same or

different nucleosome) to form a distinct "readout/code" for recognition by specific proteins. In this way, different PTMs can "cross-talk" with each other and regulate chromatin dynamics. It is possible that one PTM influences the addition or removal of another PTM on the same or different histone tail(25). An interesting example of how histone modifications direct cellular processes can be understood with the help of histone H3 phosphorylation.

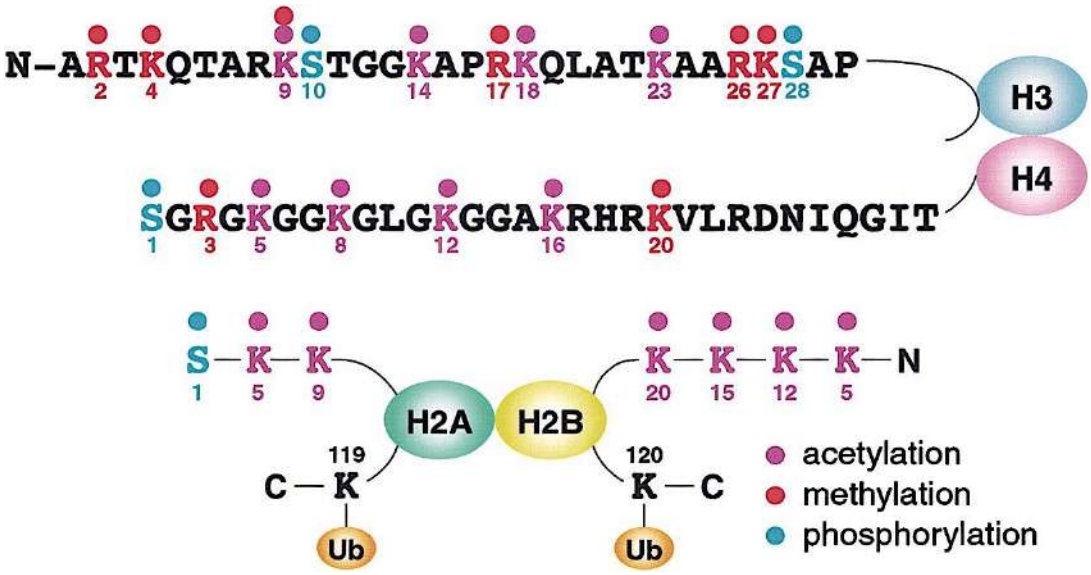

Figure 1.4 Histone Post-Translational Modifications (PTMs) on N and C-terminal extensions. *Cartoon depicting histone PTMs such as acetylation, methylation and phosphorylation, occurring on histone N and C-terminal extensions that protrude out of the nucleosome.*

Adapted from Hendzel, M. J. et al. Mitosis-specific phosphorylation of histone H3 initiates primarily within pericentromeric heterochromatin during G_2 and spreads in an ordered fashion coincident with mitotic chromosome condensation. Chromosoma (1997)(27) .

During mitosis, phosphorylation on H3S10 residue starts from peri-centromeric heterochromatin and then spreads throughout the condensed chromatin, making H3S10ph a mitosis specific mark(28). However, during G_1 phase, H3S10ph acts to induce transcription. The dual and contrasting roles of the same PTM may be explained by the milieu of PTMs located nearby, that create diverse codes for recognition and recruitment of effector proteins. In mitosis, H3S10ph might act alone or in concert with phosphorylation at H3S28 position to initiate chromosome condensation. On the contrary, in G_1 phase, acetylation at the nearby H3K14 residue and phosphorylation at H3S10 provide permissive chromatin milieu for recruitment of factors that drive transcription(29–31).

1.6 Histone variants

In addition to the clustered canonical histone genes, there are non-allelic genes that encode another class of proteins called histone variants. Histone variants are unique in their sequence, structure and timing of synthesis and incorporation into chromatin. Unlike canonical histones, the synthesis of histone variants is not restricted to S-phase only, and can take place throughout the cell cycle. Thus the replacement of a canonical histone with a structurally dissimilar variant potentially alters the size, stability and the amount of DNA wrapped around such nucleosomes(32). Mammalian histone H3 has replication independent variants H3.3 and CENtromere specific histone H3 (CEN-H3), along with replication dependent isoforms H3.1 and H3.2(33). The nucleosomes present in transcriptionally active regions have the combination of histone H2A variant H2A.Z and H3.3, which makes the overall nucleosome unstable and permits

access to underlying DNA(34). Another level of regulation is added for processes such as transcription by variant-specific PTMs. Histone variant H3.3 (differing from canonical H3 by 5 amino acids) has PTM patterns that mark transcription activation while H3.2 mainly consist of transcription repression PTMs, thus attributing different biological functions to histone variants(33).

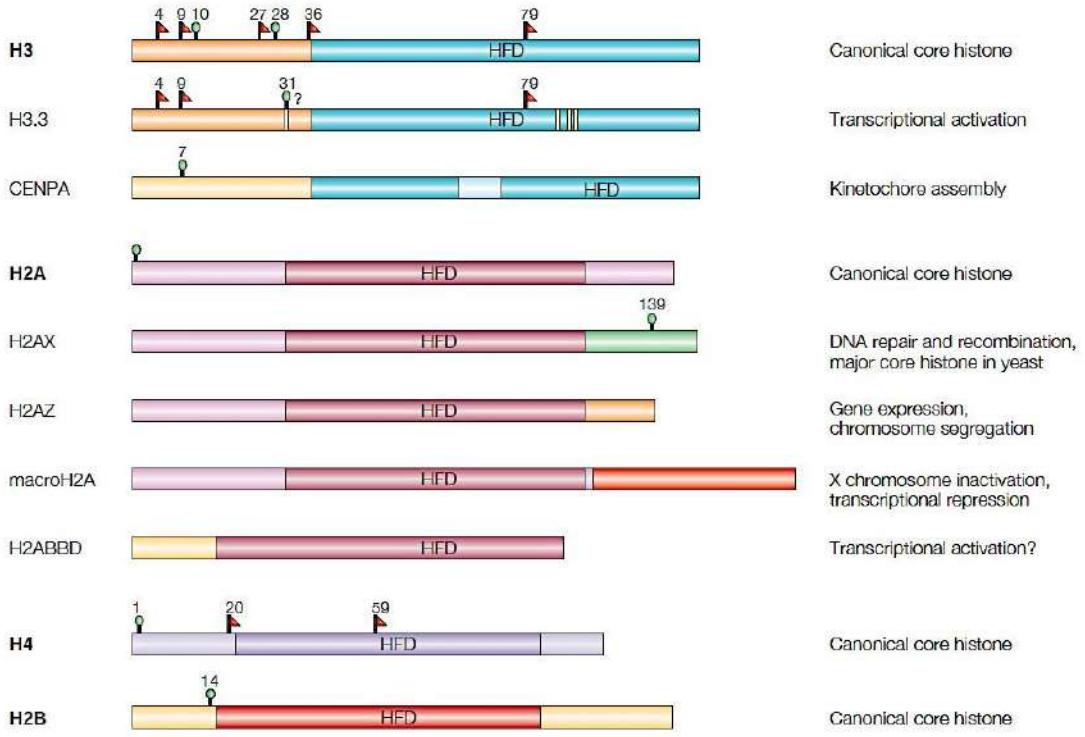

Figure 1.5 Representative image for variants of histone H2A and H3.

Image depicting several variants for histone H2A and H3 along with their cellular function. HFD- Histone Fold Domain.

Adapted from Sarma K, Reinberg D. Histone variants meet their match. Nature Reviews Molecular Cell Biology. 2005 (35).

Histone PTMs, DNA Damage Response and cell cycle

1.7 Epigenetic regulation of the cell cycle

The cell cycle consists of 4 phases- G_1, S, G_2 and mitosis through which a cell is able to faithfully duplicate its genome and form a new daughter cell after completion of mitosis. De-regulation of the levels or activity of enzymes that regulate cell cycle can lead to a diseased state like cancer. The oscillations between different cell cycle phases and chromatin architecture are tightly linked, with a specific state of chromatin and its modifying enzymes being associated with a different cell cycle phase. Chromatin conformation is broadly classified into two categories- the de-condensed and transcriptionally active euchromatin and the condensed and transcriptionally silent heterochromatin(36). Both these states are spatially and temporally regulated throughout the cell cycle, in part due to the distinct sets of histone PTMs that they harbor. The opportunity of chromatin re-structuring mostly occurs during the S-phase, where the entire genome is duplicated and epigenetic marks have to be passed on to the newly synthesized DNA and histones(37).

Since chromatin de-condensation is required for cells to initiate division, histone PTMs are crucial for marking important loci like the origin of replication. A report suggests that the pre-Replication Complex (pre-RC) assembly takes place on sites of enriched histone H4 acetylation(38). Replication licensing also correlated with another histone PTM, H4K20me (mono-methylation), presence of which was found to be sufficient to load the pre-RC complex on chromatin(39–41). Reports also suggest that the newly synthesized histones are marked with H3K56ac and H4K5/12ac, and could assist in coordinated events of nuclear

import and assembly of nucleosomes, and undergo rapid de-acetylation upon chromatin recruitment(42–44). The process of DNA replication and histone synthesis and incorporation are so intricately linked that the absence of histone chaperone Chromatin Assembly Factor 1 (CAF1) leads to cell cycle arrest and reduced cell proliferation(45).

After DNA replication, the cell has to faithfully segregate the genome into two daughter cells. This process requires high-level compaction of a de-condensed interphase chromatin in the form of mitotic chromosomes. Histone modifications that correspond with chromatin condensation include hyper-phosphorylation of the linker histone H1 and Aurora kinase mediated H3S10/28 phosphorylation(46–48).

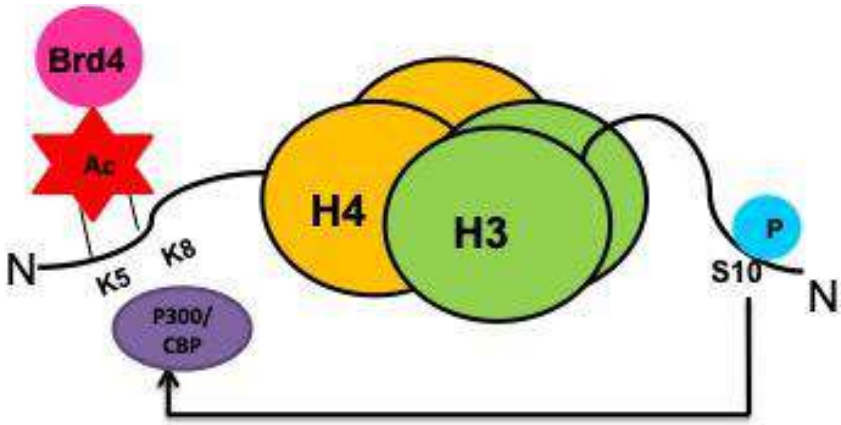

Figure 1.6 Functioning of histone PTMs explained by histone code hypothesis. *Cartoon depicts the cross talk between H3S10ph and H4K5/8ac that ensues upon transcriptional elongation and involves p300/CREB Binding Protein (CBP) histone acetyl transferase as well as Bromodomain-containing 4 (Brd4).*
Cartoon based on Hu, X. et al. Histone crosstalk connects Protein Phosphatase 1α (PP1α) and Histone Deacetylase (HDAC) pathways to regulate the functional transition of Bromodomain-containing 4 (Brd4) for inducible gene expression. Journal of Biological Chemistry (2014)(49).

While the compact chromatin of mitotic cells suggests the exclusion of transcription machinery and factors from chromatin, the presence of DNaseI hypersensitive sites in mitotic chromatin indicate that in spite of loss of higher order contact between distal chromatin domains, the proximal regions elements can still recruit factors(50,51). This "mitotic bookmarking" is necessary to preserve features that are crucial for re-initiation of transcription upon mitotic exit(37)' (50,51).Thus, specific global and local epigenetic changes mark distinct phases of cell cycle and control cellular processes essential for an unperturbed cell division process.

1.8 Chromatin, DNA damage response and genome stability

Our DNA is under constant threat from both exogenous and endogenously present DNA damaging agents. The most deleterious types of lesions that arise are DNA Double Strand Breaks (DSBs), which if not repaired properly, can lead to potentially lethal events such as chromosome translocation and deletion. To counter this genomic instability, cells mount a DNA Damage Response (DDR) that leads to cell cycle arrest, DNA repair. A classical DDR response consists of tightly regulated signaling cascade and the key levels of regulation are signals, sensors, transducers and effectors that ultimately lead to activation of the DDR.

Upon damage to the DNA, the site/lesion acts as a signal to the cell, which leads to activation of the sensor proteins, primarily Ataxia Telangiectasia Mutated (ATM) kinase, DNA-dependent Protein Kinase (DNA-PK) and Ataxia Telangiectasia and Rad3- related (ATR) kinase. These sensor proteins activate several downstream effector proteins like Checkpoint Kinase 1/2 (CHK1/2),

transcription factor p53 that leads to an inactivation of Cyclin Dependent Kinases (CDKs) to halt cell cycle progression and initiate DNA repair at the G_1/S, Intra-S or G_2/M cell cycle checkpoints(52). Perturbations in the DDR signaling cascade have potentially catastrophic implications that lead to diseased state such as cancer.

To counter DNA DSBs, cells have two major pathways, Non-Homologus End Joining (NHEJ) and Homologus Recombination (HR). NHEJ pathway is active throughout the interphase and is a process where re-ligation of broken DNA ends takes place, with minimal or no processing of the broken ends.

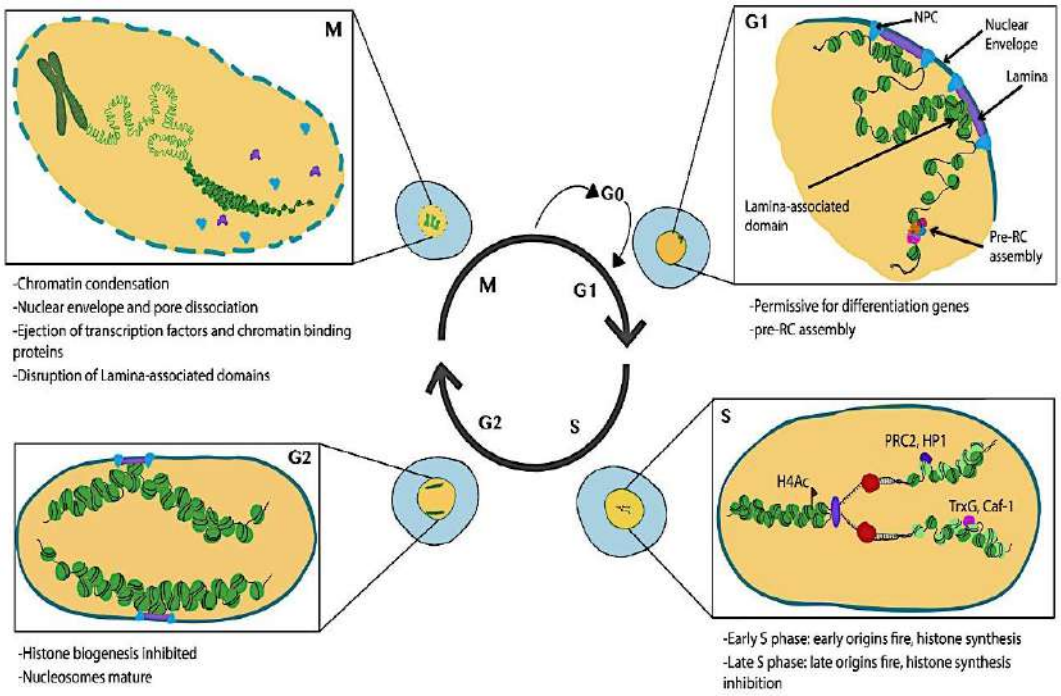

Figure 1.7 Representation of chromatin associated changes during different cell cycle phases. *Image represents alterations in global alterations in the structure of chromatin as cell progresses through the cell cycle. Adapted from Ma, Y., Kanakousaki, K. & Buttitta, L. How the cell cycle impacts chromatin architecture and influences cell fate. Frontiers in Genetics (2015)*(36).

This repair pathway is coordinated by Ku70/80 heterodimer that binds to broken DNA ends. Recruitment of DNA-dependent Protein Kinase Catalytic Subunit (DNA-PKcs) then leads to formation of a holozyme complex, further leading to activation of the nuclease Artemis and a DNA ligase IV/XRCC for ligation of DNA ends(53). Apart from NHEJ, alternative end joining mechanisms like Micro homology-Mediated End Joining (MMEJ) also take place that scans for small stretches of homologues sequences for broken end joining(54). Homologus Recombination, on the contrary, relies on the presence of a homologues strand of the damaged DNA for sequence regeneration. HR uses the replicated sister DNA strand as a template for producing a complement of the broken strand and hence, is considered to be an error free repair process that only operates during and after S-phase of the cell cycle(55). HR involves the process of end resection to produce single stranded 3' overhangs termed as recipient (damaged) strand and mainly involves resection protein C-terminal binding protein Interacting Protein (CtIP)(56). Rad51 recombinase protein then aids the process of extensive homology search, aided by endonucleolytic activity of the MRN (MRE11- Rad50-NBS1) complex(57,58). Upon encountering a homologus sequence, DNA re-synthesis ensues, thus leading to accurate repair of the broken end. It is interesting that both NHEJ and HR pathways can operate during interphase, what determining factors influence activation of either pathway. End resection and CDK activity are considered to be an important parameters influencing choice of repair pathways in *S. cerevisae*(59). However, all DNA related processes like replication, transcription require modulation of chromatin architecture. Therefore,

it is important that DNA repair also be studied in the perspective of chromatin organization.

Chromatin poses as a barrier to the repair machinery, hence global and local chromatin architectural changes help in gaining access to damage site and aid in the DNA repair process. Interestingly, altered chromatin configuration is one of the foremost events that trigger the activation of DNA repair proteins. Bakkenist *et. al.* reported activation of DNA repair protein ATM (by S1981 auto-phosphorylation) in presence of hypotonic conditions, chloroquine and HDAC inhibitor Trichostatin A (TSA) treatment. Notably, none of these agents caused breaks in the DNA or induced DNA damage responsive γH2AX, yet their treatment led to ATM activation as they caused perturbations in the overall chromatin architecture(60). Hence, it can be speculated that DNA repair proteins are sensitive to chromatin architecture change, making it one of the earliest events that signal DNA damage to a cell. The ability of DNA to form loops upon radiation exposure had been reported as early as 1987 and was attributed to loss of topological constraints upon damage induction(61). Furthermore, neuronal cells exposed to DNA damage also displayed decreased topological constraints and enhanced chromatin accessibility, as assessed by MNase and DNaseI immediately after radiation(62).

To understand the role of chromatin and chromatin- associated factors in the DDR, a prime-repair-restore model had been proposed (Fig. 1.8) (63). The model suggests the role of both histones and chromatin associated proteins like remodelers in facilitating a series of structural alterations of chromatin that enable DNA repair, and after completion of the process, chromatin is restored to its

original conformation. These changes are mediated by incorporation of histone H2A and H3 variant by their specific chaperones, ultimately leading to a permissive state for DNA repair at the damaged loci. A chromatin "toolbox" consisting of histone modifying enzymes, chaperones and remodelers has been demonstrated to function at each step of the DDR.

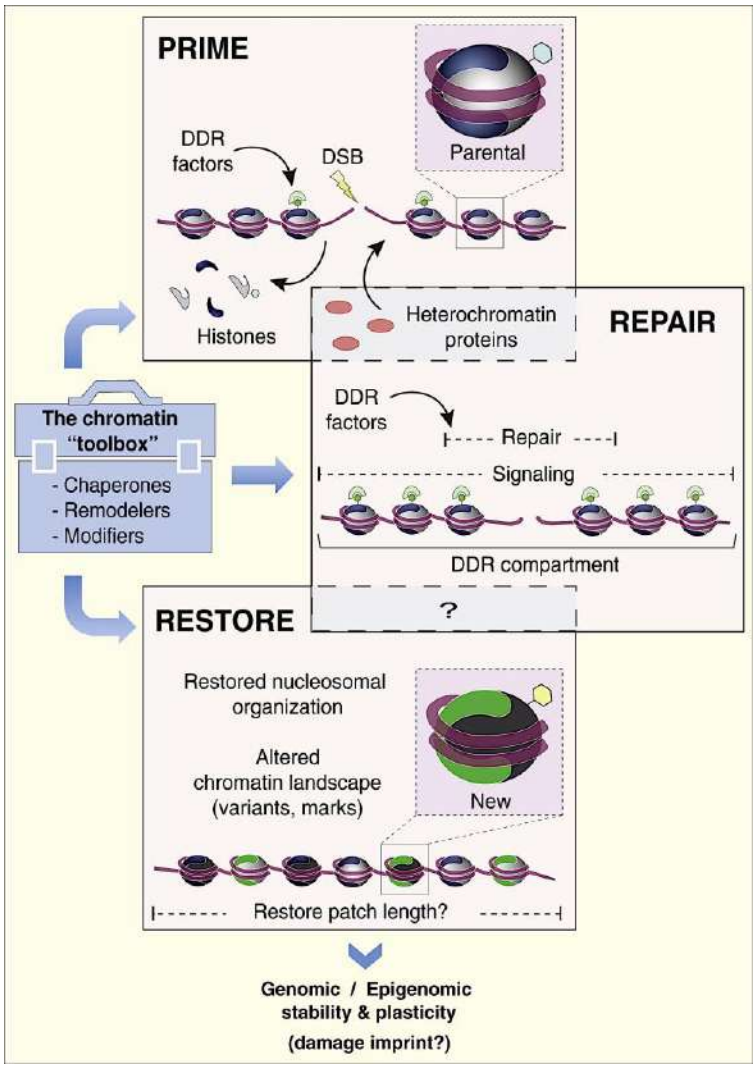

Figure 1.8 Representation of the phases of a DNA Damage Response and its associated chromatin modifiers. *The DNA Damage Response is divided into three phases called prime, repair and restore. DNA repair is associated with chromatin modifying proteins such as remodelers, modifying enzymes and chaperones that alter chromatin architecture and facilitate DNA repair.*

Adapted from Soria, G., Polo, S. E. & Almouzni, G. Prime, repair, restore: the active role of chromatin in the DNA damage response. Molecular cell (2012)(63).

Notably, histone eviction has been reported to take place after DNA damage. A study that used histone H2B- Green Fluorescent Protein (GFP) to investigate the mobility of chromatin reported chromatin to be locally expanded upon DSB induction, occurred independently of ATM activation or γH2AX induction and in an ATP dependent manner(64). Further, loss of H2B-GFP was also reported to be dependent upon the MRN complex that is recruited at the site of DNA damage(65). The action of Poly-ADP Ribose Polymerase (PARP), especially PARP1 had been implicated in regulating histone eviction and caused a state of de-condensed chromatin(66). The linker histone H1.2 had also been reported to undergo PARylation and subsequent proteasome-dependent degradation upon exclusion from chromatin after DSB induction. Interestingly, failure of eviction of H1.2 compromised ATM activation and reduced cell survival(67). The topological changes observed in chromatin as a consequence of DNA damage are attributed to the action of chromatin remodeling complexes (reviewed in (68)). Therefore, these reports strongly suggest that regulated chromatin organization movement at or around a DSB is critical for DNA repair protein activation and initiation of DNA repair process.

In conjunction with the activity of histone remodelers, histone PTMs as well as the activity of their respective modifying enzymes and readers plays a decisive role during the DDR. An interesting hypothesis emerged from several studies that suggested the role of pre-existing histone PTMs in defining a DNA repair pathway choice decision(69). This hypothesis seems plausible since chromatin

state and global/local histone modification milieu is disparate across the genome and different cell cycle phases. In complete concordance with this hypothesis, regions of the genome harboring transcription elongation mark H3K36me3 were identified to be more "HR prone" for DNA repair in a Chromatin Immuno-Precipitation (ChIP)-seq based analysis(70). This suggested that histone PTMs that distinguish specific regions of the genome (e.g. euchromatin from heterochromatin) could decide the pathway of pathway for DNA repair. Recently, an approach utilizing artificially induced DSBs coupled with ChIP-Seq was used to map histone PTM alterations at the DSB and in regions upto 1 Kilo-base (Kb) and 1 Mega-base (Mb) in its vicinity. This comprehensive study reported a reduction in H1 occupancy and increased ubiquitylation over mega base windows. Local changes included decreased levels of H3, H3K36me2, H3K79me2, H2B120Kub and increased levels of H4K20me1, H2B120Kac and ubiquitin in a window of 1Kb from the DSB. Further, an identification of NHEJ and HR specific chromatin signatures revealed that DNA lesions repaired by HR had lower levels of H3, H3K36me2, H3K79me2 and H4K12/16ac marks, while NHEJ-repair specific lesions had decreased H3K36me3 and H4K20me1 upto a distance of 1Kb from the DSB. The depletion of linker histone and enhanced ubiquitylation occurred irrespective of the DNA repair mechanism, but was more pronounced in sites under repair by HR than NHEJ, detected upto 1Mb from the lesion(71). Hence, it can be speculated that the chromatin undergoes long and short-range alterations in its PTM milieu in response to DSB induction. Such changes could strongly influence the DNA repair pathway choice. However, while performing and interpreting such studies, it is very important to note firstly, the degree and

extent of chromatin de-stabilization, secondly, the intensity of damage and type of lesion produced, thirdly, the temporal kinetics of histone PTM alteration after damage induction and finally, the cell cycle phase under study.

1.9 Histone phosphorylation and DNA damage response

Phosphorylation and de-phosphorylation events are critical for regulation of cell cycle and signaling pathways. In context of chromatin-based changes in the DNA damage response, histone H2AX phosphorylation is one of the best-studied examples. In 1997, it was first identified that Histone H2AX (a variant of canonical H2A) undergoes phosphorylation at Serine-139 residue response to DNA damage induced by ionizing radiation, and this form of H2AXS139P was known as γH2AX(72). It was reported to spread upto mega-base regions in vicinity of the DNA damage site and formed chromatin domains that could be visualized as Ionizing Radiation Induced Foci (IRIF)/γH2AX foci(73). This phosphorylation occurs in the unique SQ motif of H2AX variant in its extended C-terminal tail (absent in canonical H2AX) that acts as a recognition motif for phosphatidylinositol-3 kinase–like kinases (PIKKs) ATM, DNA-PKcs and ATR kinases(74). In case of yeast (*Saccharomyces cerevisae*), phosphorylation on H2A at position S129 by kinases Mec1 and Tel1 marks a similar response to DNA damage like mammalian γH2AX(75). The phosphorylation of γH2AX takes place as early as 1 minute after DNA damage induction and serves to recruit DNA repair proteins like Mediator DNA damage Checkpoint 1 (MDC1), Nijmegen Breakage Syndrome 1 (NBS1), Meiotic Recombination 11 (MRE11) and Breast Cancer type 1 susceptibility protein (BRCA1)(76). Contrary to S139P, Y142P

undergoes de-phosphorylation by phosphatase Eyes Absent Homolog (EYA) in response to DNA damage and the balance between γH2AX and Y142ph sets the stage for distinction between DNA repair and apoptosis(77–79). Phosphorylation as well as de-phosphorylation of histone H3 at several sites has been reported in context of DNA damage and transcription repression. A residue present at the histone-DNA interface, H3T45 has been reported to undergo phosphorylation in response to apoptosis, with the potential to also modulate nucleosome accessibility. Additionally, a report also suggested that H3T45ph mediated by protein kinase B (AKT kinase) regulated the termination of gene transcription in response to DNA damage(80,81). The dissociation of CHK1 from chromatin occurred in a PIKK dependent manner and resulted in reduced H3T11ph. This further caused reduced levels of H3K9ac by impaired recruitment of HAT General Control Non-Derepressible 5 (GCN5), leading to decreased expression of genes such as cyclin B and Cyclin Dependent Kinase 1 (CDK1) as a consequence of DNA damage response(82).

Phosphorylation of H3 at position S10 is a unique modification, with implications in cellular events like transcription and chromatin condensation(83). In response to DNA damage, there have been several ambiguous reports about alterations in levels of H3S10ph. A report suggested an increase in the levels of H3S10ph, mediated by direct action of ERK1/2 and p38 kinases, both *in vitro* and *in vivo* in response to UVB induced DNA damage(84). Also, several mitotic H3 phosphorylation such as H3S10ph, H3S28ph, H3T11ph and H3.3S31ph were reported to be unchanged after phleomycin induced DNA damage(85). Another study suggested a bi-phasic reduction in the level of H3S10ph in response to

nitroso-compound N-Methyl-N-Nitroso-Urea (MNU) treatment that was observed to be regulated by both Poly-(ADP-Ribose) Polymerase 1 (PARP1) and p53. Concomitantly with H3S10ph, decreased H3S28ph and increased H4K5/K8/K12 and K16 acetylation marks were also observed upon MNU treatment in a time dependent DNA damage kinetics study. Interestingly, contrary to the observed globally increased H4 acetylation, reduced H4 acetylation at the promoters of cell cycle regulated genes Serine/Threonine Kinase 6 (STK6) and Centromere Protein A (CENPA) that led to their transcriptional repression(86). Decreased levels of histone PTMs H3S10/28ph were also reported as early as 15 minutes after DNA damage induced by H_2O_2, independent of cell cycle progression. Reduced H3S10/28ph occurred in an inverse correlation with increasing levels of γH2AX and was regulated by PIKKs. Notably, this study also reports mutual exclusivity of γH2AX and H3S10/28ph during mitotic DNA damage(87). Additionally, our group has previously published a report about the G_1 cycle phase specific loss and recovery of H3S10ph in response to ionizing radiation induced DNA damage. This loss of H3S10ph, in an inverse correlation with γH2AX, is independent of the type of cell line, DNA damaging agent and intensity of radiation, thus indicating it to be a universal phenomenon(88). Enzymes MAP Kinase Phosphatase-1 (MKP-1) and Mitogen and Stress activated protein Kinase-1 (MSK1) govern this de-phosphorylation and subsequent re-phosphorylation, respectively. Both MKP-1 and MSK1 are also negative and positive regulators of the MAP Kinase (MAPK) pathway. Inhibition of the activity of either the phosphatase or the kinase leads to reduced survival of cells post radiation. This indicated that both loss as well recovery of H3S10ph are essential during G_1 phase

specific DDR(89). H3S10ph had also been reported to be induced in apoptotic cells by pro-apoptotic Protein Kinase C δ (PKCδ)(90). It is not only the activation but the inactivation also of the DDR that needs to be critically regulated. In *Saccharomyces cerevisae*, phosphorylation of H4 at T80 position by Cla4 kinase led to removal of checkpoint adaptor protein Rad9 from chromatin and marked the termination of the DNA damage checkpoint(91).

1.10 Histone acetylation and DNA damage response

Acetylation of lysine (K) residues of histones is one of the earliest identified and well-characterized histone PTMs. Acetylation reduces the overall positive charge of histones and leads to chromatin de-condensation, thus is generally associated with transcription activation. However, extensive local chromatin re-arrangement that occurs to facilitate access of repair machinery to damaged DNA indicates an essential role of this PTM during the DNA damage response.

A recent report that aimed to create a high-resolution map of histone PTMs suggests a switch of H2BK120ub to H2BK120ac in regions as close as 1kb near AsiSI induced DSBs, using a ChIP-based approach. Abrogation of the SUPT7L de-ubiquitinase and acetyltransferase subunit of Spt-Ada-Gcn5 Acetyltransferase (SAGA) complex hampered this conversion as well as DNA repair by both NHEJ and HR mechanisms(71). This indicated an increase of H2BK120ac to be an important local event that occurs in vicinity of a DSB and contributes to DNA repair. Other than phosphorylation, H2AX also undergoes acetylation at position K5, mediated by Histone Acetyltransferase (HAT) Tip60, essential for localization of DNA repair protein NBS1 on chromatin. It has been further

reported that Tip60 is present in a complex with ubiquitin conjugating enzyme UBC13, with the acetylation-dependent ubiquitylation of H2AX to be critical for H2AX eviction from chromatin(92,93). At a global level, an exhaustive study reported GCN5 mediated H3K9ac and H3K56ac marks to be reduced after phleomycin induced DNA damage in mitosis as well as interphase, with minimal variation in their levels throughout the cell cycle(85). This reduction in H3K56ac was attributed as a consequence of HDAC1/2 localization to chromatin in response to DNA damage, and particularly promoted NHEJ-mediated DNA repair. This report also suggested a reduction in H4K16ac after DNA damage(94). On the contrary, two independent reports also suggested p300/CBP to be the acetyltransferases that mediated H3K56ac, but reported an increase in the level of this PTM and co-localization with γH2AX in response to several DNA damaging agents(95,96). It has recently been reported that TRIM66 (Tripartite motif containing 66) protein recognized H3K56ac via its bromodomain and deemed this interaction to be crucial for recruitment of HDAC Sirt6, which allowed permissive environment for DNA repair in mouse embryonic stem cells(97). In response to DNA damage, abrogation of Human Males-absent-on-the First (hMOF) mediated acetylation of H4K16 position was reported to cause increased number of γH2AX foci and defective DNA DSB repair(98). Notably, structural studies demonstrated H3K56ac and H3K122ac not to be a part of the N-terminal region of histones. H3K56ac is positioned at the interface of the DNA entry/exit site of the nucleosome while H3K122ac is present at the symmetry axis of the nucleosome dyad. Due to this critical placement, it is possible that alteration of these PTMs in

response to DNA damage lead to local as well as global changes in chromatin configuration and facilitate DNA repair(99,100).

1.11 Histone Methylation, Ubiquitylation and PARylation and the DNA damage response

Histones undergo methylation at both lysine and arginine (R) residues and upto stoichiometry of mono-, di- or tri-methylation. Histone methylation does not cause any charge neutralization of histones and is extensively studied for its role in mediating transcription activation or repression. In response to DNA damage in mammalian cells, a report suggested enrichment of lysine (K) Demethylase KDM1A at the DNA damage site and led to reduction of H3K4me2. Depletion of KDM1A affected the chromatin recruitment of DNA repair proteins 53BP1 and BRCA1(101). Recruitment of KDM5B at the DNA damage site was also reported to aid in recruitment of both Ku70 and BRCA1 to the DNA damage site, hence promoted both NHEJ and HR. Depletion of KDM5B also led to spontaneous appearance of lesions and persistence of γH2AX foci, indicating the critical role of KDM5B in maintaining genome stability(102). Interestingly, a recent report suggested KDM5A mediated de-methylation of H3K4me3 to be crucial for chromatin recruitment of bromodomain- containing factor ZMYND8 [Zinc finger and MYND (Myeloid, Nervy and DEAF-1) domain containing 8] and Nucleosome Remodeller (NuRD) complex, for transcription repression and HR mediated repair promotion at transcriptionally active DNA damage sites(103,104). Additionally, p53 binding protein 1 (53BP1) has also been reported to recognize histone marks H4K20me3 by its two tandemly occurring tudor domains(105). A

report suggested histone methyltransferase MMSET mediated increased levels of H4K20me2 (at ISce-I induced DSBs) was crucial in recruitment of 53BP1 to damaged sites(106). Apart from histone methyl marks, 53BP1 also recognizes H2AK15ub by its unique Ubiquitin-Dependent Recruitment (UDR) motif.(107) Hence, 53BP1 acts as a "dual-modification reader" protein that recognizes both histone methyl and ubiquitin moieties for chromatin recruitment in response to DNA damage. Another histone methyl mark, H3K36 methylation plays a critical role in determining the pathway for DNA repair. Reports suggest H3K36 methyl-transferase KMT3A to be crucial for recruitment of CtIP and Rad51 at ISce-I induced DNA DSBs and promote repair by HR(108). Interestingly, a DNA repair protein named Metnase, which also had SET domain for methyltransferase activity, reportedly induced H3K36me2 in the vicinity of DSBs and helped in recruitment of NHEJ repair pathway proteins NBS1 and Ku70(109).

Ubiquitylation of histones plays an important role for recruitment of proteins involved in the DNA repair process. It has been deciphered that RNF8 E3 ubiquitin ligase created a hierarchy of events that involved linker H1 ubiquitylation and caused recruitment of another ubiquitin ligase RNF168. Subsequent ubiquitylation of H2AK13/15 by RNF168 led to recruitment of DNA repair protein 53BP1(110–113). Additionally, it has also been reported that H2AK27ub is critical for RNF168 based histone ubiquitylation and recruitment of DNA repair proteins like BRCA1 and 53BP1 and proper DNA repair foci formation(114).

Poly-ADP ribosylation is an important aspect of the DNA repair pathway. Enzymes called Poly-ADP Ribose Polymerases (PARPs) mediate addition of the

PAR moiety on substrates, including histones. A very recent study suggests the role of histone PARylation in PARylated histone eviction from the DNA damage site, mediated by the FACT complex(115). The major residue upon which PAR group is added is Serine (S). Reports suggest H3S10 and H3S28 to be major sites of PARylation during the DNA damage response, with H3S10 as a better PAR acceptor than S28 (116). Interestingly, using DNA barcoded mononucleosome libraries, having several permutations of histone PTM combinations, it was reported that presence of lysine acetylation at -1 position potentially disrupted Serine-PAR interaction. Hence, this strongly indicated a negative cross-talk between histone PTM acetylation and PAR, both of which are implicated to alter during DNA damage and repair(117).

1.12 H3S10ph and its dual but contrasting roles during interphase and mitosis

The role of histone PTM H3S10ph during DDR has been elaborated previously. H3S10ph lies within the "ARKS" motif present in histone H3 and is associated with two distinct phases of the cell cycle- G_1 and mitosis. The chromatin architecture in both these phases is drastically different, with interphase having a de-condensed and transcriptionally active state, while mitosis comprises of chromatin present in the form of highly condensed chromosomes for segregation into daughter cells. During G_1 phase, H3S10ph and its acetylation of its nearby lysine residues, H3K9/14ac are involved in promoting gene transcription at specific gene loci. In the year 2000, several reports independently confirmed the role of histone phospho-acetylation in activation of gene transcription. Cheung *et.*

al. also reported H3S10ph on the promoters of immediate early genes to be a result of Epidermal Growth Factor (EGF) stimulation, mediated by the action of MAP kinase regulators. They also reported the synergistic nature of H3S10ph and its propensity to recruit HAT GCN5, thereby stimulating the process of histone acetylation(118). Clayton *et. al.* reported that dual modifications of H3 phosphorylation and acetylation on the same histone tail resulted in expression of immediate early genes *c-fos* and *c-jun*(119). On similar lines, a study published by Sheng Lo *et. al.* also reported a positive cross-talk between H3S10ph and its role in recruitment of GCN5, to acetylate H3K14 residue. However, it was also reported that not all GCN5 regulated genes required H3S10ph for their transcription, indicating the necessity of dual phospho-acetyl mark essential only for a subset of genes(120). 14-3-3 proteins were later on identified to act as a reader of H3S10ph mark with an increased affinity for phospho-acetylated histones, where 14-3-3 recruitment was necessary for transcription(121).

The role of H3S10ph in mitosis is in complete contrast to its function in interphase. Late G_2/M onwards, from the peri-centromeric regions, H3S10ph begins to spread across the chromosome arms, peaks at metaphase and co-incides with chromatin condensation(28). Hence, H3S10ph is considered to be a mitotic mark. However, H3S10ph was reported to be required only for initiation of chromatin condensation(46), while another independent report suggested H3S10A mutants displayed aberrant chromatin condensation and segregation, making H3S10ph an essential mark for chromatin condensation in *Tetrahymena*(47).

1.13 DNA damage response during mitotic phase of cell cycle

The mitotic phase of the cell cycle is characterized by a dramatic change in chromatin architecture compared to rest of the interphase. In an attempt to faithfully segregate the duplicated genome, chromatin undergoes several fold of condensation to form distinct chromosomal entities, and the nuclear envelope is degraded(37). Mitosis being the shortest phase of the cell cycle is divided into sub-phases- Prophase, Pro-metaphase, Metaphase, Anaphase and Telophase. Another feature that distinguishes mitotic cells from interphase is its lowest tolerability for radiation induced DNA damage (termed radio-sensitivity). Several studies have reported mitotic phase to be the most radiosensitive phase of the cell cycle, partly attributed to its characteristic condensed chromatin state (122,123). Elaborate explanations about enhanced radio-sensitivity of mitotic cells remain elusive. The reasons contributing to this could be firstly, the highly dynamic nature of this process and secondly, presence of a small percentage mitotic population at a given time. Several synchronization procedures like using spindle tubule poisons (nocodazole, taxol and CDK1 inhibitors) allow arrest of the mitotic population in different phases of mitosis, thus enabling experimentation on pure mitotic population.

In response to DNA damage, generation of DNA DSBs can prove to be cytotoxic if left unrepaired. Cell cycle checkpoints in other phases of cell cycle (G_1/S, Intra-S and G_2/M) and activation of the DDR pathway are responsible for maintaining genome integrity. A checkpoint has been reported to exist during early prophase, but not late prophase, DNA damage induction led to reversal of mitotic cells to interphase. This was accompanied by reversal of mitotic events such as

centrosome maturation and de-phosphorylation of histone H3 and H1. However, DNA damage induction in late prophase did not activate this checkpoint and cells progressed through mitosis(124). Hence, a "commitment point" was proposed to be late prophase, beyond which, no reversal of mitosis- associated events too place. A preliminary study about comparison of γH2AX foci appearance and disappearance in both G_1 and mitotic phase suggested a reduced rate of γH2AX foci disappearance either due inaccessibility of the phosphatase or trapped γH2AX in condensed metaphase chromatin(125). It was interesting to note from several studies that even in highly condensed chromatin architecture, mitotic cells marked DNA damage site by formation of generation of γH2AX, but not initiate a full scale DDR. Instead mitotic cells prioritized completion of mitosis over repairing DNA only to commence a DDR in the subsequent G_1 phase. It had previously been observed that upon DNA damage induction, mitotic cells displayed early DDR signaling events like ATM activation and MRN/MDC1 complex recruitment on chromatin. However, downstream processes like ubiquitylation by E3 ubiquitin ligases RNF8/168 or DNA repair protein 53BP1/ BRCA1 recruitment were not observed in DNA damage induced mitotic cells, while repair initiation only occurred in the G_1 phase (126),(127). However, another report suggested recruitment of RNF8/168 on chromatin in late mitosis to mark sites for 53BP1 activation as an early G_1 phase associated event(128). However, 53BP1 was observed to be recruited on kinetochore region of mis-aligned chromosomes, thus also functioned to ensure unperturbed mitosis(129). An interesting report by Orthwin *et. al.* aimed to understand the consequences of DDR activation in mitosis. The study reported that CDK1 dependent phosphorylation of DNA repair

factor 53BP1 and E3 ubiquitin ligase RNF8 abrogated their recruitment on chromatin during mitosis, also reported by another independent study(130). However, activation of the DDR in mitosis by overexpression of non-phosphorylatable mutants led to hypersensitivity of such mitotic cells. Further, inhibition of NHEJ rescued the phenotype like the wild type mitotic population. This was mediated by de-protected mitotic telomeres that led to mitotic telomere fusion and further caused aneuploidy(131). Hence, a very important conclusion from this report was that activation of the DDR pathway during mitosis did not lead to better survival, rather caused radiation hypersensitivity. Apart from inhibition of HR pathway, even NHEJ process was reported as suppressed, but not inactivated during mitosis. This was attributed to CDK1 and Polo-like kinase (Plk1) dependent phosphorylation of LigaseIV complex component XRCC. However, XRCC activation during mitosis led to formation of anaphase bridges, again suggesting that initiation of DNA repair process during mitosis promotes genomic instability(132).

1.14 Epigenetic alterations and cellular radio-resistance

Chromatin architecture as well as its modulation has a profound impact on the process of DNA repair. Since the chromatin architecture changes from once cell cycle phase to another, so does the intrinsic cellular radio-sensitivity of different cell cycle phases. S-phase cells are considered to be the most radio-resistant, while mitotic cells are the least radio-resistant. In terms of radiobiology, the response of a patient towards radiotherapy is governed by factors called the 4Rs of Radiobiology, namely - Repair, Redistribution, Repopulation and Reoxygenation.

Additionally, Radio-resistance was introduced as the 5th R of radiobiology owing to its significant contribution in determining the response to radiotherapy(133). However, till date, the exact reasons that lead to intrinsic or acquired radio-resistance remain elusive and multifactorial, such as tumor microenvironment (134), cell cycle phase (123) and DNA repair pathways (135),(136).

Since the DNA damage response is critically influenced and regulated by epigenetic factors, it could be possible that certain chromatin alterations are linked with radio-resistance. Studies report increase in the heterochromatin content of fibroblasts and salt-dependent solid phase chromatin modulation lead to reduced radio-sensitivity (122,137,138). Additionally, human lung carcinoma cells also showed increased heterochromatinization and increased levels of H3K9me3(139) while reduction of histone mark H4K20me3 was observed in mice subjected to total body irradiation, but at a low dose (140).

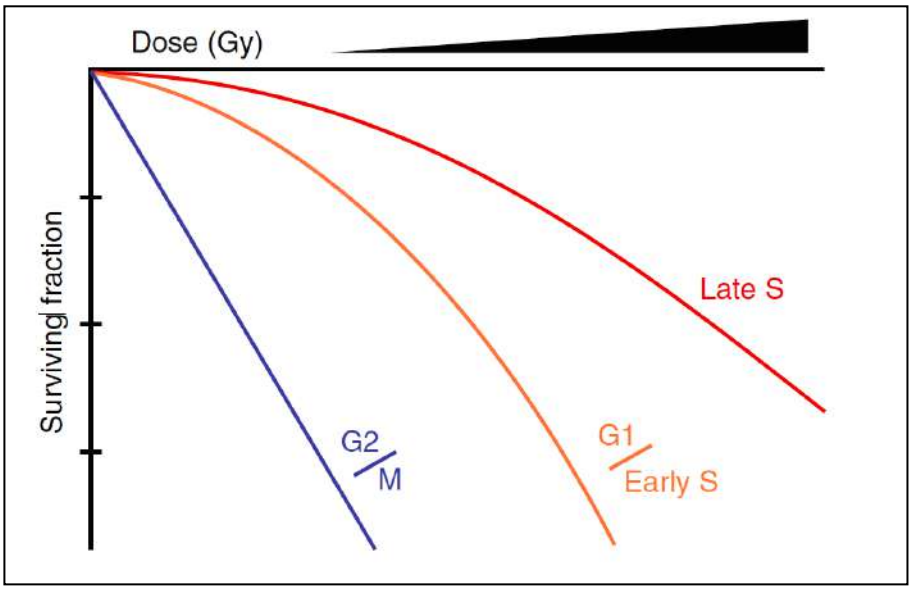

Figure 1.9 Representation of distinct cellular radio sensitivity of different cell cycle phases. *Adapted from D.S. Chang et al., Basic Radiotherapy Physics and Biology, (2014).*

Therefore it is plausible that an epigenetic signature pattern could be associated with altered cellular radio- sensitivity.

Indeed, HDAC inhibitors are currently being explored for their radio-sensitization potential. Thus, elucidation of epigenetic changes that take place during radiotherapy treatment could be helpful in gaining a better understanding of radio-resistance acquirement (141–145)

Chapter 2

Aims and Objectives

2.1 Statement of the problem

Histone PTMs are crucial regulators of the DNA damage response. The local and global patterns of histone PTMs get altered during each phase of the cell cycle. Since DNA repair pathways are also selectively activated in a cell cycle dependent manner, it is possible that the histone PTM milieu of a particular cell cycle phase influences the activation od a distinct repair pathway. In this way, histone PTMs can play a very important role as molecular switches that regulate DNA repair, and subsequently dictate the cell fate. It is also possible that in response to DNA damage, histone PTMs exhibit distinct patterns of alterations that correspond with activation of a specific repair pathway. Each cell cycle phase has different radio-sensitivity. Hence, histone PTM alterations could also be involved in determining the cell fate after DNA repair.

2.2 Hypothesis- *Previous studies by our group suggest bi-phasic alterations of histone PTM H3S10ph during the G_0/G_1 phase of the cell cycle. Therefore, we hypothesize that histone H3 PTMs such as H3S10ph and its nearby acetylation marks could play an important role in governing the cell cycle phase specific DNA damage response and acquired radio sensitivity of cells.*

The following questions were put forward to address the hypothesis:

1. Does H3S10/S28ph follow a bi-phasic kinetics during the mitotic DNA damage response?
2. How are the H3S10/S28ph modifying kinases and phosphatases regulated in the M phase of cell cycle in response to radiation induced DNA damage?

3. Does a cross talk exist between the phosphorylation on H3S10/S28 and acetylation on nearby histone marks H3K9 and K14 in response to mitotic DNA damage?
4. Do histone modifications play an important role in imparting radio-resistant phenotype to cancer cells?

To answer the above-mentioned questions, the following objectives for the thesis were formulated:

2.3 Objectives

1. To investigate the mechanism of de-phosphorylation and phosphorylation of H3S10 in response to DNA damage.
2. To understand the role of histone modifications in radio-resistant behavior in cancer cells.

2.4 Work-plan for the objectives

To answer the objectives, we employed the below detailed work plan.

Objective 1

To investigate the mechanism of de-phosphorylation and phosphorylation of H3S10 in response to DNA damage.

1. Analysis of levels of histone PTMs H3S10ph, H3S28ph and H3K9ac by western blotting and cell cycle progression by flow cytometry of mitotic synchronized cells exposed to ionizing radiation.

2. Immunofluorescence analysis of cellular morphological features using α-Tubulin, Lamin A and DAPI markers and live cell microscopy analysis of cell division defects arising after radiation of mitotic cells.
3. Comparison of cell cycle markers by western blotting in G_1 synchronized population versus mitotic cells exposed to radiation.
4. Analysis of histone PTMs H3S10ph, H3S28ph and H3K9ac in response to exposure of mitotic cells to several DNA damaging agents, in different cell lines and a range of radiation doses.
5. Mono-nucleosomal immuno-precipitation of mitotic nucleosomes for co-occurrence of histone marks γH2AX, H3S10ph, H3S28ph and H3K9ac.
6. Regulation of alteration in histone modification profile by their modifying enzymes, MKP-1, PP1α, MSK1 and Aurora Kinase B (AURKB) by real time-Polymerase Chain Reaction (PCR) and western blotting.
7. To understand the transcriptional regulation and translation stability of histone modifying enzymes, MKP-1, PP1α, MSK1 and AURKB.

Objective 2

To understand the role of histone modifications in radio-resistant behavior in cancer cells.

1. Generation of MCF7 breast cancer radio-resistant cell line by fractionated irradiation.
2. Analysis of cellular morphology (by electron microscopy), physiological features (cell proliferation, colony forming ability, cell migration capacity,

analysis of apoptotic population), gene expression profile (real-time PCR) and biochemical features (Raman spectroscopy).

3. Micrococcal nuclease assay of parental and radio-resistant cells to understand chromatin organization and immunofluorescence analysis of heterochromatin protein1α.
4. Analysis of activating and repressive histone PTM marks in parental versus radio-resistant population and activity of HDACs and HATs.
5. HDAC activity in human tumor samples from different sites of origin and HDAC 1-3 expression analysis for normal versus breast cancer and normal versus pan-cancer cohorts using TCGA database.
6. Efficacy of HDAC inhibitor, valproic acid for radio-sensitizing ability against acquired radio-resistant and inherently radio-resistance.

Chapter 3

Materials and Methods

3.1 Cell culture lines and growth conditions

The following cell lines were used/generated* in the study:

Table 3.1: Cell lines used in the study

Cell Line	Origin	Culture Medium
MCF7	Breast Adenocarcinoma	DMEM (Invitrogen)
U87	Glioblastoma Multiforme	DMEM (Invitrogen)
AGS	Gastric Adenocarcinoma	RPMI (Invitrogen)
MCF7 10GyRR*	Breast Adenocarcinoma	DMEM (Invitrogen)
MCF7 20GyRR*	Breast Adenocarcinoma	DMEM (Invitrogen)
MDA-MB231	Breast Adenocarcinoma	DMEM (Invitrogen)
MDA-MB231RR*	Breast Adenocarcinoma	DMEM (Invitrogen)

2mM glutamine (Sigma) and 1X non-essential amino acids were used to supplement the medium. 10% Fetal Bovine Serum (FBS) (Gibco) and 100X antibiotic antimycotic solution (Himedia) was used to prepare complete growth medium. Cells were maintained at 37°C and 5% CO_2 growth conditions. Cells were trypsinized and sub-cultured using 1X Phosphate Buffered Saline (PBS) and Trypsin-EDTA solution (0.25% trypsin powder w/v and 0.2% EDTA dissolved in PBS and filter sterilized). Viable cells were detected using 0.4% Trypan blue or Erythrosin B dye and counted on a haemocytometer slide. The formula for calculation of number of cells was as follows:

No. of cells per ml = Avg. number of cells per WBC chamber * dilution factor $*10^4$

$2*10^4$ cells were seeded according to experimental requirement or maintained at 60% confluency.

3.2 Cell cycle phase synchronization

Cells were synchronized in the G_0/G_1 phase and mitosis for the study. Synchronization in the G_0 phase was performed by serum starvation. Cells were grown in 10% serum containing medium till 60% confluency. Subsequently, cells were washed three times with 1X PBS to remove residual serum and then grown in 0.02% serum containing medium for 72 hours. After 72 hours, the 0.02% serum-containing medium was replaced by 10% serum containing medium. After 6 hours of media replacement, experiments for G_1 phase were initiated. To synchronize cells in mitosis, treatment was given with 200ng/ml nocodazole (Sigma) for 18 hours at 80% cell confluency. After this incubation, experiments for mitotic cells were performed. Mitotic cells were separated from non-mitotic cells by mitotic shake off method for all experiments(146,147). Nocodazole release was performed by collecting mitotic cells followed by centrifugation. The spent medium was discarded and cells washed with 1X PBS before re-plating into fresh plates and medium without nocodazole for G_1 phase progression.

3.3 Cell Irradiation

Cells were exposed to ionizing radiation through a Cobalt-60 radioactive source present in Bhabhatron-II (Panacea Medical Technologies Ltd. and Bhabha Atomic Research Centre (BARC), India). The machine is present at the Department of Radiation Oncology, ACTREC. Field size for cell irradiation was constant at as 25cm x 25cm for all cell radiation experiments. The Source-to-skin distance (SSD) was set at 80cm and cells plates were placed at 180° to the gantry. The radiation dose was kept constant at 8Gy for all experiments unless specified.

3.4 Treatment of cells with other DNA damage inducing agents

Mitosis synchronized MCF7 cells were treated with DNA damage inducing agents like Cisplatin (2μg/ml for 4 hours), Ultra Violet (10J/m^2 for 15 minutes) rays, Adriamycin (10μg/ml for 4 hours) and H_2O_2 (500μM for 15 minutes). Mitotic shake off and subsequent nocodazole release was performed as described above.

3.5 Cell cycle analysis by Fluorescence Activated Cell Sorting

Cells were trypsinized in 1ml of medium and washed twice with chilled PBS by centrifugation at 5000 rpm for 10 minutes at 4°C. 1/10^{th} of the total cell volume was shifted to a fresh Micro-Centrifuge Tube (MCT) and fixed with 1ml of chilled 70% ethanol and the remaining cells were used for histone/lysate preparation. Ethanol was added drop-wise while gently swirling the cells on a vortex and stored at -20°C. Processing for cell cycle analysis was performed by washing the fixed cells twice with chilled PBS by centrifugation at 5000 rpm for 10 minutes at 4°C to remove traces of ethanol. The cell pellet obtained was re-suspended in 500μl 1X PBS. To this cell suspension, 0.1% Triton X-100 and 100μg/ml of RNase A were added and incubated for 30 minutes at 37°C. After incubation, propidium iodide (Sigma, 25 μg/ml) was added to the cell suspension and incubated for 15 minutes in dark. Samples were immediately processed for cell cycle analysis in FACS Calibur flow cytometer (BD Biosciences) and analysis was performed by MODFIT software by Verity house. Cell sorting was performed using VYBRANT green dye (Invitrogen), as per manufacturer's instructions.

3.6 Clonogenic assay

MCF7 cells sorted after VYBRANT dye treatment were counted and seeded in 6 well plates. 1000 cells were seeded per well, per cell cycle phase. Cells were irradiated, seeded at 1000 cells per well and cultures for 14 days. Colonies were fixed with 4% paraformaldehyde, washed with 1X PBS and stained with 0.5% crystal violet(148).

3.7 Histone isolation

Histones were extracted from cells by acid extraction method(149). Cells were trypsinized and washed with 1X PBS. Thereafter, 1ml of chilled MKK lysis buffer was added to the cells (Composition in Table 9.1). Protease inhibitors were added to the chilled buffer just before use. Cells resuspended in the buffer were incubated on ice for 30 minutes with intermittent mixing and thereafter centrifuged at 18000 rpm for 30 minutes at 4°C. The supernatant was discarded and 300µl of 0.2M H_2SO_4 was added to the nuclear pellet. The pellet was vigorously vortexed for 2 hours with intermittent incubation on ice. After vortexing, the pellet was centrifuged at 18000 rpm for 30 minutes at 4°C. The supernatant was collected in a fresh MCT and 4 volumes of chilled acetone were added to it. Histones were precipitated by overnight incubation at -20°C. The pellet was washed with chilled acidified acetone (acetone containing 50mM HCl) and subsequently twice with chilled acetone. Residual acetone was vacuum evaporated from the pellet. Pellet was resuspended in 0.1% β-Mercaptoethanol and stored at -20°C.

3.8 Total cell lysate preparation

Cells were trypsinized and washed with 1X PBS. Thereafter, 300µl of chilled MKK lysis buffer was added to cells (Composition in Table 9.1). Protease inhibitor cocktail was added to the chilled buffer just before use. Cells resuspended in the buffer were incubated on ice for 30 minutes with intermittent mixing and thereafter centrifuged at 18000 rpm for 30 minutes at 4°C. Thereafter, the nuclear pellet was subjected to pulse sonication at 30% amplitude for 3-5 seconds. After breakdown of the nuclear pellet, the suspension was centrifuged at 18000 rpm for 30 minutes at 4°C. Supernatant was collected in a fresh MCT and stored as the Total Cell Lysate (TCL) while the pellet was discarded.

3.9 SDS-PAGE based separation of histones and TCL

The denaturing system of Sodium Dodecyl Sulphate (SDS) was utilized for poly-acrylamide based separation of proteins according to their molecular weight(150). A sandwich of 2 glass plates and 0.1cm thick spacers was created and sealed from the sides to prevent leakage. Varying percentages of polyacrylamide gels were prepared as per molecular weight of protein of interest. Resolving gel (18% for histones and 10% for TCL) were poured into the plates and allowed to polymerize (composition in table 9.2 and 9.3). Thereafter, stacking gel of 4% polyacrylamide was used as stacking gel (composition in table 9.4), with a 0.1cm thick plastic comb inserted as space for wells. After polymerization wells were cleaned and washed with 1X SDS Running buffer (composition in table 9.5). Samples to be separated were prepared by mixing thoroughly with 2X SDS sample buffer (0.005M Tris-Cl pH 6.8, 20% v/v glycerol, 4% SDS, 2% β-Mercaptoethanol and bromophenol blue) and boiling for 10 minutes. The

boiled samples were chilled and again mixed before loading into the wells. The gels were run at 15mA constant current till the tracking dye reached resolving gel, after which the current was increased to 30mA till tracking dye reached bottom of the gel. The assembly was then dismantled and polyacrylamide gel was processed for western blotting.

3.10 Western Blotting of histones and proteins from polyacrylamide gel

The proteins on the resolving gel were transferred onto an inert, porous and adsorbent material such as Polyvinylidene diflouride (PVDF, Millipore, pore size 0.4μm)(151). The PVDF membrane was activated by immersing in 100% methanol for 30 seconds followed by immersing in distilled water until required. A sandwich of the gel and membrane of equal size was created between six sheets of Whatmann no.1 paper for support and the assembly was immersed in chilled 1X transfer buffer (composition in table 9.6). Current was applied from the electrodes in the transfer assembly (BioRad). The process was performed at 4°C, for 4 hours using 300mA constant current. Subsequently, the PVDF membrane was stained with 0.05% Fast green solution to visualize the transferred proteins.

Western blotting was performed in 4 steps- Blocking, primary antibody incubation, washing off excess antibody and secondary antibody incubation. This was followed by visualization of the protein of interest by chemiluminesence-based detection. Blocking of the membrane was performed for one hour using blocking agents such as milk or BSA prepared in 1X TBS-T (1X Tris buffered saline containing 0.1% Tween-20)(152). This was followed by an overnight incubation with a specific dilution of the primary antibody at 4°C. Next day, the excess primary antibody was removed by

washing it four times (10 minutes each) with 1X TBST. The membrane was incubated with secondary antibody for one hour at RT, washing off excess secondary antibody and then visualization with Enhanced Chemiluminescent Reagent (ECL, Thermo Scientific), Femto West (Thermo Scientific) or Clarity Max (BioRad) as per the manufacturer's instructions. The list of antibodies used along with their specific dilution is provided in Table 8.8.

3.11 Immunofluorescence Microscopy

Cells were seeded in 100mm^2 tissue culture dishes along with sterilized glass coverslips. The cover slips containing cells were washed twice with 1XPBS and fixed with 4% Paraformaldehyde (Sigma) for 20 minutes or with chilled absolute methanol for 10 minutes. The fixative was washed off twice with PBS and cells were permeabilized using 0.2% Triton X-100 in PBS for 10 minutes. Cells were washed twice with 1X PBS and placed in primary antibody dilution (Table no. 9.7) at 4°C overnight. Next day, the cells were washed three times each, with 1X PBS and 0.1% NP-40 containing 1X PBS, and placed in fluorophore conjugated secondary antibody (Invitrogen) dilution for two hours in dark conditions. All the subsequent steps were performed in dark. Excess secondary antibody was washed with 1X PBS and 0.1% NP-40 containing 1X PBS and coverslips were DAPI stained (0.1µg/µl) for 5 minutes and excess stain was washed with 1X PBS. Mounting medium for fluorescence was added on clean glass slides and coverslips were carefully placed on the glass slides and imaged using Zeiss 510 Meta-confocal imaging system. Image analysis was performed using Image J or FIJI software.

3.12 Micrococcal nuclease (MNase) digestion assay

Cells were harvested by trypsinization and washed twice with 1X PBS at 5000 rpm at 4°C. Cell pellet was resuspended in 500 µl of MNase digestion buffer (Table 9.8) and incubated on ice for 30 minutes with intermittent shaking. The cells were then centrifuged at 5000 rpm at 4°C for 10 minutes. Supernatant was discarded and the nuclear pellet was washed again with 500 µl of MNase digestion buffer. The subsequent pellet was carefully resuspended in 300 µl of MNase digestion buffer supplemented with $CaCl_2$ (Sigma, 2mM for G_0/G_1 phase cells and 10mM for mitotic cells). The amount of DNA in the final suspension was quantified using nuclei lysis buffer (5M NaCl-2M Urea). 50µg chromatin was used for MNase digestion per time point and MNase enzyme (5Units/ µl) was used at ac concentration of 200Units/mg chromatin. The digestion was carried out at 37°C for desired duration and terminated by addition of 10mM EDTA. 2ug/ml Proteinase K was added and incubated overnight at 55°C, followed by DNA extraction by phenol chloroform method. The DNA obtained was dissolved in TE buffer, quantified by Nano-drop. 500µg chromatin was loaded on 1.8% TAE-Agarose gel containing ethidium bromide at a concentration of 0.5 µg/ml. The gel was resolved at constant voltage and visualized under UV. Image analysis was performed using FIJI software.

3.13 Mononucleosomal Immunoprecipitation

Mononucleosome isolation from mitotic nuclei was done in MNase digestion buffer containing 10mM $CaCl_2$. Mononucleosomes were prepared by incubating 1mg chromatin with 200 units of MNase for 30 minutes at 37°C. 200µg of chromatin was incubated with 2µg of anti- γH2AX, anti- H3S10ph and IgG antibodies. 20µl of

magnetic DYNA beads (Thermo Fischer) were added to chromatin-antibody mixture and incubated for 4 hours on a rotating platform. Separation of antibody-nucleosome complex and washing of bound complex was done using magnetic rack. 2X SDS loading dye was added to the bead bound complex. The samples were boiled, chilled and loaded on 18% SDS-PAGE gel, followed by western blotting with respective antibodies.

3.14 Generation of Radio-resistant cell line

Cells were made radioresistant by fractionated irradiation. Cells were exposed to 10 rounds of Co-60 radiation dose of 2Gy each and allowed to recover. Parental cells were maintained at the same passage number and mock irradiated. After the final dose of 20Gy was delivered, cells were cultured without any radiation treatment radiation for 21 days.

3.15 Clonogenic assay for radioresistant cells

Clonogenic assay was performed as described in 3.6. Parental and radio-resistant cells were irradiated and allowed to recover for 6 hours after radiation. Colonies were allowed to form for 14 days. Colonies having more than 50 cells were considered to be viable and counted under a light microscope. All data are expressed as average obtained ± standard deviation (SD) from n=3 experiments. Statistical significance was determined by conducting an un-paired students *t*-test.

3.16 Cell migration assay

Cell migration assay was carried out in a 6 well plate with 100% confluent cells, serum starved for 72 hours before the experiment. Three scratches were made in the monolayer and debris of dislodged cells was washed off carefully with sterile 1X PBS. Cell migration was monitored for 20 hours using an inverted microscope. Cells were kept at 37°C and 5% CO_2 for the entire duration of the experiment. All data are expressed as average obtained ± standard deviation (SD) from n=3 experiments. Statistical significance was determined by conducting an un-paired students *t*-test.

3.17 Cell proliferation assay

Cell proliferation was monitored using MTT method. 1000 cells were seeded in a 96 well plate and analyzed for 96 hours. 10µl of MTT (3-(4,5-dimethylthiazol-2-yl)-2,5-diphenyl tetrazolium bromide) reagent (5mg/ml in sterile PBS) was added, followed by 100µl of solubilizing solution (10% SDS-0.01N HCl) after 4 hours. Absorption was measured at 540 and 690nm using Spectrostar Nano Biotek LabTech 96-well plate reader. All data are expressed as average obtained ± standard deviation (SD) from n=3 experiments. Statistical significance was determined by conducting an un-paired students *t*-test.

3.18 AnnexinV/PI staining

Analysis of presence of apoptotic population was performed by Annexin- Fluorescein Isothiocyanate (FITC) apoptosis detection kit (Sigma), strictly following manufacturer instructions. The population was analyzed by a FACS Calibur flow cytometer and analysis performed using CELLQUEST software. All data are

expressed as average obtained ± standard deviation (SD) from n=3 experiments. Statistical significance was determined by conducting an un-paired students *t*-test.

3.19 Transmission Electron Microscopy

Samples were fixed using 3% glutaraldehyde and 1% osmium tetraoxide and post fixation was done by 1%. Alcoholic uranyl acetate treatment for 1 minute and lead citrate treatment for 30seconds. Imaging was performed using Carl Zeiss LIBRA120 EFTEM.

3.20 Raman Spectroscopy

Cells pellets were fixed using 1% PFA and washed with sterile PBS. Total 30 spectra were analyzed for all cell types. Raman Spectra were recorded using a commercial Raman micro spectroscope (WITec alpha300RS, λ_X-532nm, 10mW, 600 grooves/mm). Preprocessed Raman spectra (smoothening, fifth point, baseline, fifth order and vector normalization) in 650-1750 cm^{-1} were subjected to Principle Component Analysis using commercial Unscrambler® X software.

3.21 Quantitative PCR

RNA was extracted by Trizol method, followed by DNase1 treatment and cDNA synthesis using random hexamer primers (Revert-Aid cDNA Synthesis Kit, Thermo Scientific), strictly as per manufacturer's instructions. Real-time PCR was performed using gene specific primers. Amplification conditions for all primers were denaturation for 30 seconds at 94°C, annealing for 1 minute at 60°C and extension for 1 minute at 72°C. 30 cycles of amplification were followed by 10 minute final

extension. Sequence of primers used in the study is provided in Table 9.9. All data are expressed as average obtained ± standard deviation (SD) from n=3 experiments. Statistical significance was determined by conducting an un-paired students *t*-test.

3.22 Human tissue sample collection

Approval from Institute Ethics Committee III (Project number 164) was obtained for working on human tumor samples, collected retrospectively with approved waiver of consent. Samples were collected from Biorepository of ACTREC-TMC. Samples were stored in -80°C and used as required.

3.23 HDAC and HAT Activity assay

Assays were performed using the colorimetric HDAC and HAT activity assay kits from BioVision (BioVision Research Products, USA) as per manufacturer instructions, using 100µg of cell lysate or 1mg of tissue powder resuspended in MKK lysis buffer (composition in table 9.1). All data are expressed as average obtained ± standard deviation (SD) from n=3 experiments. Statistical significance was determined by conducting an un-paired students *t*-test.

3.24 *In silico* analysis of The Cancer Genome Atlas (TCGA) breast cancer and pan cancer dataset

To analyze the expression levels of HDAC1, HDAC2 and HDAC3 in normal and tumor samples of pan cancer, TCGA PANCAN normalized RSEM counts were obtained from UCSC cancer genome browser. p-value was determined using Wilcoxon-Mann- Whitney test analysis.

Chapter 4

Results

4.1 Alterations in cell cycle profile and levels of H3S10ph in response to DNA damage induced during mitosis

The effect of Ionizing Radiation (IR) induced DNA damage was investigated in mitosis synchronized MCF7 cells. During mitosis, the radiated population showed an immediate induction of γH2AX, while H3S10ph remained comparable to the non-radiated population (Fig. 4.1 A and B). Cell cycle analysis showed that 4 hours after nocodazole release, a majority of the cells had progressed to the G_0/G_1 phase, concomitant with decreased levels of H3S10ph. This reduction was attributed to mitotic exit and entry into G_0/G_1 phase and occurred irrespective of radiation exposure.

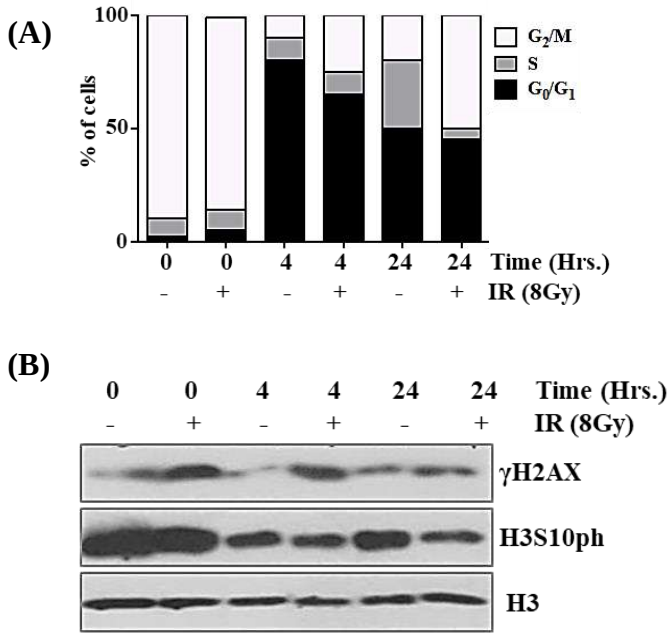

Figure 4.1 Alterations in cell cycle profile and H3S10ph levels upon mitotic DNA damage. *(A) Cell cycle profile of MCF7 cells synchronized in mitosis as analyzed by flow cytometry. Mitotic cells were collected at 0 hour time point, re-plated into fresh medium without nocodazole and harvested at specific time points. (B) Western blotting of acid extracted histones using antibodies against H3S10ph and γH2AX at specified time points. Histone H3 serves as loading control. Hrs. – Hours, Gy- Gray*

Compared to the non-radiated cells, the radiated population showed persistent γH2AX levels and a high percentage of cells in the G_2/M phase of the cell cycle 24 hours after radiation. However, it was intriguing that despite enrichment in the G_2/M phase, the radiated population showed reduced levels of mitotic mark H3S10ph (Fig. 4.1 B).

4.2 Changes in histone marks H3S28ph and H3K9ac in response to mitotic DNA damage

Histone marks H3S10ph and H3S28ph are unique as they are present in the two "ARKS" motifs of histone H3 and are enriched during mitosis. The neighboring residue of H3S10, i.e. H3K9, has the propensity to undergo acetylation and (along with H3S10ph and H3K14ac) enable the transcription activation in the G_0/G_1 phase of the cell cycle. Hence, the levels of both H3S28ph and H3K9ac after mitotic DNA damage were assessed. A time-dependent analysis was performed to analyze the cell cycle progression and histone PTM alterations after radiation and nocodazole release of mitotic cells (Fig 4.2 A and B). It was observed from the cell cycle profile that the non-radiated cells exit mitosis and enter the G_0/G_1 phase within 2 hours of nocodazole release, whereas in this duration, only a small percentage of the radiated population was able to enter the G_0/G_1 phase. The mitotic exit and G_0/G_1 phase entry of both radiated and non-radiated population was marked by increased levels of H3K9ac and reduced mitotic marks H3S10ph and H3S28ph.

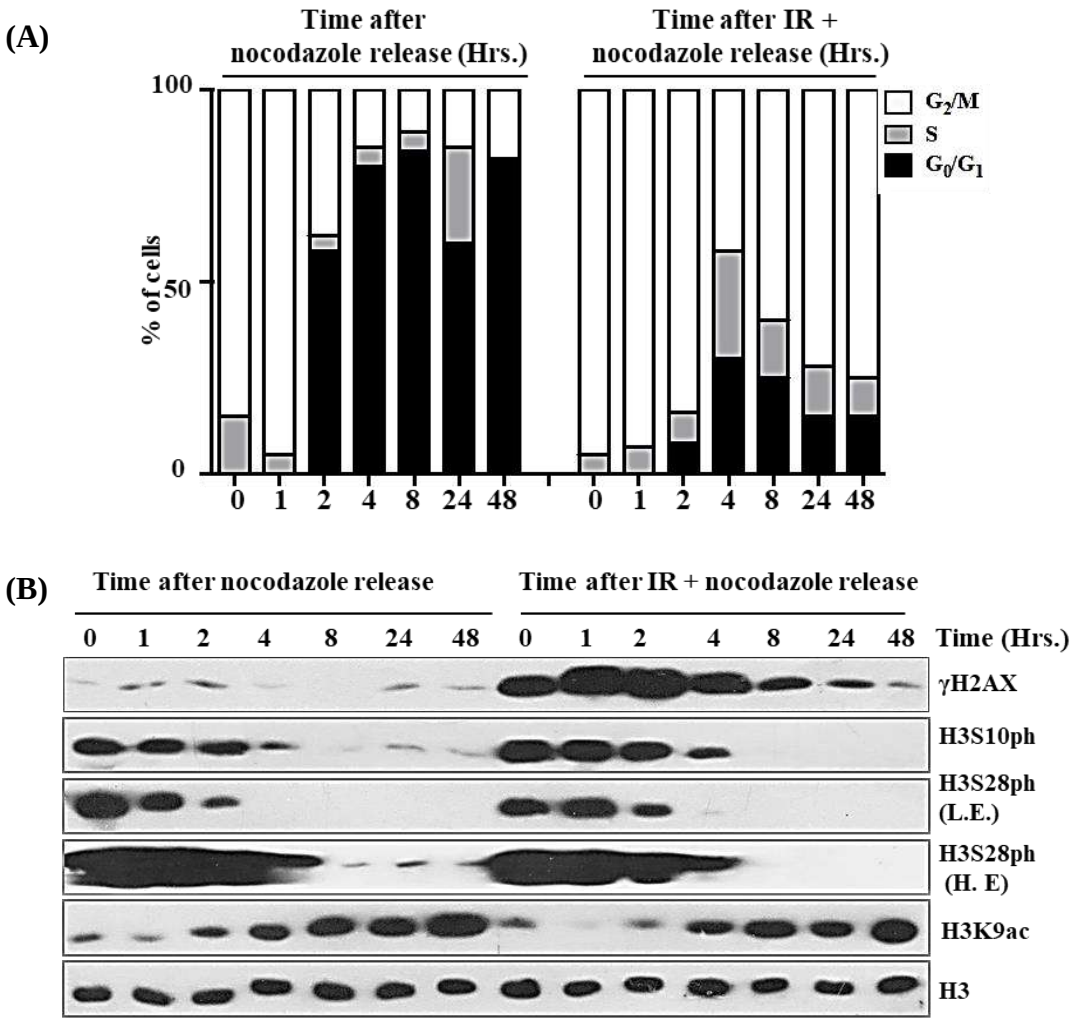

Figure 4.2 Alterations of H3S28ph and H3K9ac marks upon DNA damage induction of mitotic cells. *(A) Time point based cell cycle profile of MCF7 cells synchronized in mitosis, subjected to DNA damage and released from nocodazole arrest (B) Western blotting of acid extracted histones against γH2AX, H3S10ph, H3S28ph and H3K9ac at indicated time points. Histone H3 serves as loading control. L.E. – Low exposure, H.E. – High exposure. Hrs. – Hours, Gy- Gray.*

These changes were observed at 2 hours and 4 hours (after nocodazole release) for control and radiated cells, respectively. This indicated that DNA damage during mitosis could lead to delayed mitotic progression and interphase entry.

The non-radiated cells had attained an asynchronous cell cycle profile 8 hours after nocodazole release. However, a different pattern was observed in the radiated cells, which showed an incremental increase in the G_2/M phase population at both 8 and 24 hours after nocodazole release.

Similar to our previous observation, γH2AX levels persisted up to 24 hours after radiation. Regardless of radiation treatment, the levels of both H3S10ph and H3S28ph were unchanged during mitosis but decreased upon cell cycle progression. However, in the radiated cells, there was complete absence of H3S10/S28ph levels, co-incident with the time points that reflected G_2/M phase enrichment (8 hours and onwards). Surprisingly, neither the radiated cells attained levels of H3S10/S28ph comparable to an interphase population, nor the levels of these mitotic marks increased upon G_2/M enrichment.

In the non-radiated as well as radiated cells, entry into the G_0/G_1 phase was concomitant with an increase of H3K9ac levels that indicated the conversion of condensed mitotic chromatin to a de-condensed interphase conformation. Thus, a paradoxical situation existed, where a G_2/M enriched cell population had low levels of mitotic marks H3S10/S28ph but increased H3K9ac.

4.3 Analysis of cellular and nuclear morphology of the cells after mitotic radiation.

Given the perplexing situation of high G_2/M population but increased H3K9ac, an immuno-fluorescence based analysis was performed to microscopically observe the distribution of histone PTMs γH2AX, H3S10ph, H3S28ph and H3K9ac (Fig 4.3A). Histone mark H3K9ac mark was distributed uniformly throughout the nuclei of both radiated and non-radiated populations. Corroborating our western blot analysis, the radiated cells had lower levels of H3S10ph than the non-radiated cells (Fig 4.3 A). However, the intensity of H3S28ph was not found to be sufficient to comment upon any difference (Fig 4.3 A). An analysis of overall cellular and nuclear morphology at specific time points post nocodazole release showed that the condensed mitotic chromatin of both non-radiated and radiated cells was converted to a de-condensed conformation (reminiscent of an interphase nucleus), thereby indicating cell cycle progression (Fig 4.3 A). While assessing cellular and nuclear morphology, it was observed that as early as 8 hours after radiation, there were nuclear structure aberrations and presence of more than one nucleus within a single cell (Fig 4.3 B). This data provided strong evidence that the observed G_2/M state (with high H3K9ac and low H3S10ph and H3S28ph) of radiated cells could be due to the presence of 2 interphase-like nuclei (of ploidy 2N) within a single cell but detected by flow cytometer as a tetraploid G_2/M phase. Thus, it became essential to investigate the cause behind the generation of such bi-nucleated cells.

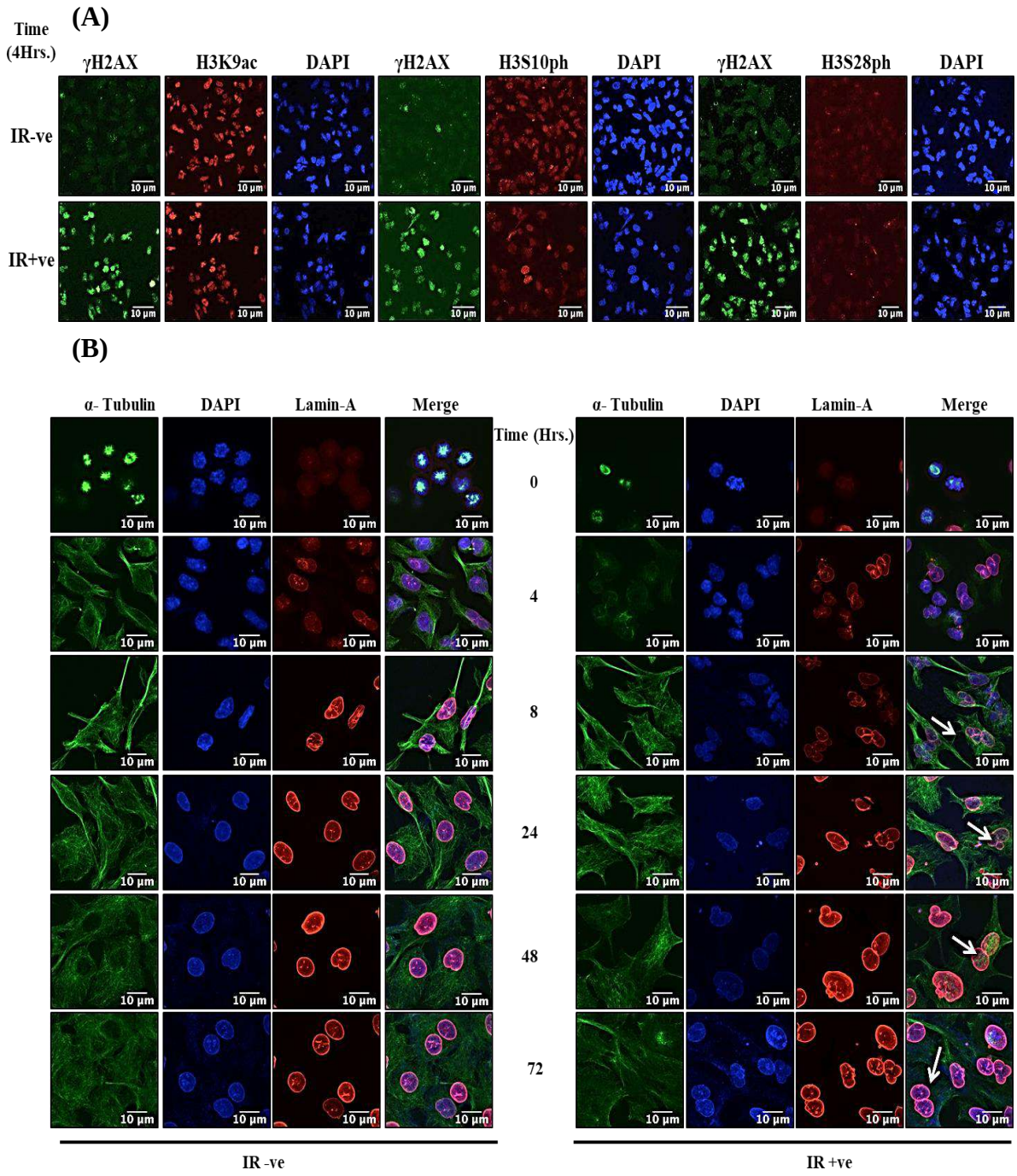

Figure 4.3 Cellular and nuclear morphological features of cells post mitotic radiation. *(A) Co-Immunofluorescence images for histone PTMs H3K9ac, H3S10ph, H3S28ph with γH2AX of radiated and non- radiated cell at 4 hour time point. (B) Co-Immunofluorescence images of non-radiated and radiated cells at specific time points post nocodazole release. α- tubulin acts as cell boundary marker, Lamin-A marks the nuclear boundary and DAPI acts as nuclear marker*

for all images. White arrows indicate alterations in nuclear architecture. Scale bar for all images is 10µm. Hrs. – Hours and radiation dose is 8Gy for all samples.

4.4 Analysis of cell division defects in mitotic cells subjected to radiation

Live cell microscopy was performed to ascertain if the radiated mitotic cells actually completed mitosis and entered the G_0/G_1 phase of the cell cycle. It was observed that the radiated population had a delayed initiation of the cell division events compared to the non-radiated cells (Fig 4.4 A white arrows and B). observed (Fig 4.4 A zoom out).

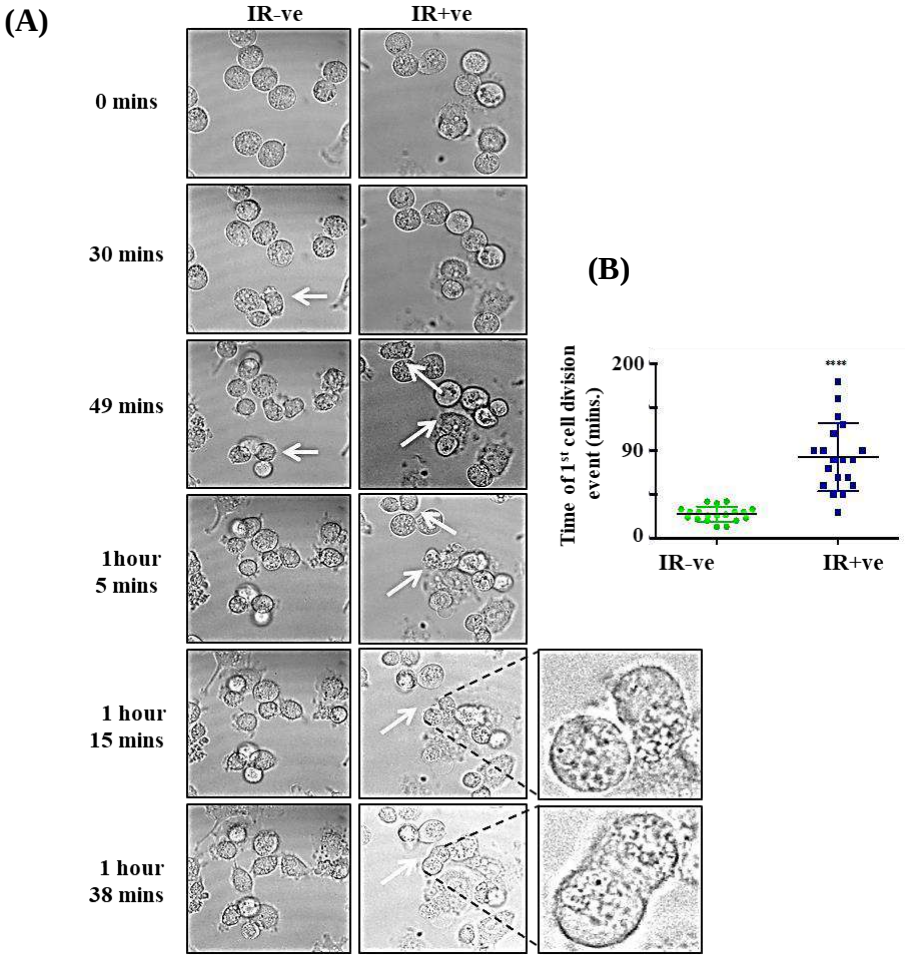

Figure 4.4 Defects in cell division process associated with DNA damage induction in mitotic cells. *(A) Live cell microscopy images of radiated and non-radiated cells at specific time points showing induction of first cell division (pointed by white arrows). (B) Graph depicting delay in time of first cell division event (n=27) Mins- Minutes.*

Events where fusion of daughter cells took place after initiating cell division were also observed (Fig 4.4 A zoom out). It was interesting that the observed G_2/M arrest was not actually a G_2/M population but comprised of bi-nucleated tetraploid cells, as a result of aberrant mitotic progression. Therefore it became important to investigate the differences between this bi-nucleated population and an actual G_0/G_1 phase population.

4.5 Presence of distinct cellular phenotypes during or after mitotic exit

In addition to delayed initiation of cell division, there were four other distinct phenotypes displayed by the radiated cells (Fig 4.5 A and B). The mitotic cells had either (a) completed cell division successfully and divided into two daughter cells, (b) did not initiate cell division, (c) displayed fusion of two the daughter cells and (d) gave rise to two daughter cells that were asymmetric in size. Therefore, as a result of incomplete or faulty mitotic progression after DNA damage, the unique phenotypes (b) and (c) could contribute to the observed tetraploid state, initially thought to be a G_2/M arrest. These observations are also summarized in Model 1.

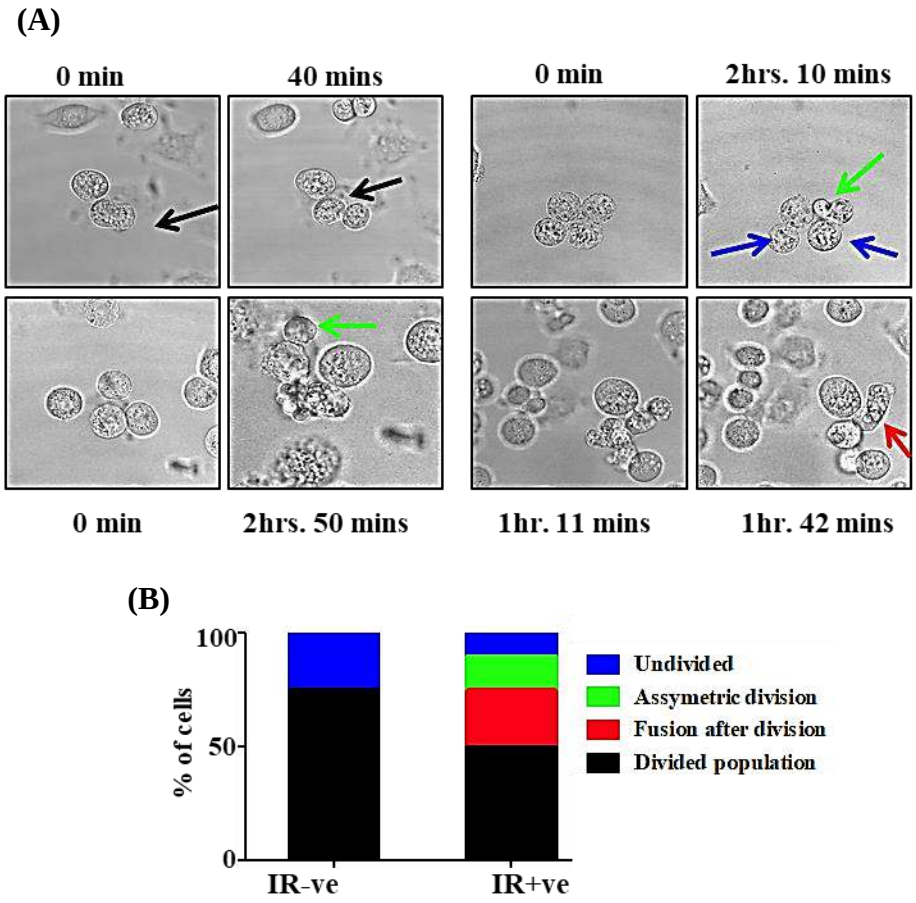

Figure 4.5 Defects in cell division process associated with DNA damage induction in mitotic cells. *(A) Images showing cell phenotypes that arise after radiation of mitotic cells. Black arrows indicate mitotic cells that divide into two daughter cells. Green arrows point to cells that show differences in size of the daughter cells. Blue arrows depict cells that did not initiate cell division during the course of experiment and red arrows indicate cells that have initiated cell division but the two daughter cells undergo cell fusion. (B) Graph depicting quantification of above described events as a percentage of cells that display these phenotypes. Mins- Minute.*

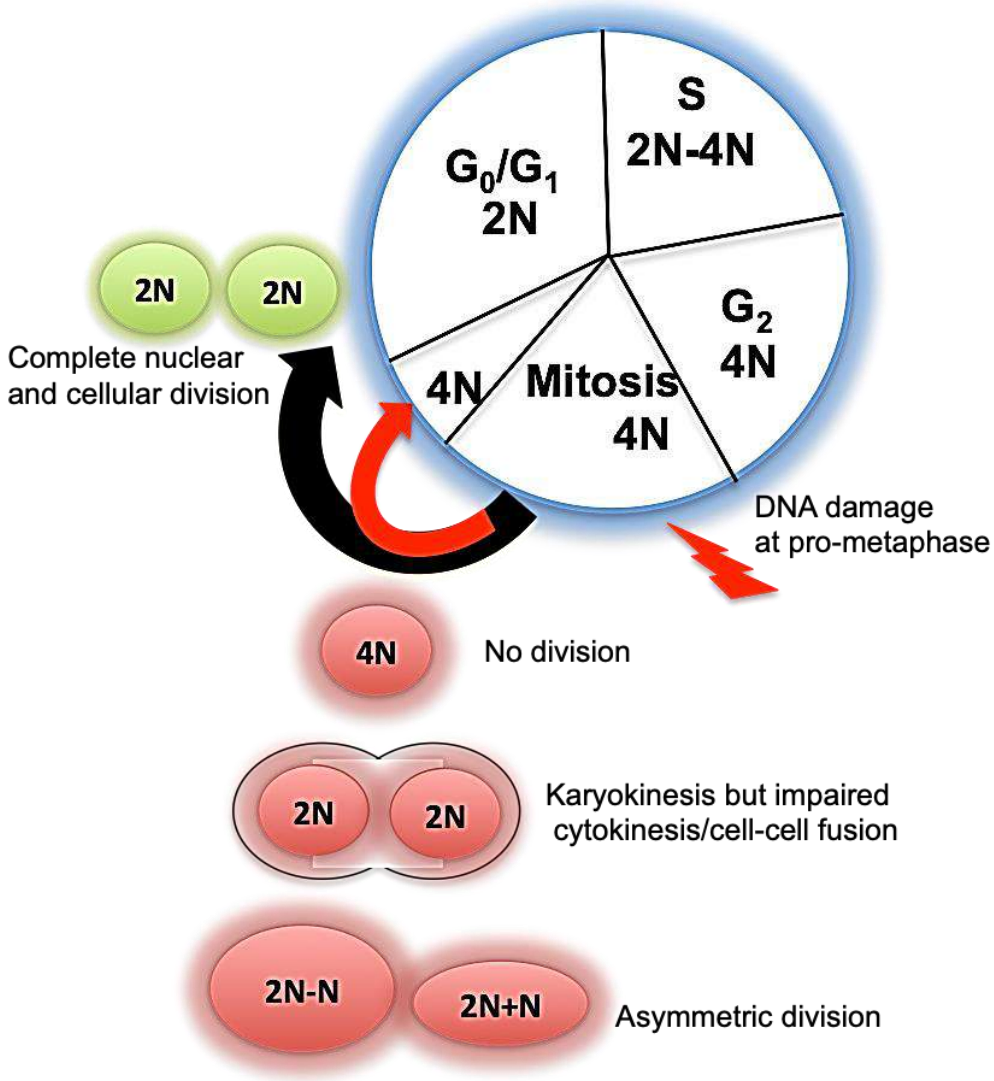

Model 1- Events describing the generation of a 4N intermediate state after DNA damage during mitosis. *Black arrow signifies normal cell cycle progression and red arrow signifies phenotypes generated by defects during mitotic progression.*

4.6 Analysis of the cell cycle and DNA repair-related proteins during and after radiation exposure to mitotic cells

A comparison of cell cycle specific cyclin proteins for both M and G_0/G_1 phase of the cell cycle was performed for mitotic cells, with and without radiation. Absence of M-phase specific cyclin B from both the radiated as well as non-radiated mitotic population after nocodazole release indicated mitotic exit. However, 4 hours after radiation, reduced (but not undetectable) levels of cyclin B strengthened our previous observation of incomplete/faulty mitotic progression.

The radiated mitotic population had reduced levels of G_0/G_1 phase specific cyclin D, as compared to nocodazole released non-radiated cells and G_0/G_1 phase synchronized cells. These data suggests that radiated mitotic cells did undergo mitotic progression, but synthesized reduced levels of G_0/G_1 phase specific cyclin D. This situation could lead to a state that was intermediate between mitosis and G_0/G_1 phase, henceforth termed as 4N-intermediate state. Our previous data showed that the mitotic cells were able to induce γH2AX in response to radiation induced DNA damage. However, an analysis of chromatin recruitment of DNA repair proteins revealed that mitotic cells were unable to recruit neither NHEJ repair protein Ku70 nor HR specific repair Rad51 proteins on chromatin while in mitosis. The recruitment of these proteins was observed 4 hours after nocodazole release, when the mitotic cells had progressed to the subsequent phase of the cell cycle. Recruitment of these repair proteins on chromatin was also concomitant with a reduction in the levels of γH2AX that indicated ongoing DNA repair.

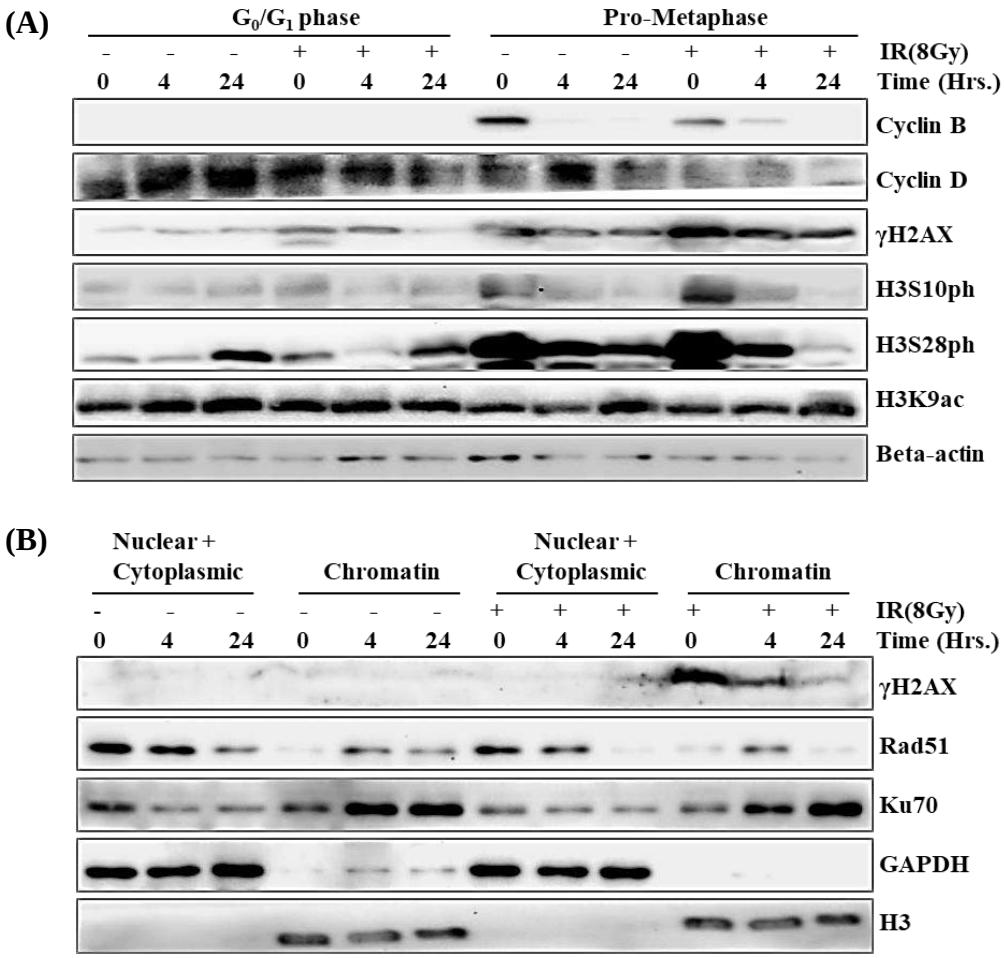

Figure 4.6 Alterations of cell cycle and DNA damage associated proteins in response to DNA damage in mitotic cells. *(A) Western blotting of Cyclin B, Cyclin D and histone PTMs from total cell lysates of cells synchronized in G_0/G_1 and mitotic phase of cell cycle at specified time points, with and without radiation. Beta-actin serves as loading control. (B) Western blotting of DNA repair associated proteins Ku70 and Rad51 in the nucleo-cytoplasmic and chromatin fraction of mitotic cells with and without radiation, at indicated time points. GAPDH and Histone H3 serve as loading controls for nucleo-cytoplasmic fraction and chromatin fraction, respectively. Hrs. – Hours, Gy- Gray.*

4.7 Alteration in levels of H3S10ph, H3S28ph and increase of H3K9ac occurs independent of DNA damaging agent, radiation dose and cell line origin.

To understand if the alterations in the levels of H3S10ph, H3S28ph and increase of H3K9ac were specific to ionizing radiation induced DNA damage, mitotic cells were treated with a variety of DNA damage inducing agents. Treatment with cisplatin (causes intra-strand cross links), Adriamycin (induces DNA double strand breaks), H_2O_2 (causes DNA double strand breaks) and ultraviolet rats (form thymidine dimers) all led to the absence of H3S10ph and H3S28ph in interphase but not mitosis. This was concomitant with increased H3K9c, similar to ionizing radiation exposure (Fig 4.7 A). Additionally, it was also observed that these alterations were independent of the dose of radiation used to induce DNA damage and the cell line under context (Fig 4.7 B-D). It was interesting to note that each DNA damaging agent used caused a different type of cell cycle arrest and different type of DNA damage lesion, yet there was a decrease in the levels of H3S10/S28ph and increase of H3K9ac. These data indicated that such epigenetic changes occurred when mitotic cells were exposed to DNA damage, irrespective of the type of lesion, cell line origin and intensity of DNA damage.

4.8 Co-localization analysis of histone PTMs γH2AX, H3S10ph, H3S28ph and H3K9ac during and after mitotic DNA damage.

It was observed in previous experiments that there was a co-occurrence of γH2AX and H3S10ph/S28ph in mitotic cells subjected to DNA damage (as assessed by western blotting).

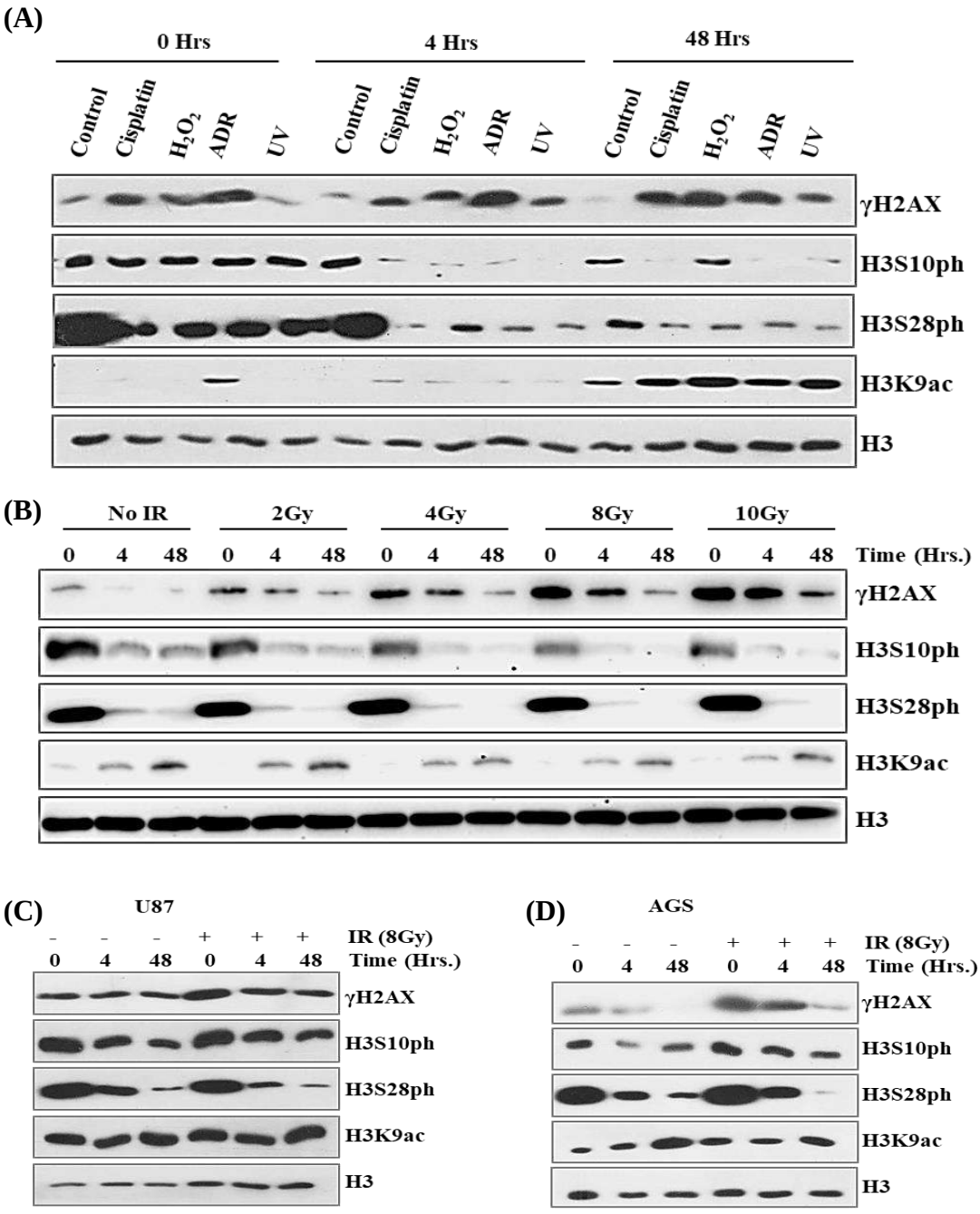

Figure 4.7 Effect of different DNA damaging agents, cell lines and radiation doses in response to mitotic DNA damage *(A) Western blotting for histone PTMs γH2AX, H3S10ph, H3S28ph and H3K9ac from acid extracted histones of mitosis synchronized MCF7 cells treated with cisplatin, H_2O_2, Adriamycin and UV rays, (B) different doses of ionizing radiation to induce DNA damage. (C) U87 glioblastoma and AGS gastric adenocarcinoma cell line. Histone H3 serves as loading control. Hrs. – Hours, Gy- Gray.*

After mitosis, as the cell cycle progressed into the G_0/G_1 phase, the levels of γH2AX were still detectable, but levels of H3S10/S28ph were not comparable to interphase cells. This was reminiscent of a previously reported inverse co-relationship that γH2AX and H3S10ph followed in the G_0/G_1 phase specific DNA damage response. Therefore, an immuno-fluorescence analysis was performed to understand if any co-relation existed between H3S10/S28ph and γH2AX localization and levels, both during and after the mitotic DDR (Fig 4.8 A-C).

In mitosis-synchronized cells, it was observed that γH2AX co-localized with both mitotic marks H3S10ph and H3S28ph. However, the pattern of distribution of these marks on the chromosomes was different, with H3S10ph showing a more pan-chromosome staining as compared to H3S28ph. Secondly, the areas of H3S28ph and γH2AX co-localization were found to be more randomly dispersed as compared to H3S10ph. The levels of H3K9ac were undetectable in mitotic cells. As previously observed, 4 hours after radiation and nocodazole release, mitotic progression and exit caused chromatin relaxation, concomitant with increased levels of H3K9ac. However, the co-localization of γH2AX and H3S10/28ph (as seen during mitosis) was not observed in this de-condensed chromatin state. Upon mitotic exit, H3S10ph was observed to form foci, H3K9ac showed a pan-nuclear staining while H3S28ph dropped to undetectable. Remarkably, neither H3S10ph nor H3K9ac co-localized with γH2AX, despite being present in the same nucleus (Fig 4.8 A-C zoomed out images). Additionally, it was also seen that cells having more intense staining of γH2AX had dramatically reduced intensity of H3S10ph.

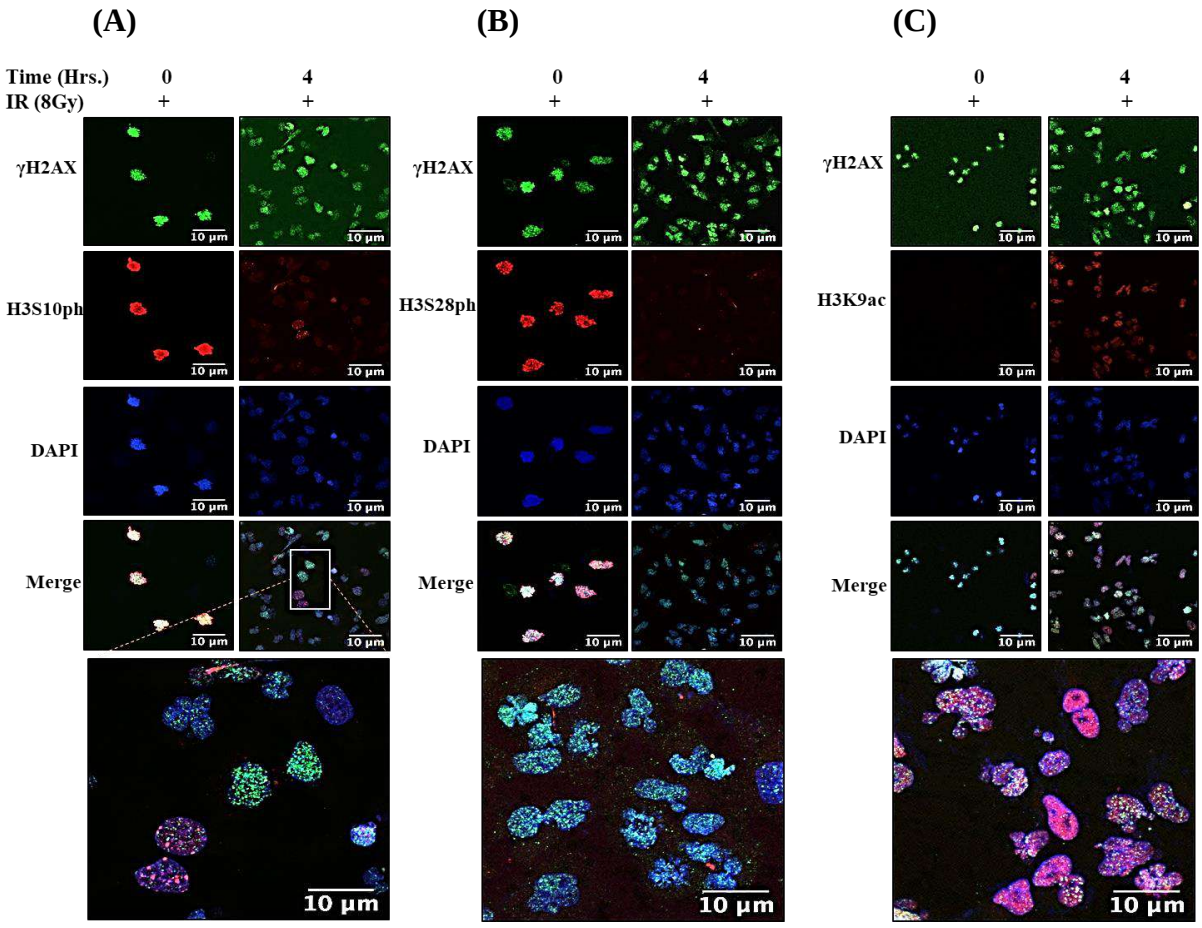

Figure 4.8 Immunofluorescence analysis of γH2AX, H3S10ph, H3S28ph and H3K9ac co-localization during and after the mitotic DNA damage response. *Immunofluorescence based co-localization analysis of (A) γH2AX and H3S10ph (B) γH2AX and H3S28ph and (C) γH2AX and H3K9ac at specified time points after radiation and nocodazole release. Time points 0 hour depicts time when cells were still in mitosis and 4 hours denotes time elapsed after nocodazole release and radiation. Inset shows zoomed in area of image. Scale bar for all images is 10µm. Yellow color denotes co-localization of indicated histone marks. DAPI acts as nuclear marker for all images. Hrs. – Hours, Gy- Gray.*

These data strongly indicated that an inverse correlation of localization existed between histone marks H3S10ph, H3S28ph and H3K9ac with γH2AX upon mitotic exit.

4.9 Mono-nucleosomal association of γH2AX, H3S10ph, H3S28ph and H3K9ac marks in during and after mitotic DNA damage

One of the reasons for the observed co-localization of histone marks H3S10/S28ph and γH2AX could be the highly condensed chromatin state during mitosis. The close proximity of the red and green fluorophores (representing H3S10/S28ph and γH2AX, respectively) in condensed mitotic chromatin could lead to an illusion of co-localizing regions (seen as yellow). Moreover, upon mitotic progression and subsequent chromatin de-condensation, the fluorophores could be spatially apart, causing complete absence of co-localization. Therefore, a mono-nucleosomal immuno-precipitation was performed to ascertain if H3S10/S28ph, H3K9ac and γH2AX actually co-localized in mitosis (Fig 4.9 D). Co-Immunoprecipitation with both anti-γH2AX and anti-H3S10ph antibody showed that γH2AX, H3S10ph, H3S28ph and H3K9ac marks co-occurred on the same nucleosome during mitosis. However, 4 hours after radiation and nocodazole release, when chromatin attained a de-condensed state after mitotic progression, the marks H3S10ph, H3S28ph and H3K9ac ceased to co-occur on nucleosomes harboring γH2AX, thereby corroborating our immunofluorescence based observation. Interestingly, in the de-condensed chromatin state after DNA damage, the marks H3S28ph and H3K9ac were present on nucleosomes containing H3S10ph. These observations indicated that H3S10/S28ph, H3K9ac and γH2AX co-occurred on the same nucleosome in damage induced mitotic cells. However, an inverse co-relationship existed between these H3S10ph and γH2AX in G_0/G_1 phase.

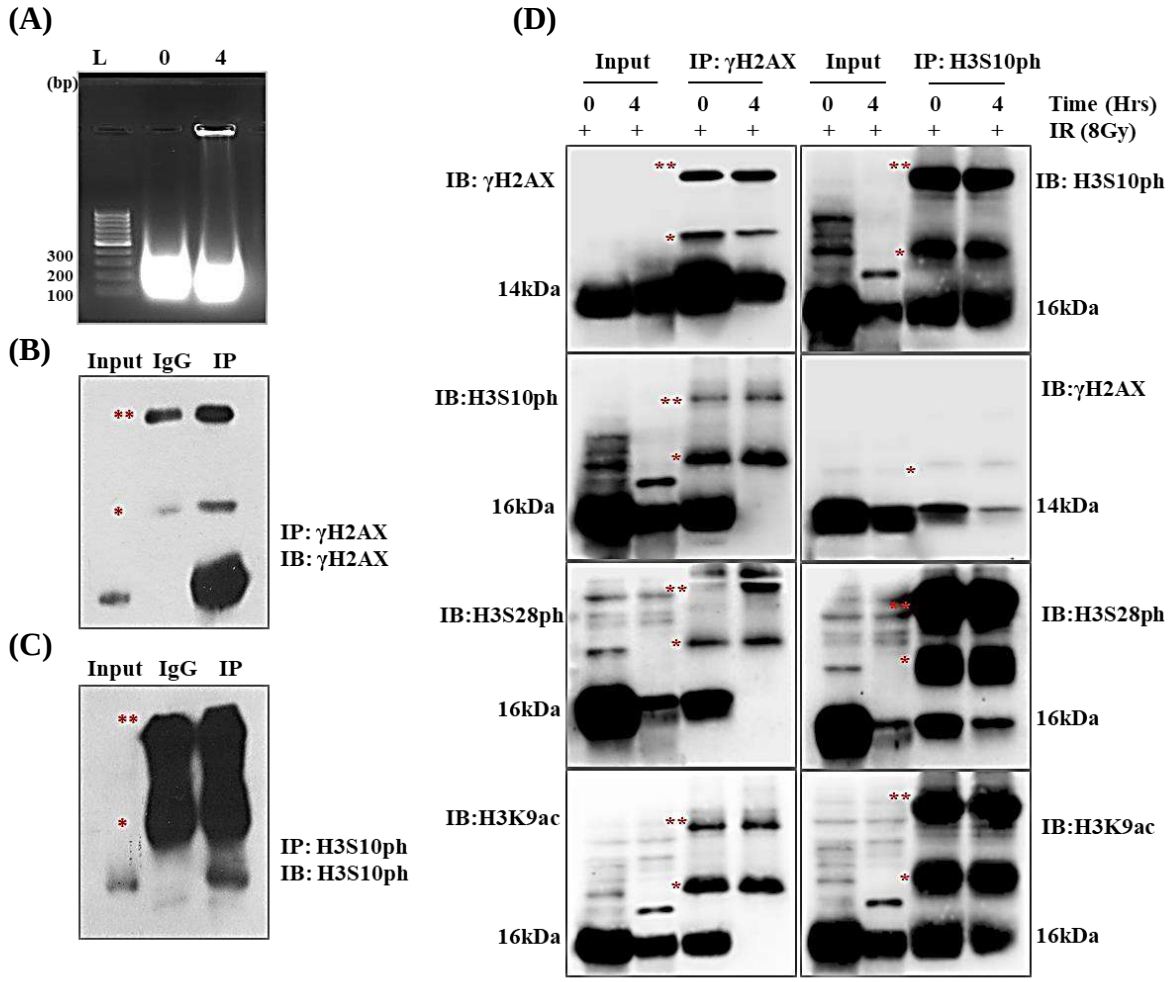

Figure 4.9 H3S10ph, H3S28ph and H3K9ac do not co-exist on nucleosomes containing γH2AX after mitotic progression. *(A) Mononucleosomes prepared from IR exposed mitosis synchronized MCF7 cells. Time points indicate time after nocodazole release. (B) Validation of anti-γH2AX and IgG anti-mouse antibody and (C) anti-H3S10ph and IgG anti-rabbit antibody by immuno-precipitation and immuno-blotting. (D) Mono-nucleosomal immuno-precipitation performed with anti-γH2AX and anti-H3S10ph antibody at the indicated time points after radiation and nocodazole release. Immuno-blotting performed with anti-γH2AX, anti-H3S10ph, anti-H3S28ph and anti-H3K9ac antibodies. Input is 10% amount of mononucleosomes used for immuno-precipitation. * and ** denote antibody heavy chain (55kDa) and light chain (25kDa), respectively. L= DNA ladder. Hrs. – Hours, Gy- Gray.*

4.10 Analysis of H3S10ph modifying enzymes during and after mitotic DNA damage

As mitotic cells progressed to G_0/G_1 phase, a cell cycle dependent reduction of H3S10ph was observed. But the interphase population so formed was not able to attain levels of H3S10ph comparable to non-radiated cells. The reduced levels of H3S10ph could be due to alterations in levels of its modifying kinases and phosphatases. Thus, western blotting was performed to assess the protein levels of H3S10ph modifying in a time dependent manner. (Fig. 4.10 A and B). The phosphatases PP1α, MKP-1 and the kinases MSK1, MSK2 and AURKB modify H3S10 in a cell cycle dependent manner. It was seen that the level of mitotic H3S10ph phosphatase PP1α rapidly increased at one-hour time point, but decreased 2 hours after radiation and nocodazole release. In the control population, a similar pattern of increase followed by decrease was observed. In both control and radiated cells, PP1α was persistent up to 48 hours after radiation, but at higher levels in the radiated population. Likewise, an increase in MKP-1 phosphatase was also observed in both control and radiated cells 2 hours after re-plating, but higher levels of MKP-1 persisted up to 24 hours after radiation. There was a reduction in the levels of kinases MSK1 and AURKB, while MSK2 levels increased after radiation.

The levels of the three kinases were reduced at 8 hours and significantly diminished at 24 hours and undetectable at 48 hours after radiation and nocodazole release.

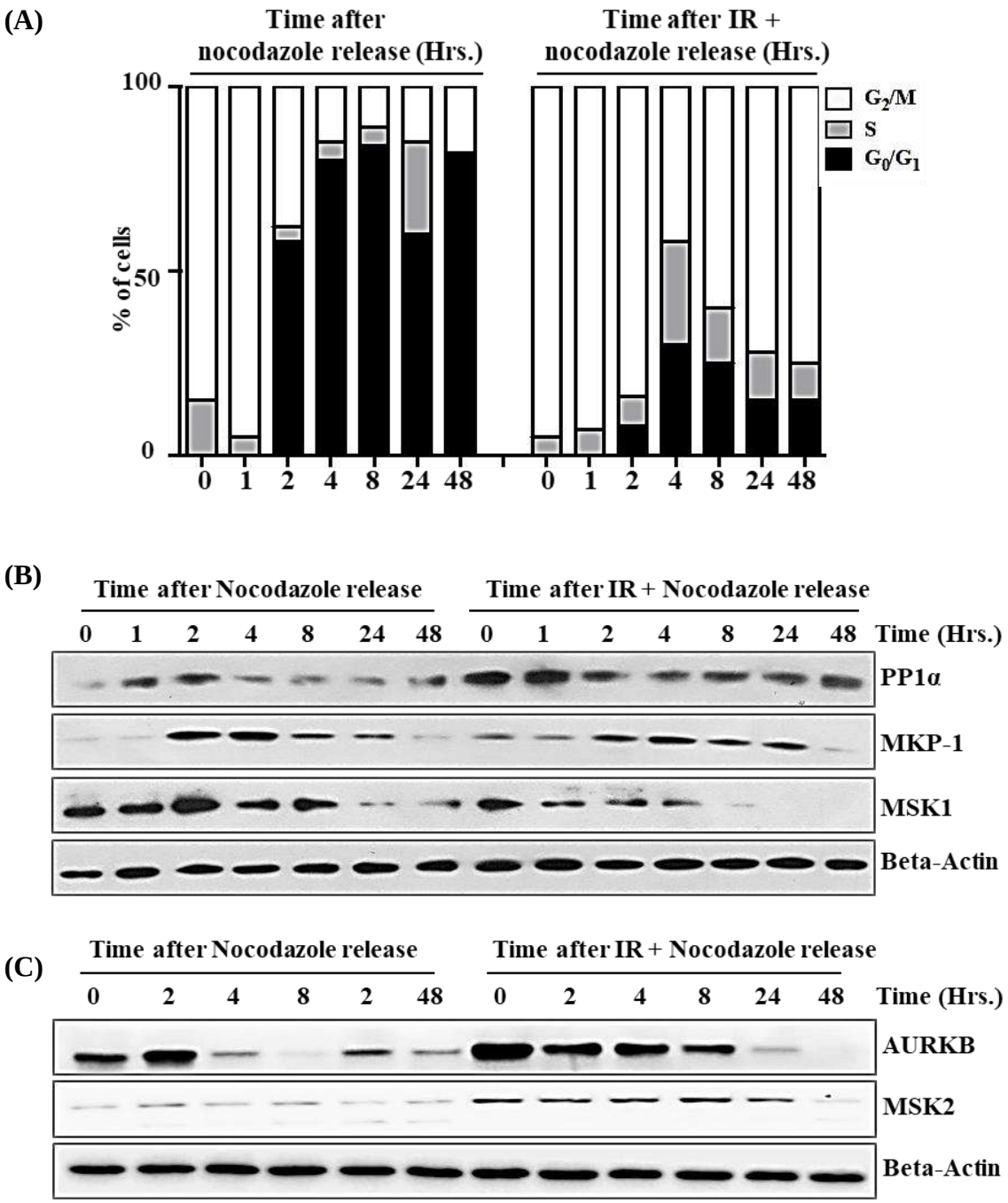

Figure 4.10 Alterations in the level of H3S10ph and H3S28ph modifying kinases and phosphatases during mitotic DNA damage. *(A) Cell cycle profile of mitosis synchronized MCF7 cells. Indicated time points denote time after nocodazole release, with and without radiation. (B) Western blotting of H3S10ph modifying enzymes PP1α, MKP-1, MSK1, MSK2 and AURKB from total cell*

lysates of mitosis synchronized MCF7 cells at the specified time points after radiation and nocodazole release. Beta actin serves as loading control.
Hrs- .Hours, Gy- Gray.

Interestingly, the levels of MSK1 kinase were not increased at time point 4 hours after radiation. MSK1 kinase and MKP-1 phosphatase are both immediate early genes that gets transcriptionally activated as cells enter the G_0/G_1 phase of the cell cycle, where they act as regulators of MAPK pathway. Therefore, as reflected by cell cycle analysis at 2-hour time point, exit of mitosis and entry into interphase (of non-radiated population) was accompanied by an escalation in the levels of MKP-1 and MSK1. In response to radiation and nocodazole release, the level of MKP-1 increased at 2 hours while MSK1 did not increase but continued to decline. The persistent levels of the mitotic H3S10 kinase AURKB up to 8 hours after radiation and nocodazole release also corroborated our previous finding of delayed mitotic exit or a prolonged mitotic stage. These data suggested that continuous presence of the phosphatases coupled with diminished levels of kinases could be responsible for non-recovery of H3S10ph and H3S28ph after radiation and mitotic progression.

4.11 Alterations in transcript levels of H3S10ph and H3S28ph modifying enzymes upon IR exposure during and after mitosis.

To understand the mechanism of regulation of H3S10ph modifying enzymes, real-time PCR was performed to analyze transcript-level alterations in response to radiation during and after mitosis (Fig. 4.11).

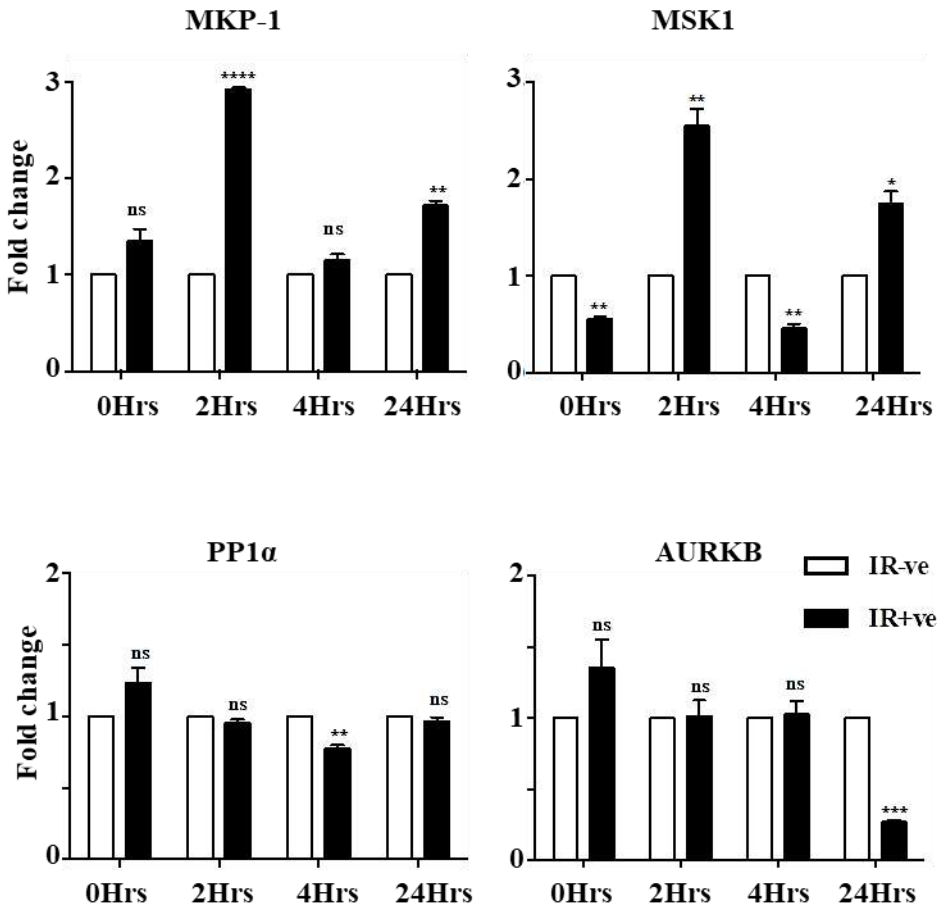

Figure 4.11 Altered transcript levels of MKP-1, PP1α, MSK1 and AURKB in response to DNA damage during mitosis. *Graphs depict real-time PCR based analysis of transcript levels of MKP-1, PP1α, MSK1 and AURKB at specific time points after radiation and nocodazole release represented as fold change. Values normalized to non-radiated control of each time point, represented as fold change 1. n.s – non- significant. Hrs. – Hours.*

It was observed that compared to the non-radiated controls, the transcript levels of MKP-1 phosphatase and MSK1 kinase showed an increased expression 2 hours after radiation, followed by decrease at 4 hours and again an increase at 24 hours after radiation. This cyclical pattern could be due to MKP1 and MSK1 being immediate early genes, whose transcription and synthesis peaks transiently in the early G_1 phase of cell cycle. However, the peak in transcript levels was not reflected by any increase in the protein level of MSK1 at 2 and 24 hours after radiation and nocodazole release, as previously observed. Additionally, the transcript levels of both PP1α and AURKB had not changed significantly, except for decreased AURKB transcript levels 24 hours after radiation. The drastic increase observed in protein levels of PP1α were seemed unlikely to be due to a non-significant increase of its transcript levels. Overall, the transcript level analysis of H3S10ph modifying enzymes could not provide detailed insight about the changes observed at the protein level after radiation, thus emphasizing the need for further experimentation.

4.12 Regulation of histone modifying enzymes MKP-1, MSK1, PP1 and AURKB in response to DNA damage during mitosis.

Transcript level alterations provided insufficient detail about the alterations in the H3S10 modifying enzymes. This indicated that these proteins could be regulated by mechanisms like translation and degradation (Fig. 4.12 A and B).

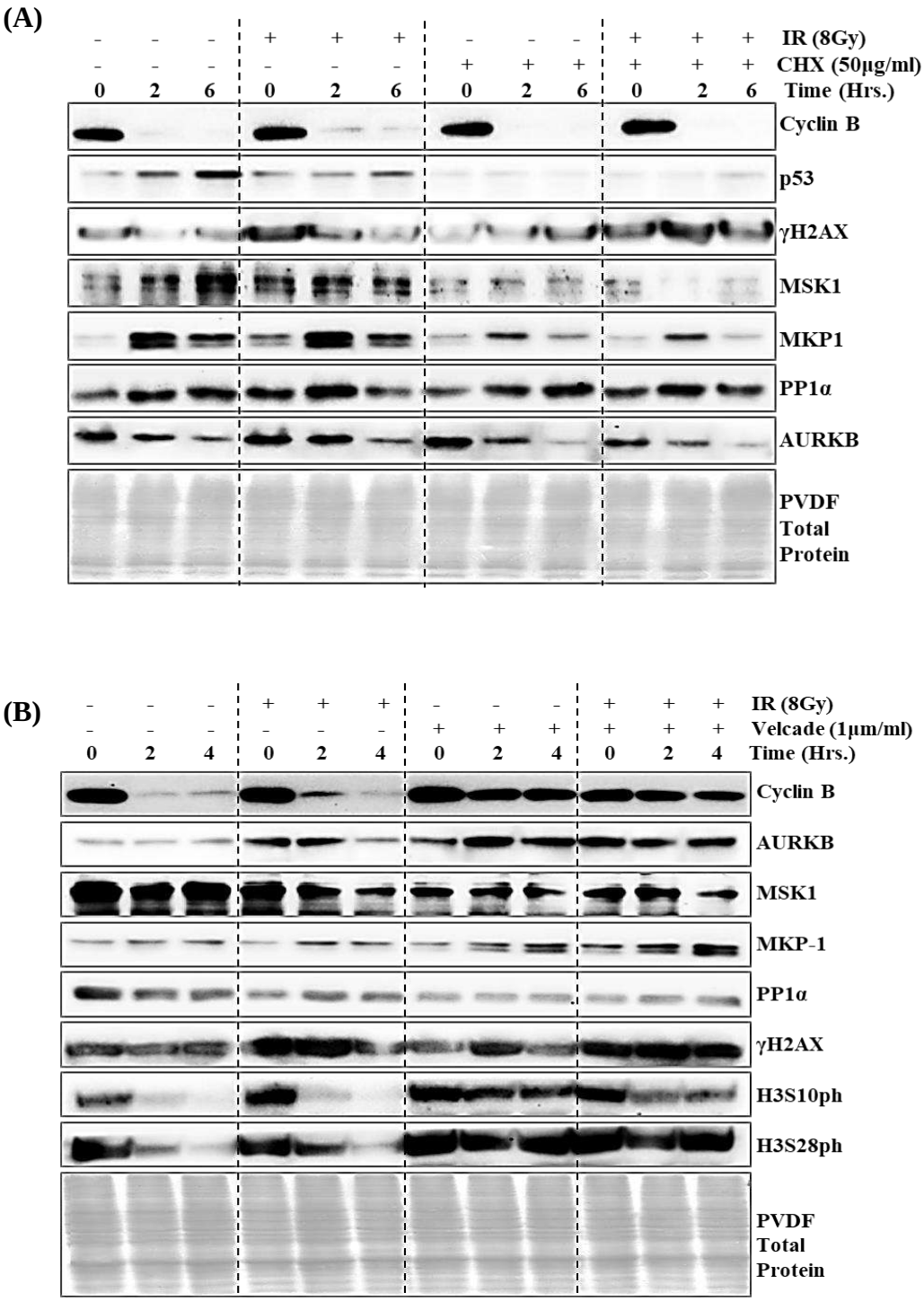

Figure 4.12 Regulation of MKP-1, PP1, MSK1 and AURKB protein levels in response to radiation during and after mitosis. *Western blotting against MKP-1 PP1, MSK1 and AURKB in total cell lysates prepared from (A) cycloheximide and (B) velcade treated mitotic cells at specified time points. PVDF membrane serves as loading control. Hrs.- Hours, Gy- Gray.*

Treatment of mitotic cells with protein translation inhibitor cycloheximide (CHX) had no effect on cell progression from mitosis to G_0/G_1 phase, irrespective of radiation exposure, release in non-radiated cells. Such an induction was not observed in the radiated population. Notably, similar effect was observed when cells were treated with CHX, irrespective of radiation exposure. This strongly pointed that MSK1 protein level was regulated by mRNA translation upon mitotic exit and G_0/G_1 phase entry. Therefore, due to translation-related defects, there was no increase in MSK1 protein levels despite transcriptional up-regulation, compared to non-radiated cells. The phosphatase MKP-1 followed a cyclical pattern of increase of protein levels at 2 hours after radiation, followed by a reduction at 4 hours. A similar pattern, but with a more pronounced reduction in MKP-1 protein level was observed upon CHX treatment. This indicated that MKP-1 phosphatase was also regulated by protein translation. The protein level of the phosphatase PP1α showed an increase even upon CHX treatment, but as observed previously, there was no transcriptional up-regulation. These data indicated that protein stabilization could play an important role in maintaining the level of PP1α, even up to 48 hours after radiation.

In contrast to the other H3S10ph modifying enzymes, the protein level of AURKB declined irrespective of radiation and CHX treatment. This suggested that the levels of AURKB were not regulated by translation of its mRNA but could be regulated by protein degradation. Thus, mitotic cells were also treated with velcade, an inhibitor of the proteasome machinery (Fig. 4.12 B).

The velcade untreated mitotic cells that progressed to the G_0/G_1 phase showed reduced protein levels of AURKB, cyclin B, H3S10/28ph. However, in the velcade treated cells (both with and without radiation), the levels of cyclin B, AURKB and H3S10/28ph were unchanged, along with a cell cycle profile that reflected no progression from mitotic phase. This indicated that AURKB protein undergoes proteasome-mediated degradation as mitotic cells progress to G_0/G_1 phase, and its levels are regulated in a cell cycle dependent manner. As observed upon CHX treatment, MKP-1 levels changed in a cyclical pattern, but an accumulation of the protein was observed upon velcade treatment. This implied that MKP-1 was regulated both by protein synthesis and degradation upon cell cycle progression, irrespective of radiation treatment. However, inhibition of protein degradation was unable to rescue the levels of MSK1 kinase, compared to untreated as well as radiated controls, therefore indicating that MSK1 level were solely regulated by its synthesis upon mitotic progression. PP1α levels remained unchanged upon both protein translation and degradation inhibition, suggesting the role of protein stabilization, possibly through some PTM (of itself or a regulatory subunit) in this context. Thus it was concluded that non-recovery of H3S10/28ph after mitotic DNA damage could be due to (a) reduced translation of the kinase MSK1, (b) synthesis of MKP-1 phosphatase or (c) stabilization of PP1α phosphatase.

4.13 Molecular modelling based affinity interaction and chromatin recruitment of histone H3 modifying enzymes in response to mitotic DNA damage.

In addition to non-recovery of H3S10ph after mitotic DNA damage, an increase in H3K9ac was also observed. Previous reports suggested that hyper-acetylated histone tails were poor substrates for H3 kinase AURKB. Additionally, *in silico* modelling studies showed that MSK1 kinase has reduced affinity towards H3 peptides acetylated at positions H3K9 and K14. Therefore, there could be two possibilities for non-recovery of H3S10ph after mitotic DNA damage and exit. Firstly, reduced affinity of the kinase/ increased affinity of the phosphatase due to nearby acetylated residues, or secondly, reduced recruitment of the kinases on chromatin. To investigate the first condition, molecular modelling was performed using Swiss model software. Modelling was carried out for protein structures available for PP1α and MKP-1 with a set of differentially modified histone H3 peptides (Fig 4.13 A). The modifications on the histone peptides were H3S10ph, H3K9ac and H3K14ac in combinations of unmodified, dual and triply modified residues. A haddock score was calculated that predicted the extent of affinity a protein had to bind to a specific combination of H3 PTMs. It was observed that both MKP-1 and PP1α had comparable affinity for unmodified H3 peptides and peptides having only H3S10ph in conjunction with either one or both (H3K9ac/H3K14ac) marks.

(A)

Histone peptide	MKP-1 Haddock score	PP1α Haddock score
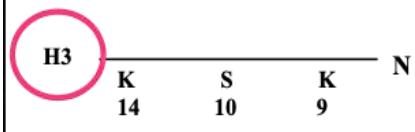	-61.8 ± -6.8	-65.3 ± -8.6
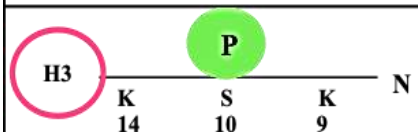	-90.3 ± -3.8	-106.3 ± -2.0
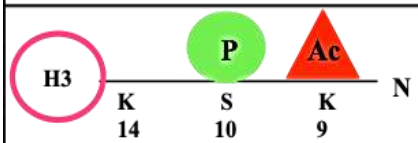	-121.6 ± -16.4	-139.1 ± -8.9
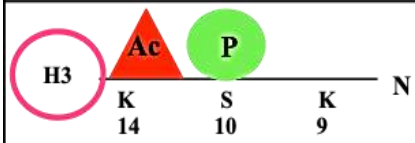	- 122.6 ± -17.7	-116.6 ± -9.3
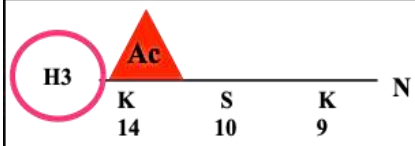	-67 ± -6.3	-99.0 ± -9.9
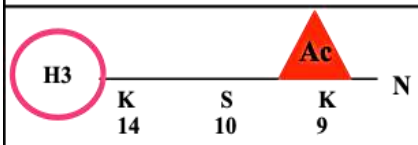	-56.8 ± -6.9	-98.7 ± -7.0
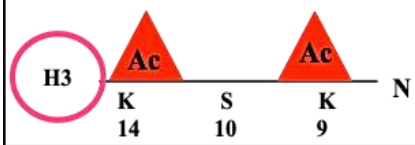	- 61.9 ± -4.4	-107.6 ± -6.9
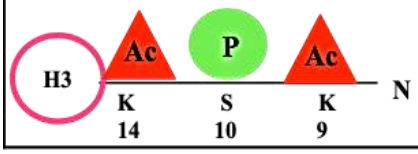	-138.6 ± -12.1	-139.1 ± -10.4

Figure 4.13 (A) Molecular modelling of phosphatases MKP-1 and PP1α using differentially modified H3 peptides. *Molecular modelling was carried out for MKP1 and PP1α with different sets of H3 peptides (having a combination of PTMs H3S10ph, H3K9ac and H3K14ac) Haddock score depicts affinity of interaction of particular protein and PTM combination.*

Interestingly, PP1α had higher affinity for H3 peptides that had only one or both H3K9ac/H3K14ac marks. This indicated that the *in silico* affinity of histone phosphatases MKP-1 and PP1α was influenced by PTM(s) present or absent on nearby residue(s), apart from the H3S10 position.

To explore the second possibility, cellular fractionation was performed to separate the nucleo-cytosolic content from the chromatin bound fraction. This was done to assess the chromatin recruitment of H3S10 modifying enzymes in response to mitotic DNA damage (Fig 4.13 B). It was observed that there was increased recruitment of phosphatase PP1α on chromatin as compared to MKP-1. This was concurrent with enhanced H3K9ac and recruitment of HATs GCN5 and PCAF on chromatin, irrespective of radiation exposure. This suggested that upon interphase entry and chromatin de-condensation, increased H3K9ac is accompanied by (a) recruitment of PP1α on chromatin, (b) reduction in levels of H3S10ph and (c) recruitment of HATs on chromatin. On the other hand, the levels of MKP-1 on chromatin were observed to be negligible, but substantially increased in the nucleo-cytoplasmic fraction. The kinases AURKB and MSK1 also showed an overall reduction in the protein levels (in nucleo-cytoplasmic fraction) as well as decreased chromatin recruitment after mitotic DNA damage. Therefore, the acetylation of nearby residue H3K9 could lead to enhanced recruitment of phosphatase PP1α on chromatin. Additionally, reduced overall levels as well as chromatin recruitment of kinases MSK1 and AURKB could be responsible for non-recovery of H3S10ph after mitotic DNA damage and interphase entry. Therefore, the *in silico* analysis was complemented by biochemical analysis of chromatin recruitment of histone modifying enzymes.

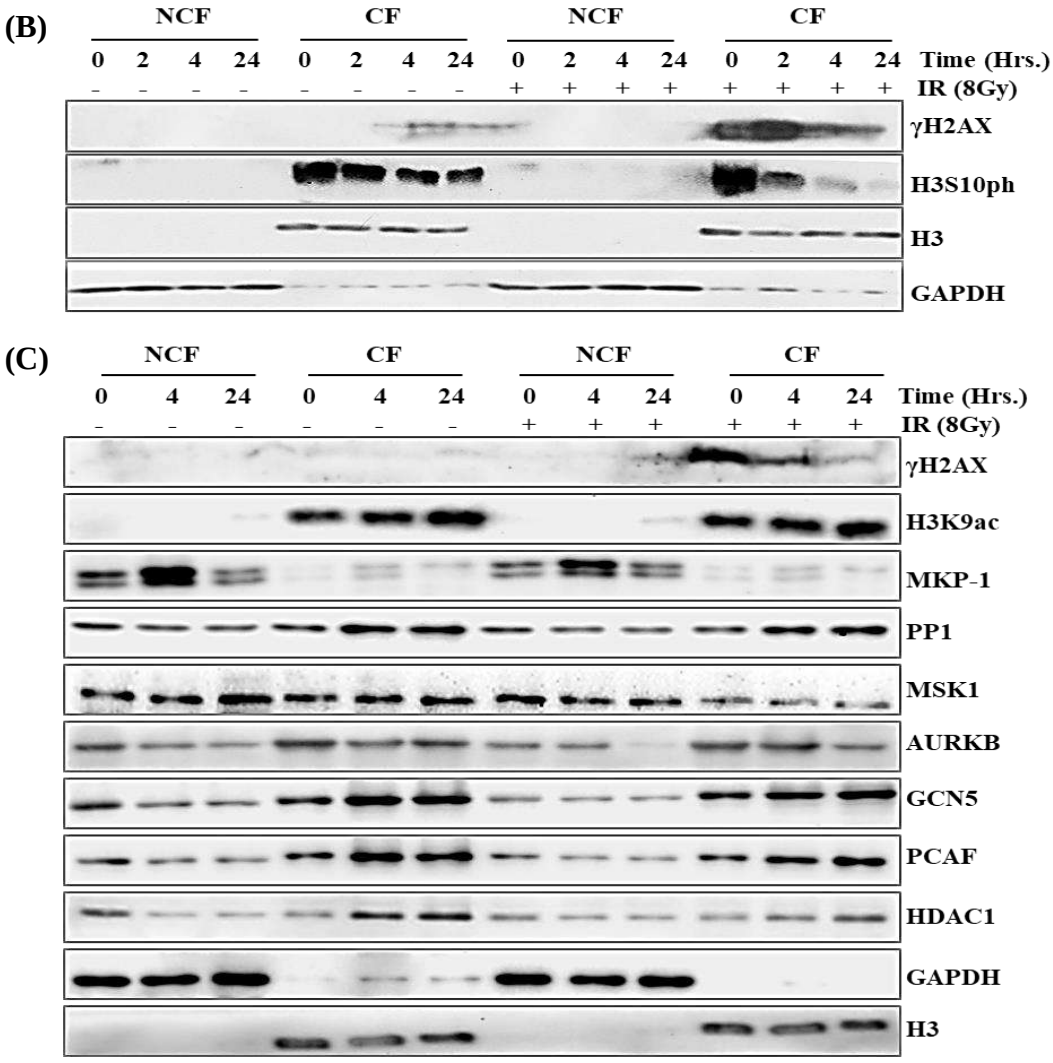

Figure 4.13 (B and C) Chromatin recruitment of histone modifying enzymes. *Mitosis synchronized MCF7 cells were fractionated into nucleo-cytoplasmic (NCF) and chromatin fractions (CF). Western blotting was performed for chromatin modifying kinases, phosphatases, HATs and histone PTMs. GAPDH and H3 serve as loading controls for NCF and CF, respectively. Hrs. - Hours and Gy- Gray.*

4.14 Mitotic cells radiated and allowed to enter interphase have reduced cell survival potential.

Analysis of the cellular and nuclear morphology of radiated cells strongly suggested that the observed G_2/M arrest was a 4N-intermediate stage between mitotic exit and interphase entry. The population generated after cell cycle progression of radiated mitotic cells was assessed for survival potential. Thus, 48 hours after mitotic cell radiation and nocodazole release, FACS was performed to sort cells (according to their ploidy) using a cell membrane permeable DNA binding dye, specific for live cells (Fig. 4.14 A). The FACS profile suggested presence of G_0/G_1, S and G_2/M phases of the cell cycle in the population. It is possible that the G_0/G_1 and S phase population could be contributed by (a) cells that had successfully completed cell division and entered interphase in a diploid state or (b) cells that had possibly resumed normal cell cycle progression after DNA repair. The G_2/M sorted cells could be the (a) 4N intermediate population generated after a prolonged mitotic arrest or (b) cells that had possibly resumed normal cell cycle progression after DNA repair or (c) mitotic cells that did not initiate cell division. Subsequent exposure of these cells to radiation led to a dramatic reduction in the cell survival potential, compared to an asynchronous population. Moreover, these cells had a marked reduction in colony formation potential even without radiation exposure that suggested an initiation of cell death (Fig. 4.14 B). It is also interesting that though the cell survival potential of these cells is reduced, there were still some surviving cells from the G_1 and S-phase populations. Survival of such cells tetraploid could have catastrophic implications such as enhanced tumorigenic potential, as reported in literature(153).

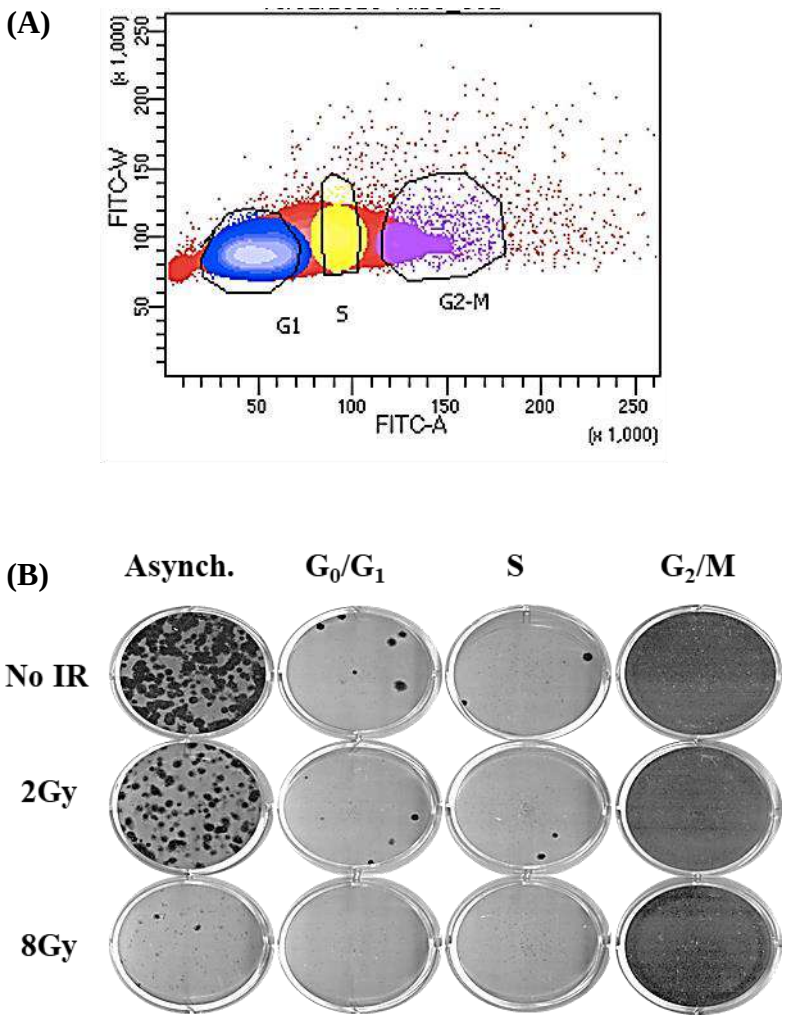

Figure 4.14 Reduced cell survival potential of cell population generated after mitotic DNA damage (A) *Graph represents the ploidy parameters used for Fluorescence Activated Cell Sorting based separation of G_0/G_1 (2N), S (2N-4N) and G_2/M (4N) cell cycle phases after mitotic DNA damage response. X-Axis represents fluorescence intensity and Y-Axis represents number of cells (X1000).* ***(B)*** *Clonogenic assay representing reduction in overall survival of the cell populations obtained after DNA damage response, compared to an asynchronous population. Gy- Gray and Asynch- Asynchronous MCF7 population.*

The above experiments carried out revealed that histone PTMs like H3S10ph, H3S28ph and H3K9ac had a variation in their pattern of alteration in response to DNA damage during both G_0/G_1 and mitotic phase of the cell cycle. Each phase of the cell cycle has different inherent radio-sensitivity and chromatin structure is one of the major determinants of this radio-sensitivity pattern. Therefore, we hypothesized that histone PTMs and modifying enzymes could also play a crucial role in clinically relevant processes like development of radio-resistance during radiotherapy. Therefore the below described sets of experiments (4.15 and onwards) were performed to investigate the epigenetic alterations that occur during the course of acquirement of radio-resistance.

4.15 Generation of MCF7 radio-resistant cell line

An *in vitro* model system was generated to understand how epigenetic modifications influence the process of radio-resistance. Since breast cancer is one of the most predominant cancers worldwide and in India, MCF7 breast cancer cell line was used for this study(153–156). Therefore, a radio-resistant MCF7 breast cancer cell line was developed to understand epigenetic alterations associated with acquired radio-resistance (Fig. 4.15 A). MCF7 cells (denoted as Parental/P) were exposed to radiation in fractions (2Gy/10 fractions) to generate a 20Gy radioresistant cell line (denoted as 20GyRR). Clonogenic assay showed increased cell survival potential at higher radiation dose, thereby confirming the radio-resistant nature of the cells. Additionally, cell proliferation assay also revealed these cells to have lower proliferation rate compared to the MCF7 parental cells (Fig. 4.15 B-C).

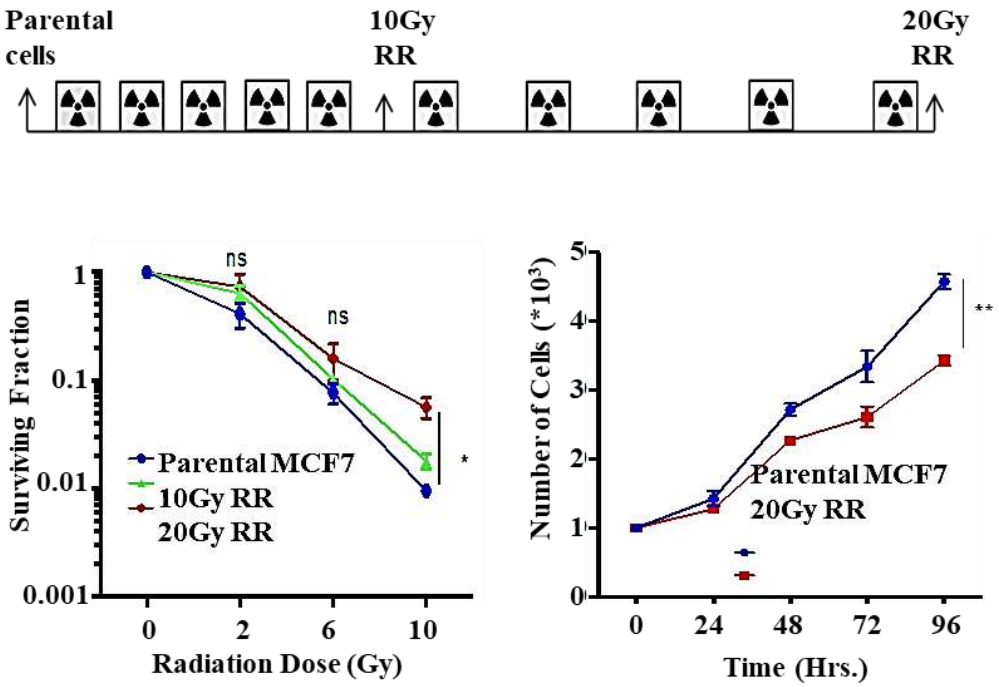

Figure 4.15 Generation of radioresistant breast cancer cell line. (A) *Schematic representation of generation of radio-resistant 20GyRR by fractionated irradiation. (B) Graph depicting surviving fraction of parental and radio-resistant cell line for a range of radiation doses. X-axis represents doses of radiation and Y-axis represents surviving fraction. (C) Graph depicting proliferation rate of parental and radioresistant cell line. X-axis represents duration of the experiment (96 hours) and Y-axis represents number of cells (x1000). P= Parental MCF7, RR= radioresistant MCF7 20GyRR. Unpaired student's t-test applied for statistical analysis for n =3 experiments.* $^{*}p < 0.05$, $^{**}p < 0.01$ *Gy- Gray, Hrs.- Hours, ns- non significant.*

4.16 Physiological alterations in acquired radio-resistant cell line

In addition to increased clonogenic potential and reduced cellular proliferation, several physiological parameters were altered upon acquirement of radio-resistance (Fig. 4.16 A-D). Firstly, the radio-resistant 20GyRR was observed to have a reduced percentage of AnnexinV-PI dual positive cells (Fig. 4.16 A). The

percentage of these dual positive cells indicated cells in late apoptosis, therefore radio-resistant cells showed reduced percentage of apoptotic cells that could contribute to enhanced cell survival at high radiation doses. Another factor that could regulate increased cell survival at high radiation doses could be the increased expression of DNA repair elated genes such as P53, BRCA1, ATR and ATM (Fig. 4.16 C). Additionally, radio-resistant 20GyRR cells also exhibited enhanced cell migration potential (Fig. 4.16 B).

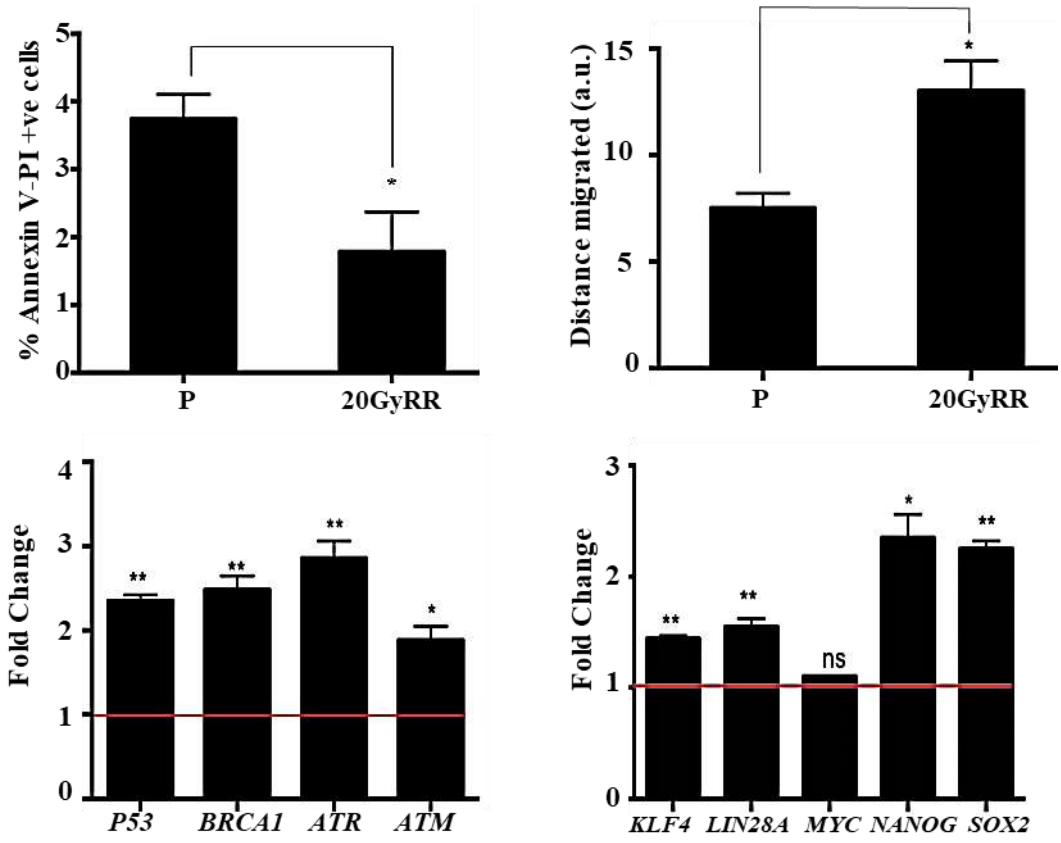

Figure 4.16 Physiological alterations in radio-resistant breast cancer cell line. ***(A)*** *Graph depicting percentage of parental and radioresistant cells having dual positive AnnexinV and Propidium Iodide cell population.* ***(B)*** *Graphical representation of cell migration potential of parental and radio-resistant MCF7 cells. Distance migrated calculated after 20 hours.* ***(C)*** *Expression of DNA repair related genes and (D) stemness related genes as analyzed by real time PCR in*

parental and radioresistant cell line. Levels plotted as fold change normalized to parental cells. Fold change 1 depicts levels of parental MCF7. P= Parental MCF7, RR= radioresistant MCF7 20GyRR. Unpaired student's t-test applied for statistical analysis for n =3 experiments. $^{*}p < 0.05$, $^{**}p < 0.01$, *ns- non significant and a.u.- arbitrary units.*

This was accompanied by an increased expression of stemness-related genes such as *Nanog,* and *Sox2* (Fig. 4.16 D). Increase of both stemness related genes and cell migration could be attributed to prolonged radiation exposure(157).

4.17 Morphological and biochemical alterations in acquired radio-resistant cell line

Apart from distinct physiological alterations that distinguish radio-resistant 20GyRR cells from parental MCF7 cells, there were distinct morphological features also observed in these cells. Morphological changes acquired during radiation treatment were analyzed by transmission electron microscopy. Analysis revealed that radio-resistant 20GyRR cells had aberrations in nuclear morphology, as compared to the smooth and well-rounded shape of parental MCF7 cells (Fig. 4.17 A, changes marked by black arrows). Additionally, it was also observed that the radio-resistant cells showed an increase in the size of mitochondria (Fig. 4.17A marked by black arrows and zoomed out images). This in concordance with a previous report that suggests mitochondrial function and structure alterations occur as a result of prolonged radiation exposure(158–160). Apart from having a different nuclear morphology, the biochemical alterations that occur during radio-resistance were assessed by a non-invasive Raman spectroscopy technique. Analysis showed biochemical alterations in the 20GyRR at wavelengths 1650-

1665 cm^{-1} (amide I), 1235-1265 cm^{-1} (amide III), 1450 cm^{-1} (δCH2 deformation) and increased peaks at 751 cm^{-1} and 1557 cm^{-1} (amino acid Tryptophan) (Fig. 4.17 B).

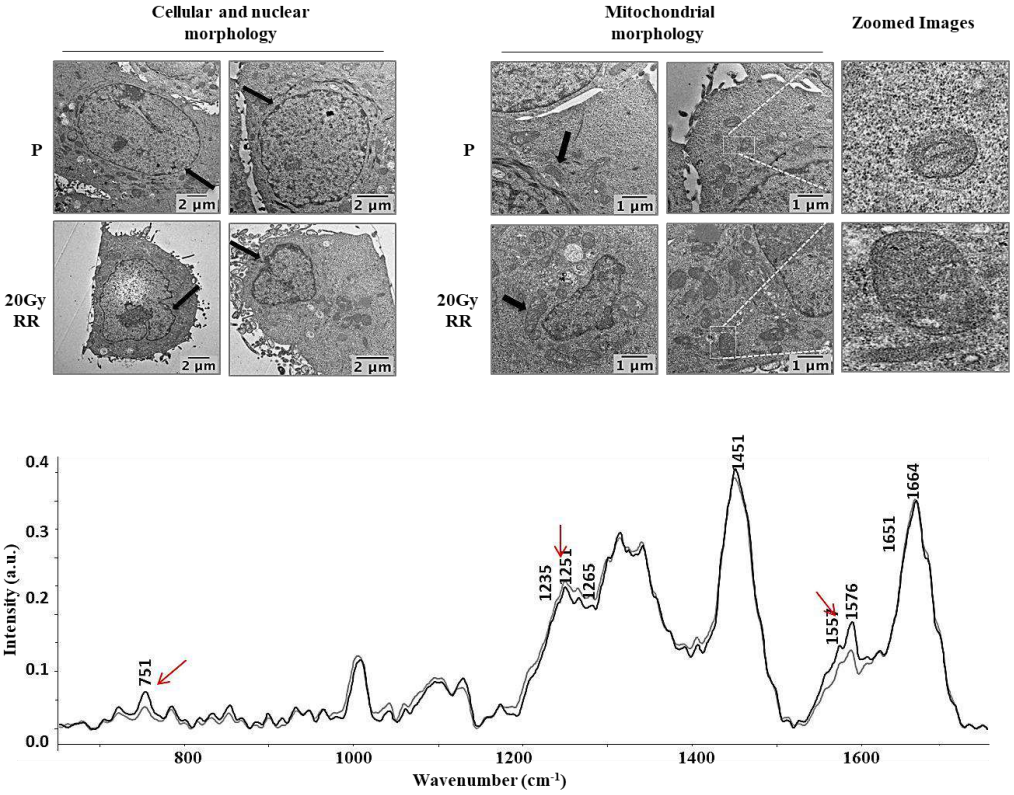

Figure 4.17 Morphological and biochemical alterations of radio-resistant breast cancer cells. ***(A)*** *Electron microscopy based analysis of morphological alterations in 20GyRR cells. Black arrows in images point towards alterations in nuclear and mitochondrial morphology.* ***(B)*** *Graph depicts spectral features of parental (grey) and 20GyRR MCF7 (black) cells analyzed by Raman spectroscopy Red arrows highlight wavelengths that show changed intensity. P= Parental MCF7, RR= radioresistant MCF7 20GyRR and a.u. is arbitrary units. Magnification- 1000X. Scale bar is 5µm and 1µm for nuclear morphology and mitochondrial morphology, respectively.*

These data suggest that acquired radio-resistant cells had specific morphological characteristics and also peculiar biochemical features that might be useful for non-invasive spectroscopic and microscopic identification of radioresistant cells.

4.18 Chromatin architecture alterations of radio-resistant breast cancer cells

Since the radio-resistant 20GyRR cells showed abnormal nuclear morphology, it became imperative to investigate if the global chromatin architecture of these cells was also modified. Therefore, MNase digestion assay was performed for radio-resistant 20GyRR cells and parental MCF7 cells (Fig. 4.18 B and C). MNase digestion revealed that overall there was no difference between the rate of mononucleosome formation after MNase digestion of radio-resistant 20GyRR cells and parental MCF7 cells. Additionally, there was also no change of the average mononucleosome length. Interestingly, the rate of formation of polynucleosomes was faster in parental MCF7 compared to 20GyRR (Fig. 4.18 B and C-indicated by red arrows). However, high molecular weight and MNase resistant undigested genomic DNA was observed in radioresistant cells, but not in parental MCF7. This indicated towards presence of compact chromatin in radio-resistant cells and which was not due to any cell cycle phase associated differences (Fig. 4.18 A). In corroboration with MNase digestion analysis, 20GyRR cells also showed an increase in global protein level and nuclear intensity of Heterochromatin Protein 1 α (HP1α), along with increased levels of linker histone H1 (Fig. 4.18 D-F). These data point towards increase in heterochromatinization upon acquirement of radio-resistance.

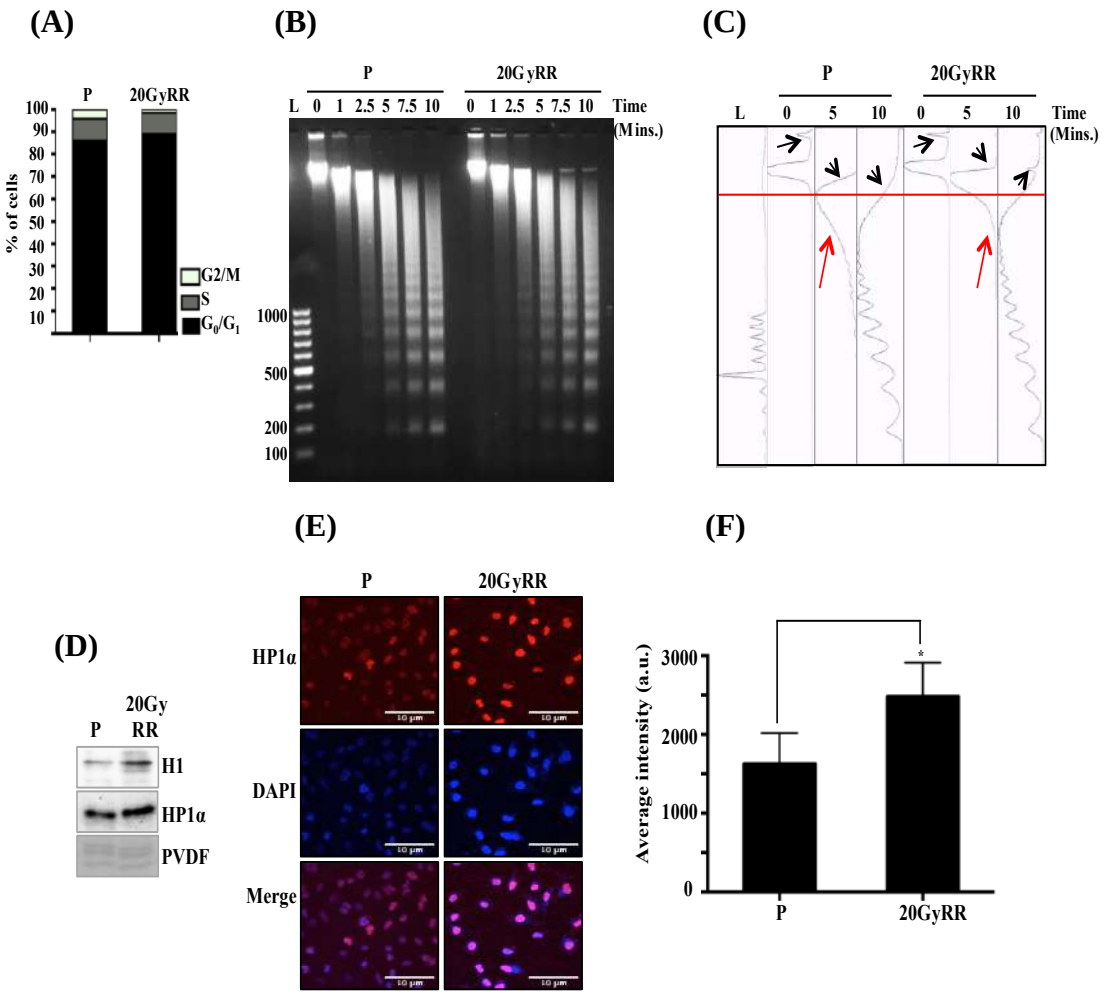

Figure 4.18 Alterations of chromatin architecture that occur upon radio-resistance acquirement. (A) *Cell cycle profile of parental and radio-resistant MCF7 cells.* ***(B)*** *MNase digestion represented on TAE-Agarose gel and (C) as densitometric representation. Time indicates incubation time of nuclei with MNase. Black arrows represent alterations in chromatin architecture. The red horizontal line and arrows mark genomic DNA conversion to poly-nucleosomes.* ***(D)*** *Protein levels of histone H1 and HP1α in P and 20GyRR cell lysates. PVDF membrane is the equal loading control. (E) Representative z-stack images for distribution of HP1α. DAPI serves as nuclear marker. (F) Graph depicting nuclear intensity of HP1α from 50 nuclei. Scale bar- 10μm. P= Parental MCF7, RR= radioresistant MCF7 20GyRR. Unpaired student's t-test applied for statistical analysis for n =3 experiments.* $^{*}p < 0.05$, $^{**}p < 0.01$, *ns- non significant and a.u.- arbitrary units and mins. – Minutes.*

4.19 Histone PTM alterations during acquirement of radio-resistance in breast cancer cells

Since radio-resistance acquirement was concomitant with increased heterochromatinization, the histone PTM milieu of radioresistant cells was assessed in both mitosis and G_0/G_1 phase (Fig. 4.19 A). Different cell cycle phases have a differential response to radiation, with mitotic cells being the most radio-sensitive and G_0/G_1 phase cells being relatively radio-resistant. Therefore, histone PTM analysis was carried out in both these populations for radio-resistant 20GyRR cells and parental MCF7 cells (Fig. 4.19 B). Interestingly, during both G_0/G_1 phase and mitosis, the transcription activation associated histone marks H3K9ac, H3K27ac and H3S10pK14ac were reduced (Fig. 4.19 B). However, only mitotic cells showed a decrease of H3K56ac upon radio-resistance acquirement. Moreover, H4K20me3 mark that is associated with transcriptional repression was increased in G_0/G_1 phase cells but decreased in mitotic radio-resistant cells. Notable changes were observed in both H3S10ph and H3S28ph, which were decreased in the G_0/G_1 phase radio-resistant cells. H3S10ph is regulated by MKP-1 phosphatase and MSK1 kinase, which are both negative and positive regulators of the MAPK pathway. Analysis of the MAPK pathway revealed increased levels of MKP-1, concomitant with decreased activated phosphorylated forms of MAPK mediator proteins p38 and ERK1//2 (Fig. 4.19 C). However, levels of kinases MSK1 and MSK2 were unchanged in radio-resistant 20GyRR cells. These data strongly suggest that global epigenetic alterations like reduced histone phosphorylation and acetylation take place during the acquirement of radio-resistance, which could contribute to enhanced heterochromatinization during

radio-resistance acquirement. Additionally, changes in the global as well as local histone PTM milieu could also affect the overall transcriptome of radio-resistant cells.

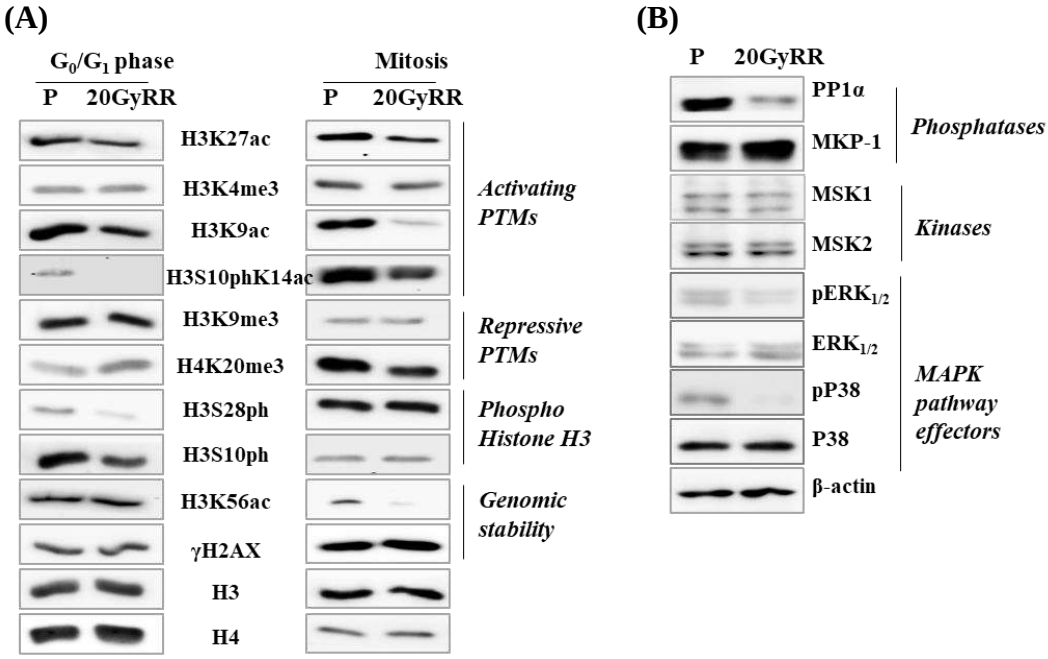

4.19 Alterations in levels of histone PTMs and MAPK pathway in radio-resistant cells. (A) *Levels of site-specific histone PTMs in G_0/G_1 and mitotic P and 20GyRR cells. Histone H3 and H4 serve as loading controls.* ***(C)*** *Levels of MAPK pathway proteins in P and 20GyRR. β-actin acts as equal loading control. P= Parental MCF7, RR= radioresistant MCF7 20GyRR.*

4.20 Radioresistant cells have increased HDAC activity and decreased HAT activity

Our previous observation of increased heterochromatinization was corroborated by decrease in the levels of site specific histone acetyl marks. Hence, the activity of HATs and HDACs was monitored in 20GyRR radio-resistant cells. Interestingly, it was observe that upon acquirement of radio-resistance, there was an increase in

HDAC activity along with a decrease in HAT activity as MCF7 breast cancer cells acquired radio-resistance (Fig. 4.20 A and B). Hence, predominant epigenetic alterations, at the levels of chromatin modifying enzyme activity could be the cause behind altered histone acetylation status and could lead to subsequent heterochromatinization during radio-resistance acquirement.

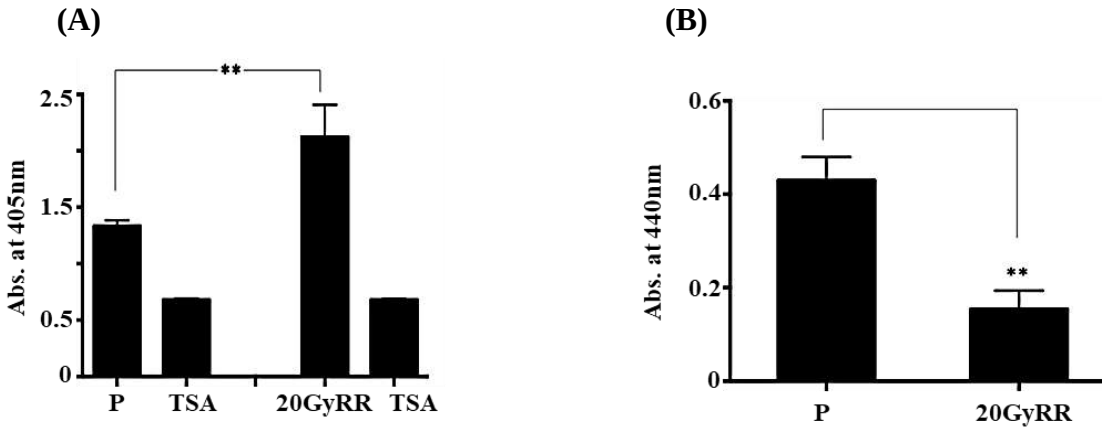

4.20 Altered HDAC and HAT activities upon radio-resistance acquirement. *Depiction of (A) HDAC and (B) HAT activities of P and 20GyRR, measured as a colorimetric readout at 405nm and 440nm, respectively. HDAC inhibitor Trichostatin A (TSA) depicts negative control. P= Parental MCF7, RR= radioresistant MCF7 20GyRR. Unpaired student's t-test applied for statistical analysis for n =3 experiments.* $^{*}p < 0.05$, $^{**}p < 0.01$, *ns- non significant and Abs. – absorbance.*

4.21 Generation of MDA-MB 231 radio-resistant cell line

Breast cancer is classified according to expression of estrogen, progesterone and Herceptin receptors, with MCF7 cell line being positive for estrogen and progesterone receptor, but not Herceptin receptor. Therefore, to extend our findings in other breast cancer subtypes, a radioresistant version of MDA-MB231 (Triple Negative Breast Cancer cell line) was generated by similar regime as used for MCF7 cells (Fig.

4.15A). Clonogenic assay revealed increased cell survival of radio-resistant cells, and confirmed their radio-resistant nature (Fig. 4.21 A and B).

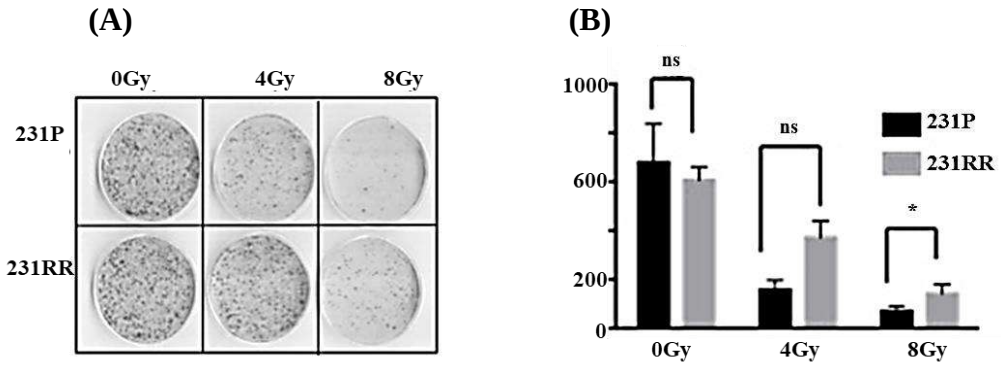

Figure 4.21 Generation of radio-resistant MDA-MB231 cell line. *(A and B) Representation of colonies after irradiation of parental and radio-resistant MDA-MB231 cells. 231P= Parental MDA-MB231 and 231RR= radioresistant cells. Statistical analysis is done by unpaired t-test.* $^{*}p<0.05$, $^{**}p<0.01$, *n.s- non significant.*

4.22 Epigenetic characteristics of radio-resistant MDA-MB 231 cells

After generation of radioresistant MDA-MB231 cells (denoted as 231RR) from parental MDA-MB231 cells (231P) MNase assay was performed to assess chromatin architecture alteration upon radio-resistance acquirement (Fig. 4.22 A and B). MNase digestion pattern revealed presence of a more open chromatin conformation in radio-resistant MDA-MB 231 cells. This was observed as increased intensity of mononucleosomes upon digestion, as well as faster conversion of genomic DNA to polynucleosomes. Interestingly, as observed in radio-resistant MCF7 cells, there was the presence of high molecular weight undigested chromatin. Further analysis of histone PTMs showed a global decrease of transcription activation marks H3K9ac, H3K27ac and H3S10phK14ac in radioresistant MDA-MB231cells, similar to

previous observations in 20GyRR MCF7 cells. These data were corroborated by detection of high HDAC activity in MDA-MB231RR cells, but with no significant change in overall HAT activity. Therefore, these results suggest that global epigenetic changes of histone hypo-acetylation and heterochromatinization, accompanied by increased HDAC activity are epigenetic alterations associated with acquirement of radio-resistance. These data also suggest that these epigenetic alterations are not limited to a specific breast cancer subtype.

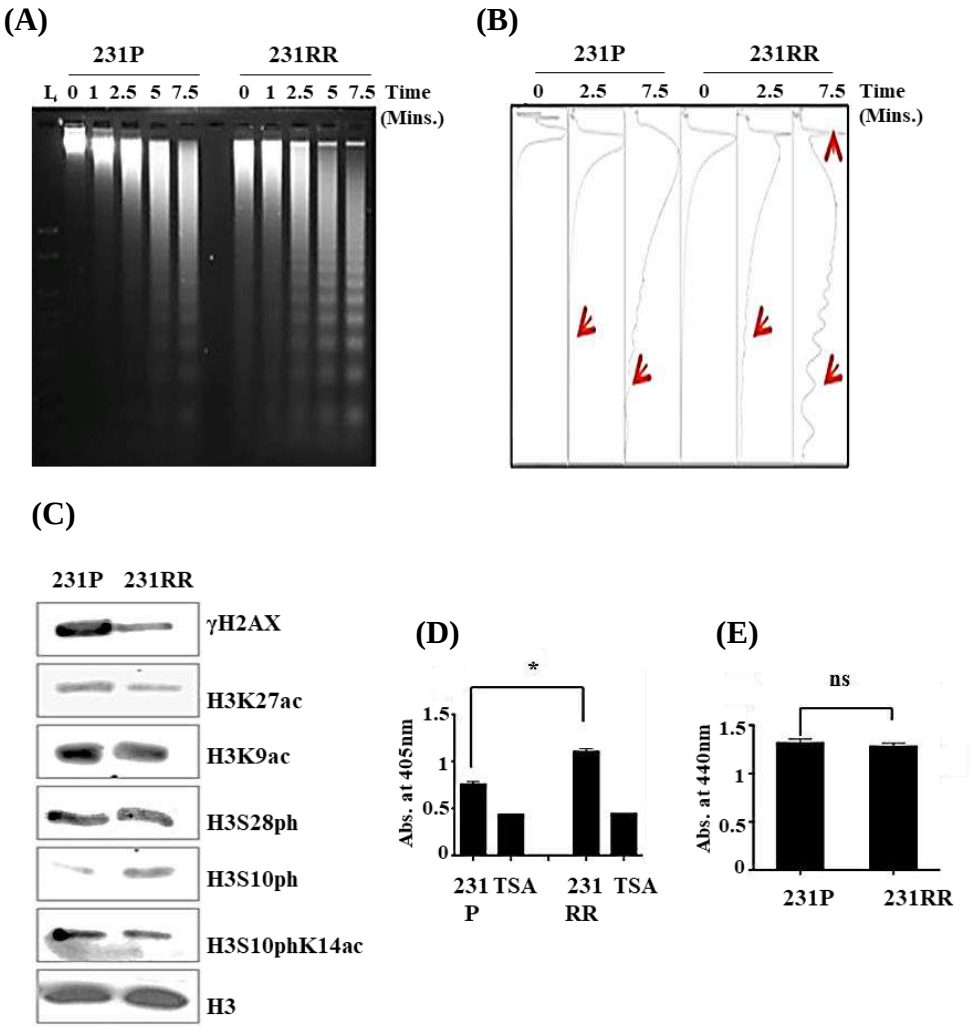

Figure 4.22 Alterations of chromatin architecture that occur upon radio-resistance acquirement. (A) *MNase digestion represented on TAE-Agarose gel and (B) densitometric representation. Time indicates incubation time of nuclei with MNase. The red arrows mark genomic DNA being converted to poly-nucleosomal entities. (C) Levels of histone PTMs in 231P and 231RR. (D) Graph depicting HDAC and (E) HAT activities of 231P and 231RR, measured as a colorimetric readout at 405nm and 440nm, respectively. HDAC inhibitor TSA acts as a negative control. 231P= Parental MDA-MB231 and 231RR= radioresistant cells. Statistical analysis is done by unpaired t-test.* $^{*}p<0.05$, $^{**}p<0.01$, *n.s- non significant, Abs. – absorbance.*

4.23 Altered HDAC activity in tumors signifies epigenetic heterogeneity within a population.

Altered epigenetic features, comprising of increased HDAC activity marked the acquirement of radio-resistance in breast cancer cells. HDAC inhibitors like Valproic Acid (VPA) are already under use in clinics as FDA-approved anti-epilepsy drugs. HDAC inhibitors are also being explored for their role as potential radio-sensitizers. However, for maximal effectiveness of epi-drug therapy, a prior assessment of the epigenetic background of the subject should be carried out. Therefore, HDAC activity was assessed across 8 human tumor types, based on usage of radiotherapy for their treatment. Tumor tissues were collected, sectioned, stained by Hematoxylin and Eosin and further validated by a pathologist for tumor content. The histopathological analysis of the samples used in the study is summarized in Table 4.1. After performing assessment of HDAC activity from as little as 1mg of biopsy tissue, it was observed that there was inter-tumoral variation in HDAC activity, even across patients with similar tumor types. This heterogeneity was observed irrespective of tissue of origin (Fig. 4.23 A). Lysates containing HDAC inhibitor TSA served as negative control.

Sample	Origin	Histopathological Analysis
BR1	Breast	IPLC[#] grade III
BR2	Breast	IBC[##] grade III
BR3	Breast	IBC[##] grade III
BR4	Breast	IPLC[#] grade III
BR5	Breast	IBC[##] grade III
BR6	Breast	IBC[##] grade III
BC1	Brain	GWG[$] Grade IV
BC2	Brain	GWG[$] Grade IV
BC3	Brain	GWG[$] Grade IV
BC4	Brain	GWG[$] Grade IV
BC5	Brain	GWG[$] Grade IV
BM1	Buccal Mucosa	MDSC[&]
BM2	Buccal Mucosa	MDKSC[%]
BM3	Buccal Mucosa	MDSC[&]
BM4	Buccal Mucosa	MDKSC[%]
BM5	Buccal Mucosa	MDSC[&]
BM6	Buccal Mucosa	MDSC[&]
TN1	Tongue	PDSC[@]
TN2	Tongue	MDSC[&]
TN3	Tongue	MDSC[&]
TN4	Tongue	MDSC[&]
TN5	Tongue	MDSC[&]

Sample	Origin	Histopathological Analysis
K1	Kidney	RCC[&]
K2	Kidney	RCC[&]
K3	Kidney	RCC[&]
K4	Kidney	RCC[&]
GB1	Gall Bladder	CCN[$$]
GB2	Gall Bladder	CCN[$$]
GB3	Gall Bladder	CCN[$$]
GB4	Gall Bladder	CCN[$$]
L1	Liver	SCC[@@]
L2	Liver	MDA[&&]
L3	Liver	MDA[&&]
L4	Liver	PDA[%%]
R1	Rectum	MDA[&&]
R2	Rectum	SCRA[@#]
R3	Rectum	MDA[&&]
R4	Rectum	MDA[&&]

[#]IPLC – Invasive Pleomorphic Lobular Carcinoma
[##]IBC – Invasive Breast Carcinoma
[$]GWG- Glioblastoma WHO Grade
[&]MDSC – Moderately Differentiated Squamous Carcinoma
[%]MDKSC – Moderately Differentiated Keratinizing Squamous Carcinoma
[@]PDSC – Poorly Differentiated Squamous Carcinoma
[&] RCC – Renal Cell Carcinoma
[$$]CCN – Cholangiocarcinoma
[@@]SCC - Squamous Cell Carcinoma
[&&] MDA – Moderately Differentiated Adenocarcinoma
[%%]PDA – Poorly Differentiated Adenocarcinoma
[@#]SCRA – Signet Ring Cell Adenocarcinoma

Table 4.1 Compilation of histopathological analysis of human tumor samples used in the study.

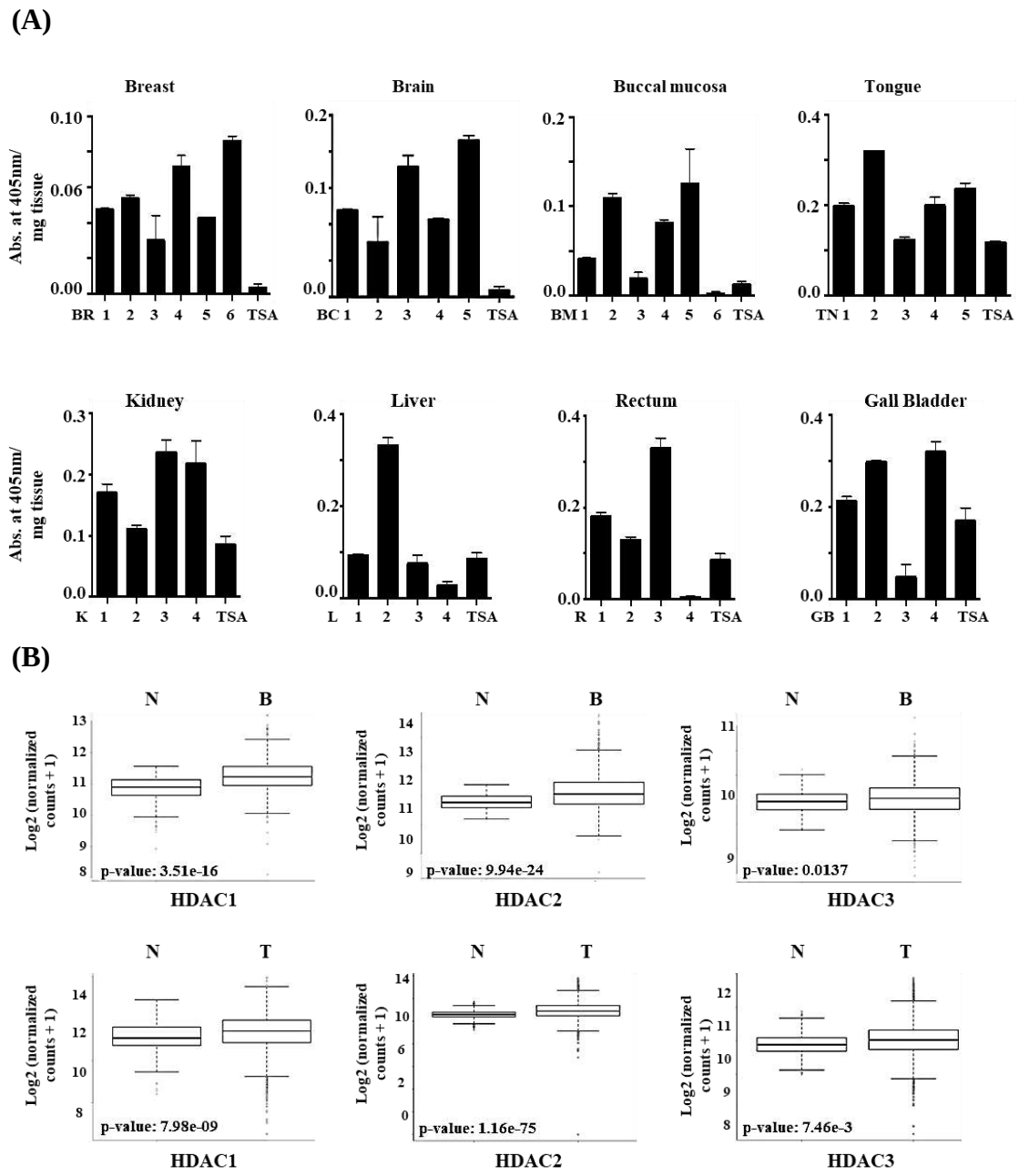

Figure 4.23 Inter-tumoral variation in levels of HDAC activity and expression emphasizes the need for patient stratification.

(A) HDAC activity of different human tumor type samples. HDAC inhibitor TSA acts as negative control. X-axis indicates sample number. ***(B)*** *Normal (N) versus breast cancer (B) and pan-cancer (T) expression levels of HDAC1-3 analyzed from RNA-seq data available in TCGA.*

Therefore, a prior assessment of tumor HDAC activity revealed presence of inter-tumoral epigenetic heterogeneity within a population. Additionally, apart from assessment of HDAC activity, an analysis of TCGA datasets revealed a variation of HDAC 1 and 2 expression for breast cancer. Likewise, a compiled analysis of TCGA datasets for multiple cancer types showed up regulated expression of HDAC 1-3 (Fig. 4.23 B). Therefore, prior assessment of the epigenetic background of the patient before treatment with epigenome modifying drugs could be helpful in selecting the correct population that would benefit from the treatment. Hence, stratification of patients based on their tumor HDAC activity status could help in better efficacy of HDAC inhibitors as radio sensitizers in poor-responders.

4.24 Histone de-acetylase inhibitor VPA causes retention of γH2AX and radio-sensitization of acquired and intrinsic radio-resistant cells.

The 20GyRR radioresistant MCF7 cells had an increased HDAC activity and variability in terms of HDAC activity and expression exists in several tumor types. Therefore, HDAC inhibitor VPA was assessed for its radio-sensitizing potential for both acquired radio-resistant MCF7 20GyRR and intrinsically radio-resistant U87 cells. Pre-treatment with VPA was done 2 hours before radiation that showed increased acetylation of histones (Fig. 4.23 A and C). A pre-treatment regime was used as previous reports suggest that HDAC inhibitor induced enhanced histone acetylation and chromatin de-condensation enhance the efficacy of radiation. Increased acetylation of H3K9/K56 position indicated potency of VPA in both 20GyRR and U87 (Fig. 4.24 A and C). Additionally, persistent levels of γH2AX upto 24 hours after radiation indicated delayed DNA repair kinetics (Fig. 4.24 A and D).

Also, the combinatorial treatment of VPA and IR caused significant enhanced cell death of MCF7-RR (Fig. 4.24 B). Interestingly, in both MCF7-RR and U87 cell lines, there was only partial recovery of H3S10p post irradiation and VPA treatment, along with high levels of histone acetylation and γH2AX (Fig. 4.24 A and C). This indicated the possibility of a cross talk between histone acetylation and phosphorylation in context of H3S10p recovery in VPA treated and radiated cells. This observation of decreased H3S10 phosphorylation and increased histone H3K9ac was also previously seen upon radiation of mitotic cells and their cell cycle progression, and correlated with reduced cell survival of mitotic cells.

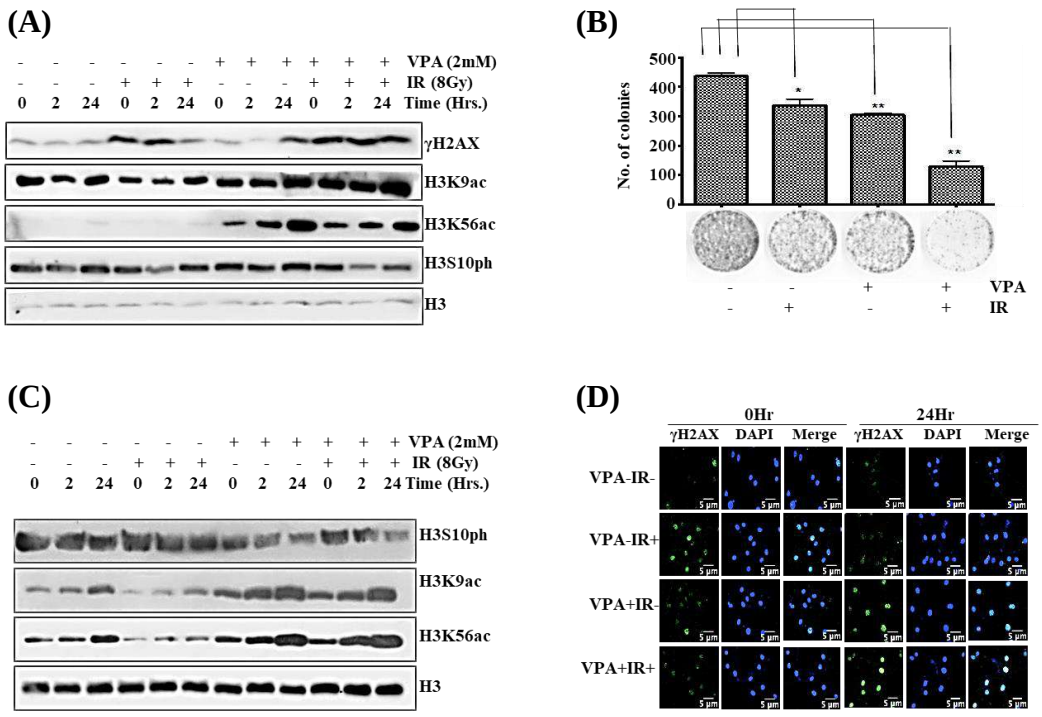

Figure 4.24 HDAC inhibitor Valproic acid causes γH2AX retention and epigenetic alterations in acquired and inherently radioresistant cells. (A) *Levels of histone PTMs in 20GyRR at different time points after treatment with VPA and radiation.* ***(B)*** *Clonogenic assay of 20GyRR cells to assess radio-sensitization potential of Valproic*

acid post radiation exposure. Graph depicts number of surviving colonies. ***(C)*** *Levels of histone PTMs post VPA treatment and irradiation in U87 cell line.* ***(D)*** *Z-stack images for depiction of γH2AX retention in U87 cells after VPA treatment and radiation. Scale bar- 20μm. Statistical analysis is done by student's t-test.* $^{*}p<0.05$, $^{**}p<0.01$, *Hrs. – Hours. Histone H3 serves as loading control for all western blots.*

Chapter 5

Discussion

Chromatin is a dynamic entity that changes both locally and globally according to the cell cycle phase and acts as a natural barrier for all DNA-related processes. The initiation and culmination of these processes requires structural alterations of chromatin, facilitated by a variety of proteins such as chromatin remodelers, histone-modifying enzymes, and chaperones. DNA double strand breaks (DBSs) are the most deleterious lesions that left unrepaired, can lead to gross chromosomal aberrations(51). Highly efficient DNA repair pathways like NHEJ and HR, in association with histone PTMs, act in a cell cycle dependent manner to detect and repair the damage(161). Since histone PTMs vary in a cell cycle dependent manner, it is highly plausible that a characteristic PTM signature at/near the break site could aid in activation of a specific repair pathway, or vice-versa. In accordance with this hypothesis, a detailed study by our group has previously demonstrated a bi-phasic kinetics followed by histone PTM H3S10ph during the G_0/G_1 phase of the cell cycle(87,88).

The study presented in this thesis is based on the above findings of the lab, with an extended aim to explore the clinical significance of histone H3 phospho-acetylation. Therefore, the target of the study was to understand the role of histone PTMs in response to ionizing radiation during mitosis and acquired radio-resistance. Special emphasis has been given to mitotic DDR in this study for two reasons. Firstly, the cellular radio-sensitivity varies throughout the cell cycle. Mitotic cells are the most radiosensitive by nature, followed by G_0/G_1 phase while cells show minimum radio sensitivity during the S-phase(121). Secondly, H3S10ph is a very unique histone PTM that plays dual and contrasting roles within the cell cycle. During the G_1 phase, H3S10ph is involved in promoting

gene transcription at specific gene loci while in mitosis, the enrichment of this mark occurs throughout the chromosome arms, making it a mitotic mark(45–47,82,162,163). Hence, the work presented in the first objective of this thesis is aimed to understand intrinsic mitotic radio sensitivity and its association with H3S10ph. Extending these findings to a clinically setting, the second objective of this thesis aimed to explore the role of histone phospho-acetylation marks and associated modifying enzymes in imparting acquired radio-resistance. The major findings of this thesis suggests that significant alterations of histone phospho-acetylation correlate with both intrinsic and acquired radio-resistance, and have the potential to govern the cellular fate of these cells. Our study suggests that the dynamic nature of the epigenome can be exploited to convert the epigenetic landscape of radio-resistant cells like that of radiosensitive cells that successfully results in enhanced cell kill. Therefore, studies like this can help in identification of novel epigenetic targets to effectively combat cellular radio-resistance.

Mitosis is the shortest but perhaps the most significant phase of the cell cycle, as it allows the cells an opportunity for propagation of its genetic material. The de-condensed and gene rich euchromatin has an increased susceptibility for DNA damage, suggesting a protective role of condensed chromatin(122,136,164). However, inspite of a highly compact chromatin state, the exact reasons for mitotic radio sensitivity are still elusive. Therefore it can be speculated that the epigenetic events orchestrating DNA repair during mitosis could differ from interphase, due to significant dissimilarities in chromatin landscapes. In this study, the role of H3S10ph and its neighboring acetyl mark H3K9ac was explored during mitotic DNA Damage Response (DDR). Additionally, this study was also

extended to understand the correlation between these PTMs after radiated mitotic cells progressed to interphase. In corroboration with other reports, our data suggests that mitotic cells can mark the sites of DNA damage by γH2AX induction. However, no chromatin recruitment of repair proteins like NHEJ-specific Ku70 or HR specific Rad51 accompanies γH2AX induction. These data are also in corroboration with reports that suggest activation of only a primary DDR during mitosis(123,165–167). As reflected by our data, the chromatin recruitment of these repair proteins takes place only when radiated cells exit mitosis and enter interphase. This is strongly in agreement with reports suggesting similar pattern of chromatin-non-recruitment of repair protein 53BP1. This can be explained due to the fact that activation of DNA repair during mitosis leads to development of chromosome segregation defects like anaphase bridges and telomere fusion of sister chromatids(123,165–167). Due to occurrence of such events, the activation of DDR during mitosis renders the mitotic cells a hypersensitive phenotype.

In context of histone phospho-acetylation alterations during mitotic DDR, our data suggests no change in global levels of H3S10/28ph. However, when radiated mitotic cells resume cell cycle, these marks decrease in a cell cycle specific manner, irrespective of radiation exposure. These data are in complete accordance with a report published by Tjeertes *et. al*, that also suggests a decrease in levels of H3K9ac after mitotic DNA damage(84),(168). However, we observe a contradictory observation in corroboration with literature that suggests increase in levels of histone acetylation upon mitotic exit. This was attributed to chromatin recruitment of Histone Acetyl Transferases (HATs) Gcn5 and PCAF. Several

factors such as duration of nocodazole treatment, specific time point analysis after interphase entry, cell line and the extent of DNA damage often lead to such contrasting observations, that reflects the dynamic nature of DDR associated epigenetic alterations. Interestingly, our data suggests H3S10ph and γH2AX to co-occur and co-localize during mitosis, as assessed by western blotting and immunofluorescence based studies. Our study additionally provides evidence that both H3S10ph and γH2AX co-exist on the same mononucleosome during mitosis, but this association is abrogated upon interphase entry and chromatin de-condensation. These observations held the utmost importance for the study as well as for our hypothesis that suggested histone PTM alterations to be associated with cell cycle phase specific DDR. The data in this thesis also corroborated the previous findings of that suggested G_0/G_1 phase specific inverse correlation between H3S10ph and γH2AX(87,88). The inverse correlation between H3S10ph and γH2AX (based on western blotting and immunofluorescence) has not only been reported by ours and other groups, but also recently confirmed by a mass spectrometry based analysis(85),(86),(169).

The observations of H3S10ph and γH2AX mononucleosomal co-occurrence during mitosis coincided with no recruitment of repair proteins on chromatin. This led us to several assumptions about mitotic chromatin did not provide a permissive environment of activation of DDR. H3S10ph has been previously associated with formation of DNA-RNA hybrid R-loops(170). However, the chromatin structure alterations required for formation of R-loop could be detrimental to genome stability during cell division process. Additionally, it is yet unexplored whether γH2AX-H3S10ph form homotypic or heterotypic

nucleosomes. This could add to the possibility of nucleosome structure alterations that could hinder the recruitment of chromatin remodeling factors associated with DNA repair. This seems plausible since de-condensation of chromatin associated with DNA repair could lead to enhanced genomic instability, especially during cell division process. Additionally, to further explore this possibility, it needs to be ascertained whether H3S10ph and γH2AX containing nucleosomes are present at the DNA damage site/DSB or in its vicinity. Another possibility that explains the mononucleosomal co-occurrence of H3S10ph and γH2AX and no activation of DDR during mitosis is the histone code hypothesis. It could be speculated that presence or absence of other PTMs could be a pre-requisite for mitotic DDR activation, and that such a code is only restored upon chromatin de-condensation associated with G_1 phase entry. This speculation is based upon a study that utilized artificial DSB induction system to elucidate the histone PTM milieu around a DSB, at a resolution of 1Kb-1Mb(70). A similar analysis of histone PTM landscape during mitosis and G_1 phase should be performed that sheds light on the role of histone PTMs and cell cycle phase specific DNA repair.

Perhaps the most confusing observation in this study was the observed G_2/M arrest after mitotic exit. Since G_1 phase is the longest phase of the cell cycle, it was anticipated that after mitotic exit, the radiated cells would arrest in the G_1 phase. It was later realized that the observed G_2/M enrichment was due to detection of binucleated tetraploid cells as cells in G_2/M phase. This tetraploid intermediate state has been reported as a "4N-intermediate" state(152,171–173). The absence of cyclin B and decreased cyclin D levels suggested mitotic exit, but not interphase entry for these cells. Such a binucleated population could arise due

to daughter cell fusion, as suggested by live-cell monitoring performed in this study. However, further studies are required to understand if radiated mitotic cells had undergone mitotic slippage to generate such a population, or they arise due to radiation-associated defects in the cytokinesis process. The features that characterized this population were (a) low levels of H3S10/28ph (b) high H3K9ac and (c) reduced survival potential. Further exploration is required to assess the impact of H3S10/28ph and H3K9ac in dictating the cell fate of binucleated tetraploid cells. Additionally, there was survival of few cells from the G_1 and S-phases that arise after mitotic radiation. Proliferation of tetraploid cells that get generated after cytokinesis failure is associated with an increased in the tumorigenic potential of these cells (152). Hence, it would be interesting to elucidate the epigenetic mechanisms that regulate cell survival or death of such binucleated tetraploid cells.

It was observed that H3S10/28ph levels were unchanged during mitotic DDR and decreased in a cell cycle dependent manner upon mitotic progression. However, levels comparable to non-radiated interphase cells were not attained after radiation. A report suggests enhanced chromatin recruitment of PP1δ upon histone acetylation induction during mitosis(174). Hence, based on our data, we propose that histone acetylation-associated recruitment of PP1α phosphatase could regulate the kinase activity after radiated mitotic cells enter interphase. Interestingly, PP1 is shown to negatively regulate the activity of AURKB during interphase(175). Additionally, histone acetylation status also influences substrate specificity of mitotic kinases, with AURKB mediated H3S10ph occurring only on hypo-acetylated histone tails(176). However, our data suggests PP1α chromatin

recruitment to occur irrespective of radiation exposure. Therefore the question arises that could PP1α regulate kinase activity selectively after radiation? The substrate specificity of PP1 catalytic subunit depends on its association with different regulatory subunits. Association of PP1γ with Repo-Man has been reported to regulate histone de-phosphorylation that occurs upon mitosis to G_1 transition(177,178). Formation of similar complex by PP1α could also regulate MSK1 kinase activity during interphase, in response to DNA damage. It is also likely that PP1 associates with a unique regulatory subunit upon radiation, which directs its specificity towards interphase kinases. These are interesting possibilities that can bring to light the complexity of kinase-phosphatase regulation during mitotic DDR. These data suggest that exposure of mitotic cells to ionizing radiation brings out a unique epigenetic profile of the subsequent interphase cells. These cells are characterized by reduced histone H3S10/28ph mark but have increased level of H3K9ac. This unique epigenetic profile correlates with their reduced survival and highly radiosensitive nature. Therefore, the intrinsic radio-sensitivity of mitotic cells is contributed by the epigenetic state of the population that arises after damaged mitotic cells resume cell cycle.

In addition to our understanding about epigenetic alterations of the intrinsically radio-resistant mitotic cells, this study was also extended to explore the role of histone PTMs and chromatin modifying enzymes during acquired radio-resistance. Therefore, radio-resistant cell lines were developed for ER+/PR+ MCF7 breast cancer cells. In concordance with several previous reports on mammalian systems and prokaryotes, our data also suggests increased heterochromatinization upon acquirement of radio-resistance(179),(180). This is also in concordance with

several other reports that suggest the de-condensed and gene rich euchromatin region to be more susceptible to DNA damage(136–138). Therefore, enhanced heterochromatinization observed during acquirement of radio-resistance could have a protective role against DNA damage induction, and be advantageous for survival of radio-resistant cells.

In concomitance with increased heterochromatinization, the radio-resistant cells also showed reduced histone phospho-acetylation. DDR-based studies suggest reduced histone acetylation in response to DNA damage(168). However, a major caveat of such studies is their short-term analysis that describes only transient but dynamic histone PTM alterations. These studies do not comment upon how these histone PTM alterations could influence long-term processes such as acquirement of radio-resistance. In this study, histone marks H3K9/K27ac and H3S10phK14ac marks were reduced in radio-resistant MCF7 cells irrespective of the cell cycle phase. This suggested that these alterations were true events associated with acquirement of radio-resistance. Interestingly, the histone acetyl mark reduction was accompanied by a reduction in H3S10/28ph marks also. H3S10p and S28p are both a part of the “ARKS” motifs present in histone H3 N-terminal tail, and both these PTMS are reported to occur at active promoters. Therefore, a reduction in transcription-promoting histone phospho-acetyl marks could be associated with an altered gene expression profile upon acquirement of radio-resistance. This possibility requires further exploration by ChIP-Seq and RNA-Seq based studies of these acquired radio-resistant cells, along with their validation.

Chromatin modifying enzymes play a crucial role in maintaining the dynamic histone PTM landscape. An assessment of H3S10ph modifying kinases and

phosphatases revealed up-regulation of MKP-1 phosphatase, concomitant with reduced MAPK activators ERK1/2 and p38. Notably, MKP-1 up-regulation in breast cancer correlates with poor prognosis and therapy resistance(181,182). Therefore, alteration of chromatin modifying enzymes during radio-resistance acquirement can influence the cellular pathways and also influence gene expression. Perhaps the most significant finding in acquired radio-resistant cells was an imbalance between HDAC and HAT activities. The radio-resistant cells showed increased HDAC activity and decreased HAT activity, which provides an explanation for enhanced heterochromatinization and reduced histone acetylation. This finding had important clinical implications because HDAC inhibitors are currently being explored as potential radio-sensitizing agents(142,182–184). Indeed the treatment of acquired radio-resistant MCF7 cells and intrinsically radio-resistant U87 glioblastoma cell line with HDAC inhibitor Valproic acid (VPA) rendered than sensitive towards ionizing radiation and enhanced cell kill. VPA is a preferred HDAC inhibitor for utilization in clinics as it is an FDA approved drug with little cellular toxicity(185). Interestingly, reduced H3S10ph and high levels of H3K9ac marked the sensitization of both acquired and intrinsic radioresistant cells. These epigenetic changes could be attributed to impaired de-acetylation of non-histone substrates of HDACs that could alter their activity status.

HDAC inhibitors have shown promising potential in hematological malignancies, but poor response in solid tumors. This could be due to poor pharmaco-kinetic of the drugs, reduced half-life and cellular toxicity(183). Our group had previously demonstrated a liquid biopsy based real-time monitoring approach to assess

HDAC activity in serum of normal as well as cancer patients(186). Additionally, elevated HDAC activity was the key epigenetic highlight of radio-resistant cells. Hence, based on our observations, we put forward the hypothesis that treatment with HDAC inhibitors should be based on the HDAC activity status of the patients. The potential possibilities that could influence HDAC levels or activity could be as varied as presence or absence of infection, disease, metabolic variations or even the dietary constituents. Therefore, it is difficult to identify a single reason behind variation between HDAC activities at an individual level.

Therefore, an assessment of tumor HDAC activity before starting with radiotherapy could help in identification of patients with high tumor HDAC activity that could be potential poor radiation responders. These patients would be best suited for HDAC inhibitor based radio-sensitization. Interestingly, our data suggests a HDAC activity based epigenetic heterogeneity within several tumor types. Notably, the tumor HDAC activity was checked with as little as 1mg of tumor tissue. Occurance of such epigenetic heterogeneity even within tumors of the same subtype strongly suggested that all patients would not have similar response to HDAC inhibitor based therapy. Therefore sub-grouping of patients into high and low HDAC activity groups could help to identify the most suitable candidates for HDAC inhibitor based radio-sensitization therapy. Additionally, more information about the most effective treatment regime can be obtained by animal model based studies as well as pre-clinical trials.

One of the most interesting observations from the collective analysis of this research suggests that decrease in cell survival and radio-sensitization was both accompanied by reduced H3S10ph and high levels of H3K9ac. This observation

was found applicable to both intrinsically radioresistant mitotic cells as well as HDAC inhibitor treatment of acquired radio-resistant cells. Thus, our study suggests that effective targeting of chromatin modifiers that regulate these histone marks could lead to attainment of a state that correlates with reduced cell survival. Thus, the conversion of a radio-resistant state to a radiosensitive state could be achieved by epigenetic modulation. Therefore, amalgamation of understanding the basic biology behind radio-sensitization could have tremendous clinical impact for tackling radio-resistant populations. Such studies can be utilized to create new opportunities for development of next-generation therapies or combinatorial regimes utilizing chromatin modifiers to sensitize radio-resistant cells.

Chapter 6

Conclusions and

Summary

Chromatin essentially acts as a barrier for all DNA related processes like replication, transcription and repair. Thus for all these processes to commence or cease, the modulation of chromatin architecture is inevitable. In response to DNA damage, many changes occur in the chromatin that allows access to DNA repair proteins at the site of damage. A major contributor of such changes is histone PTMs. Since histone PTMs are strong determinants of the DDR, this study explores the effect of DDR associated histone PTM alterations in a cell cycle phase specific manner. A noteworthy point is that as cell cycle phases differ in their intrinsic radio-resistance, the pattern of histone PTM alteration during DDR could specific for a particular cell cycle phase.

It is essential to understand the concept of radio-resistance in depth because of its clinical implications in the field of radiotherapy. Unfortunately, tumor recurrence may occur even after successful treatment regime. Radio-resistance is an enigmatic phenomenon and whether radio-resistant cells have different epigenetic profile compared to non-resistant cells is an important question that needs to be addressed. An understanding of the epigenetic alterations in radio-resistant tumors, could be useful to target radio-resistant cells or to decrease the incidence of radio-resistance altogether by using drugs against epigenetic modifiers (epi-drugs).

In this study, we explored the epigenetic determinants of the intrinsically radiosensitive mitotic cells and also that of acquired radio-resistant breast cancer cells. Interestingly in both the scenario, interplay between H3S10ph and histone acetylation was found to be associated with radio sensitivity of mitotic cells as well as radio resistance, as summarized in model 2.

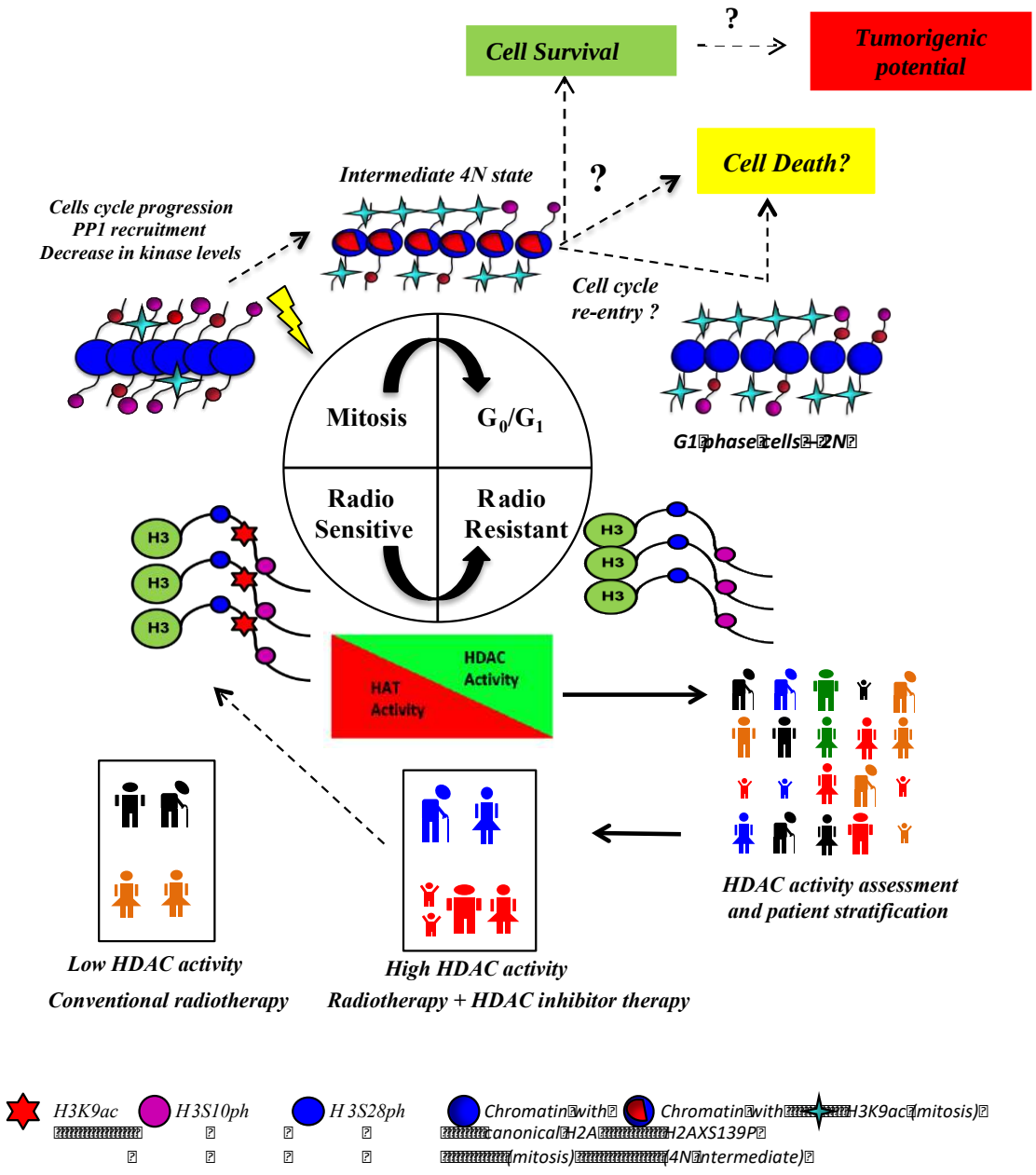

Model 2- *Diagrammatic representation depicting the role of histone H3 PTMs in DNA damage and radio-resistance.*

DNA damage in M-phase of the cell cycle induces a state of cells in which they have de-condensed nuclei with 4N DNA content because of incomplete cell division process. These cells have absence of both cyclin B as well as cyclin D, indicating exit from mitosis but in an intermediate state before G1. There is co-existence of H3 phospho-acetyl marks on same nucleosome as ϒH2AX in mitosis but not after cells have started cycling. Increase of H3K9ac takes place on those nucleosomes on which there is no ϒH2AX but presence of H3S10P. Post DNA damage in M-phase of the cell cycle, there is no recovery of H3S10P/28P. This can be attributed to decreased levels as well as reduced chromatin recruitment of histone kinases Msk1 and AURKB. Decreased levels of MSK1 are influenced by alteration in its translation, while AURKB is influenced by cell cycle dependent progression. Additionally, overall there is stabilization and chromatin recruitment of phosphatase PP1.

Radio-resistant cells developed by fractionated irradiation have compact chromatin architecture and decreased histone phospho-acetylation. This can be attributed to enhanced HDAC activity and reduced HAT activity. Inter-tumoral HDAC activity exists within a single tumor type, hence emphasizing on identifying the right population to be targeted for HDAC inhibitor therapy. Finally, treatment with HDAC inhibitor, Valproic acid is able to retain γH2AX levels up to 24 hours post IR in and increase cell death in acquired radio-resistant cell line.

Chapter 7

Future Directions

1. To investigate the cytokinesis related defects after radiation of mitotic cells and the molecular players involved in imparting a binucleated tetraploid phenotype
2. Single-cell level transcriptomic analysis of the tetraploid binucleated cells to identify alterations associated with death or cell survival of these cells.
3. *In silico* or biochemical analysis of stability or structural alterations of nucleosomes having both H3S10ph and ϒH2AX.
4. Investigation of mechanisms that influence the stability of PP1 in response to mitotic radiation. Studies also need to be carried out to find if PP1 directly regulates the activity of Msk1 kinase in interphase.
5. *In vivo* studies to be carried out to determine efficacy of VPA as a radio-sensitizer, by first determining the most effective dosage regime and radiation combination.

Chapter 8

References

REFERENCES

1. Van Holde KE. Chromatin. Springer Science & Business Media; 2012.
2. Hewish DR, Burgoyne LA. Chromatin sub-structure. The digestion of chromatin DNA at regularly spaced sites by a nuclear deoxyribonuclease. Biochemical and biophysical research communications. 1973;52(2):504–10.
3. Noll M. Subunit structure of chromatin. Nature. 1974;251(5472):249–51.
4. Sahasrabuddhe CG, Van Holde KE. The effect of trypsin on nuclease-resistant chromatin fragments. Journal of Biological Chemistry. 1974;249(1):152–6.
5. Kornberg RD. Structure of chromatin. Annual review of biochemistry. 1977;46(1):931–54.
6. Felsenfeld G. Chromatin. Nature. 1978;271(5641):115–22.
7. Kornberg RD. Chromatin Structure: A Repeating Unit of Histones and DNA. Science. 1974 May 24;184(4139):868 LP-871.
8. Kornberg RD, Thonmas JO. Chromatin Structure: Oligomers of the Histones. Science. 1974 May 24;184(4139):865 LP-868.
9. Luger K, Mäder AW, Richmond RK, Sargent DF, Richmond TJ. Crystal structure of the nucleosome core particle at 2.8 Å resolution. Nature. 1997 Sep 18;389:251.
10. Prachayasittikul V, Prathipati P, Pratiwi R, Phanus-umporn C, Malik AA, Schaduangrat N, et al. Exploring the epigenetic drug discovery landscape. Expert Opinion on Drug Discovery. 2017 Apr 3;12(4):345–62.
11. Felsenfeld G. A brief history of epigenetics. Cold Spring Harbor perspectives in biology. 2014 Jan 1;6(1):a018200.
12. Clark RJ, Felsenfeld G. Structure of chromatin. Nature: New biology. 1971 Jan;229(4):101–6.

13. Bonner J, Taft Garrard W. Biology of the histones. Life Sciences. 1974;14(2):209–21.

14. Workman JL, Abmayr SM. Fundamentals of Chromatin.

15. Ramakrishnan V. HISTONE STRUCTURE AND THE ORGANIZATION OF THE NUCLEOSOME. 1997;83–112.

16. Richmond RK, Sargent DF, Richmond TJ, Luger K, Ma AW. Crystal structure of the nucleosome ˚ resolution core particle at 2 . 8 A. 1997;7:251–60.

17. Zorich AETH, Opinion RC, Biology C, Caf- A. The histone tails of the nucleosome Karolin Luger and Timothy J Richmond *. :140–6.

18. Allfrey VG, Faulkner R, Mirsky AE. Acetylation and methylation of histones and their possible role in the regulation of RNA synthesis. Proceedings of the National Academy of Sciences of the United States of America. 1964 May;51:786—794.

19. Kouzarides T. Chromatin Modifications and Their Function. Cell. 2007;128(4):693–705.

20. Tropberger P, Schneider R. Going global: Novel histone modifications in the globular domain of H3. Epigenetics. 2010 Feb 16;5(2):112–7.

21. Di Cerbo V, Mohn F, Ryan DP, Montellier E, Kacem S, Tropberger P, et al. Acetylation of histone H3 at lysine 64 regulates nucleosome dynamics and facilitates transcription. eLife. 2014 Mar 25;3:e01632–e01632.

22. Tropberger P, Schneider R. Scratching the (lateral) surface of chromatin regulation by histone modifications. Nature Structural & Molecular Biology. 2013;20(6):657–61.

23. Lawrence M, Daujat S, Schneider R. Lateral Thinking: How Histone Modifications Regulate Gene Expression. Trends in Genetics. 2016;32(1):42–56.

24. Tropberger P, Pott S, Keller C, Kamieniarz-gdula K, Caron M, Richter F, et al. Regulation of Transcription through Acetylation of H3K122 on the Lateral Surface of the Histone Octamer. 2013;859–72.

25. Jenuwein T, Allis CD. Translating the Histone Code. Science. 2001 Aug 10;293(5532):1074 LP-1080.

26. Luger K. Nucleosomes: Structure and Function. eLS. 2001. (Major Reference Works).

27. Zhang Y, Reinberg D. Transcription regulation by histone methylation: interplay between different covalent modifications of the core histone tails. Genes & Development . 2001 Sep 15;15(18):2343–60.

28. Hendzel MJ, Wei Y, Mancini MA, Van Hooser A, Ranalli T, Brinkley BR, et al. Mitosis-specific phosphorylation of histone H3 initiates primarily within pericentromeric heterochromatin during G2 and spreads in an ordered fashion coincident with mitotic chromosome condensation. Chromosoma. 1997;106(6):348–60.

29. Jeong YS, Cho S, Park JS, Ko Y, Kang Y-K. Phosphorylation of serine-10 of histone H3 shields modified lysine-9 selectively during mitosis. Genes to Cells. 2010 Mar 1;15(3):181–92.

30. Karam CS, Kellner WA, Takenaka N, Clemmons AW, Corces VG. 14-3-3 Mediates Histone Cross-Talk during Transcription Elongation in Drosophila. PLOS Genetics. 2010 Jun 3;6(6):e1000975.

31. Sawicka A, Seiser C. Histone H3 phosphorylation - a versatile chromatin modification for different occasions. Biochimie. 2012/04/28. 2012 Nov;94(11):2193–201.

32. Kamakaka RT, Biggins S. Histone variants: deviants? Genes & Development . 2005 Feb 1;19(3):295–316.

33. Hake SB, Allis CD. Histone H3 variants and their potential role in indexing mammalian genomes: The "H3 barcode hypothesis." Proceedings of the National Academy of Sciences. 2006 Apr 25;103(17):6428 LP-6435.

34. Jin C, Felsenfeld G. Nucleosome stability mediated by histone variants H3.3 and H2A.Z. Genes & development. 2007 Jun 15;21(12):1519–29.

35. Ma Y, Kanakousaki K, Buttitta L. How the cell cycle impacts chromatin architecture and influences cell fate . Vol. 6, Frontiers in Genetics . 2015. p. 19.

36. de Castro IJ, Gokhan E, Vagnarelli P. Resetting a functional G1 nucleus after mitosis. Chromosoma. 2016/01/04. 2016 Sep;125(4):607–19.

37. Miotto B, Struhl K. HBO1 histone acetylase activity is essential for DNA replication licensing and inhibited by Geminin. Molecular cell. 2010 Jan 15;37(1):57–66.

38. Li Y, Armstrong RL, Duronio RJ, MacAlpine DM. Methylation of histone H4 lysine 20 by PR-Set7 ensures the integrity of late replicating sequence domains in Drosophila. Nucleic acids research. 2016/04/29. 2016 Sep 6;44(15):7204–18.

39. Tardat M, Brustel J, Kirsh O, Lefevbre C, Callanan M, Sardet C, et al. The histone H4 Lys 20 methyltransferase PR-Set7 regulates replication origins in mammalian cells. Nature Cell Biology. 2010;12(11):1086–93.

40. Brustel J, Kirstein N, Izard F, Grimaud C, Prorok P, Cayrou C, et al. Histone H4K20 tri-methylation at late-firing origins ensures timely heterochromatin replication. The EMBO journal. 2017/08/04. 2017 Sep 15;36(18):2726–41.

41. Clemente-Ruiz M, González-Prieto R, Prado F. Histone H3K56 Acetylation, CAF1, and Rtt106 Coordinate Nucleosome Assembly and Stability of Advancing Replication Forks. PLOS Genetics. 2011 Nov 10;7(11):e1002376.

42. Li Q, Zhou H, Wurtele H, Davies B, Horazdovsky B, Verreault A, et al. Acetylation of histone H3 lysine 56 regulates replication-coupled nucleosome assembly. Cell. 2008 Jul 25;134(2):244–55.

43. Ge Z, Nair D, Guan X, Rastogi N, Freitas MA, Parthun MR. Sites of acetylation on newly synthesized histone H4 are required for chromatin assembly and DNA damage response signaling. Molecular and cellular biology. 2013/06/17. 2013 Aug;33(16):3286–98.

44. Hoek M, Stillman B. Chromatin assembly factor 1 is essential and couples chromatin assembly to DNA replication in vivo Proceedings of the National Academy of Sciences. 2003 Oct 14;100(21):12183 LP-12188.

45. Van Hooser A, Goodrich DW, Allis CD, Brinkley BR, Mancini MA. Histone H3 phosphorylation is required for the initiation, but not maintenance, of mammalian chromosome condensation. Journal of Cell Science. 1998 Dec 1;111(23):3497 LP-3506.

46. Wei Y, Yu L, Bowen J, Gorovsky MA, Allis CD. Phosphorylation of Histone H3 Is Required for Proper Chromosome Condensation and Segregation. Cell. 1999;97(1):99–109.

47. Wei Y, Mizzen CA, Cook RG, Gorovsky MA, Allis CD. Phosphorylation of histone H3 at serine 10 is correlated with chromosome condensation during mitosis and meiosis in Tetrahymena. Proceedings of the National Academy of Sciences of the United States of America. 1998 Jun 23;95(13):7480–4.

48. Michelotti EF, Sanford S, Levens D. Marking of active genes on mitotic chromosomes. Nature. 1997;388(6645):895–9.

49. Hsiung CC-S, Morrissey CS, Udugama M, Frank CL, Keller CA, Baek S, et al. Genome accessibility is widely preserved and locally modulated during mitosis. Genome research. 2014/11/04. 2015 Feb;25(2):213–25.

50. Hu X, Lu X, Liu R, Ai N, Cao Z, Li Y, et al. Histone Crosstalk Connects Protein Phosphatase 1α (PP1α) and Histone Deacetylase (HDAC) Pathways to Regulate the Functional Transition of Bromodomain-containing 4 (Brd4) for Inducible Gene Expression. Journal of Biological Chemistry . 2014 Jun 17;

51. Ciccia A, Elledge SJ. The DNA damage response: making it safe to play with knives. Molecular cell. 2010 Oct 22;40(2):179–204.

52. Lieber MR. The Mechanism of Double-Strand DNA Break Repair by the Nonhomologous DNA End-Joining Pathway. Annual Review of Biochemistry. 2010 Jun 7;79(1):181–211.

53. Sfeir A, Symington LS. Microhomology-Mediated End Joining: A Back-up Survival Mechanism or Dedicated Pathway? Trends in Biochemical Sciences. 2015;40(11):701–14.

54. Verma P, Greenberg RA. Noncanonical views of homology-directed DNA repair. Genes & Development . 2016 May 15;30(10):1138–54.

55. Sartori AA, Lukas C, Coates J, Mistrik M, Fu S, Bartek J, et al. Human CtIP promotes DNA end resection. Nature. 2007/10/28. 2007 Nov 22;450(7169):509–14.

56. Garcia V, Phelps SEL, Gray S, Neale MJ. Bidirectional resection of DNA double-strand breaks by Mre11 and Exo1. Nature. 2011 Oct 16;479(7372):241–4.

57. Nimonkar A V, Genschel J, Kinoshita E, Polaczek P, Campbell JL, Wyman C, et al. BLM-DNA2-RPA-MRN and EXO1-BLM-RPA-MRN constitute two DNA end resection machineries for human DNA break repair. Genes & development. 2011 Feb 15;25(4):350–62.

58. Aylon Y, Liefshitz B, Kupiec M. The CDK regulates repair of double-strand breaks by homologous recombination during the cell cycle. The EMBO journal. 2004/11/18. 2004 Dec 8;23(24):4868–75.

59. Bakkenist CJ, Kastan MB. DNA damage activates ATM through intermolecular autophosphorylation and dimer dissociation. Nature. 2003;421(6922):499–506.

60. Roti JLR, Wright WD. Visualization of DNA loops in nucleoids from HeLa cells: Assays for DNA damage and repair. Cytometry. 1987 Sep 1;8(5):461–7.

61. Jaberaboansari A, Nelson GB, Roti JLR, Wheeler KT. Postirradiation Alterations of Neuronal Chromatin Structure. Radiation Research. 1988 Apr 27;114(1):94–104.

62. Soria G, Polo SE, Almouzni G. Prime, repair, restore: the active role of chromatin in the DNA damage response. Molecular cell. 2012 Jun 29;46(6):722–34.

63. Kruhlak MJ, Celeste A, Dellaire G, Fernandez-Capetillo O, Muller WG, McNally JG, et al. Changes in chromatin structure and mobility in living cells at sites of DNA double-strand breaks. J Cell Biol. 2006;172.

64. Berkovich E, Monnat RJ, Kastan MB. Roles of ATM and NBS1 in chromatin structure modulation and DNA double-strand break repair. Nature Cell Biology. 2007;9(6):683–90.

65. Strickfaden H, McDonald D, Kruhlak MJ, Haince J-F, Th'ng JPH, Rouleau M, et al. Poly(ADP-ribosyl)ation-dependent Transient Chromatin Decondensation and Histone Displacement following Laser Microirradiation. The Journal of biological chemistry. 2015/11/11. 2016 Jan 22;291(4):1789–802.

66. Li Z, Li Y, Tang M, Peng B, Lu X, Yang Q, et al. Destabilization of linker histone H1.2 is essential for ATM activation and DNA damage repair. Cell Research. 2018;28(7):756–70.

67. Dabin J, Fortuny A, Polo SE. Epigenome Maintenance in Response to DNA Damage. Molecular cell. 2016 Jun 2;62(5):712–27.

68. Clouaire T, Legube G. DNA double strand break repair pathway choice: a chromatin based decision? Nucleus (Austin, Tex). 2015/02/12. 2015;6(2):107–13.

69. Aymard F, Bugler B, Schmidt CK, Guillou E, Caron P, Briois S, et al. Transcriptionally active chromatin recruits homologous recombination at DNA double-strand breaks. Nature structural & molecular biology. 2014/03/23. 2014 Apr;21(4):366–74.

70. Clouaire T, Rocher V, Lashgari A, Arnould C, Aguirrebengoa M, Biernacka A, et al. Comprehensive Mapping of Histone Modifications at DNA Double-

Strand Breaks Deciphers Repair Pathway Chromatin Signatures. Molecular Cell. 2018;72(2):250–262.e6.

71. Rogakou EP, Pilch DR, Orr AH, Ivanova VS, Bonner WM. DNA Double-stranded Breaks Induce Histone H2AX Phosphorylation on Serine 139 *. 1998;273(10):5858–68.

72. Rogakou EP, Boon C, Redon C, Bonner WM. Megabase chromatin domains involved in DNA double-strand breaks in vivo. The Journal of cell biology. 1999 Sep 6;146(5):905–16.

73. Stiff T, Driscoll MO, Rief N, Stiff T, Driscoll MO, Rief N, et al. ATM and DNA-PK Function Redundantly to Phosphorylate H2AX after Exposure to Ionizing Radiation ATM and DNA-PK Function Redundantly to Phosphorylate H2AX after Exposure to Ionizing Radiation. 2004;2390–6.

74. Redon C, Pilch DR, Rogakou EP, Orr AH, Lowndes NF, Bonner WM. Yeast histone 2A serine 129 is essential for the efficient repair of checkpoint-blind DNA damage. EMBO reports. 2003 Jul;4(7):678–84.

75. Paull TT, Rogakou EP, Yamazaki V, Kirchgessner CU, Gellert M, Bonner WM. A critical role for histone H2AX in recruitment of repair factors to nuclear foci after DNA damage. :886–95.

76. Xiao A, Li H, Shechter D, Ahn SH, Fabrizio LA, Erdjument-Bromage H, et al. WSTF regulates the H2A.X DNA damage response via a novel tyrosine kinase activity. Nature. 2008/12/17. 2009 Jan 1;457(7225):57–62.

77. Cook PJ, Ju BG, Telese F, Wang X, Glass CK, Rosenfeld MG. Tyrosine dephosphorylation of H2AX modulates apoptosis and survival decisions. Nature. 2009/02/22. 2009 Apr 2;458(7238):591–6.

78. Krishnan N, Jeong DG, Jung S-K, Ryu SE, Xiao A, Allis CD, et al. Dephosphorylation of the C-terminal Tyrosyl Residue of the DNA Damage-related Histone H2A.X Is Mediated by the Protein Phosphatase Eyes Absent. Journal of Biological Chemistry . 2009 Jun 12;284(24):16066–70.

79. Lee J-H, Kang B-H, Jang H, Kim TW, Choi J, Kwak S, et al. AKT phosphorylates H3-threonine 45 to facilitate termination of gene transcription in response to DNA damage. Nucleic acids research. 2015/03/26. 2015 May 19;43(9):4505–16.

80. Brehove M, Wang T, North J, Luo Y, Dreher SJ, Shimko JC, et al. Histone core phosphorylation regulates DNA accessibility. The Journal of biological chemistry. 2015/07/13. 2015 Sep 11;290(37):22612–21.

81. Shimada M, Niida H, Zineldeen DH, Tagami H, Tanaka M, Saito H, et al. Chk1 Is a Histone H3 Threonine 11 Kinase that Regulates DNA Damage-Induced Transcriptional Repression. Cell. 2008;132(2):221–32.

82. Prigent C, Dimitrov S. Phosphorylation of serine 10 in histone H3, what for? Journal of Cell Science. 2003 Aug 13;116(18):3677 LP-3685.

83. Papers JBC, Doi M, Zhong S, Ma W, Dong Z. ERKs and p38 Kinases Mediate Ultraviolet B-induced Phosphorylation of Histone H3 at Serine 10 *. 2000;275(28):20980–4.

84. Tjeertes J V, Miller KM, Jackson SP. Screen for DNA-damage-responsive histone modifications identifies H3K9Ac and H3K56Ac. The EMBO Journal. 2009;28(13):1878–89.

85. Chen K, Zhang S, Ke X, Qi H, Shao J, Shen J. Biphasic reduction of histone H3 phosphorylation in response to N-nitroso compounds induced DNA damage.

Biochimica et Biophysica Acta (BBA) - General Subjects. 2016;1860(9):1836–44.

86. Ozawa K. Reduction of phosphorylated histone H3 serine 10 and serine 28 cell cycle marker intensities after DNA damage. Cytometry Part A. 2008;73(6):517–27.

87. Sharma AK, Bhattacharya S, Khan SA, Khade B, Gupta S. Mutation Research / Fundamental and Molecular Mechanisms of Mutagenesis Dynamic alteration in H3 serine 10 phosphorylation is G1-phase specific during ionization radiation induced DNA damage response in human cells. Mutation Research - Fundamental and Molecular Mechanisms of Mutagenesis. 2015;773:83–91.

88. Sharma AK, Khan SA, Sharda A, Reddy D V, Gupta S. Mutation Research / Fundamental and Molecular Mechanisms of Mutagenesis MKP1 phosphatase mediates G1-specific dephosphorylation of H3Serine10P in response to DNA damage. Mutation Research - Fundamental and Molecular Mechanisms of Mutagenesis. 2015;778:71–9.

89. Park C-H, Kim K-T. Apoptotic Phosphorylation of Histone H3 on Ser-10 by Protein Kinase Cδ. PLOS ONE. 2012 Sep 12;7(9):e44307.

90. Millan-Zambrano G, Santos-Rosa H, Puddu F, Robson SC, Jackson SP, Kouzarides T. Phosphorylation of Histone H4T80 Triggers DNA Damage Checkpoint Recovery. Molecular cell. 2018/10/25. 2018 Nov 15;72(4):625–635.e4.

91. Ikura T, Tashiro S, Kakino A, Shima H, Jacob N, Amunugama R, et al. DNA Damage-Dependent Acetylation and Ubiquitination of H2AX Enhances Chromatin Dynamics. Molecular and Cellular Biology. 2007 Oct

15;27(20):7028 LP-7040.

92. Ikura M, Furuya K, Matsuda S, Matsuda R, Shima H, Adachi J, et al. Acetylation of Histone H2AX at Lys 5 by the TIP60 Histone Acetyltransferase Complex Is Essential for the Dynamic Binding of NBS1 to Damaged Chromatin. Molecular and Cellular Biology. 2015 Dec 15;35(24):4147 LP-4157.

93. Miller KM, Tjeertes J V, Coates J, Legube G, Polo SE, Britton S, et al. Human HDAC1 and HDAC2 function in the DNA-damage response to promote DNA nonhomologous end-joining. Nature structural & molecular biology. 2010/08/29. 2010 Sep;17(9):1144–51.

94. Das C, Lucia MS, Hansen KC, Tyler JK. CBP/p300-mediated acetylation of histone H3 on lysine 56. Nature. 2009/03/08. 2009 May 7;459(7243):113–7.

95. Vempati RK, Jayani RS, Notani D, Sengupta A, Galande S, Haldar D. p300-mediated Acetylation of Histone H3 Lysine 56 Functions in DNA Damage Response in Mammals. The Journal of Biological Chemistry. 2010 Sep 10;285(37):28553–64.

96. Chen J, Wang Z, Guo X, Li F, Wei Q, Chen X, et al. TRIM66 reads unmodified H3R2K4 and H3K56ac to respond to DNA damage in embryonic stem cells. Nature Communications. 2019;10(1):4273.

97. Sharma GG, So S, Gupta A, Kumar R, Cayrou C, Avvakumov N, et al. MOF and histone H4 acetylation at lysine 16 are critical for DNA damage response and double-strand break repair. Molecular and cellular biology. 2010/05/17. 2010 Jul;30(14):3582–95.

98. Williams SK, Truong D, Tyler JK. Acetylation in the globular core of histone H3 on lysine-56 promotes chromatin disassembly during transcriptional activation. Proceedings of the National Academy of Sciences. 2008 Jul 1;105(26):9000 LP-9005.

99. Tropberger P, Pott S, Keller C, Kamieniarz-Gdula K, Caron M, Richter F, et al. Regulation of Transcription through Acetylation of H3K122 on the Lateral Surface of the Histone Octamer. Cell. 2013;152(4):859–72.

100. Mosammaparast N, Kim H, Laurent B, Zhao Y, Lim HJ, Majid MC, et al. The histone demethylase LSD1/KDM1A promotes the DNA damage response. The Journal of cell biology. 2013 Nov 11;203(3):457–70.

101. Li X, Liu L, Yang S, Song N, Zhou X, Gao J, et al. Histone demethylase KDM5B is a key regulator of genome stability. Proceedings of the National Academy of Sciences of the United States of America. 2014/04/28. 2014 May 13;111(19):7096–101.

102. Gong F, Clouaire T, Aguirrebengoa M, Legube G, Miller KM. Histone demethylase KDM5A regulates the ZMYND8-NuRD chromatin remodeler to promote DNA repair. The Journal of cell biology. 2017/06/01. 2017 Jul 3;216(7):1959–74.

103. Gong F, Chiu L-Y, Cox B, Aymard F, Clouaire T, Leung JW, et al. Screen identifies bromodomain protein ZMYND8 in chromatin recognition of transcription-associated DNA damage that promotes homologous recombination. Genes & Development . 2015 Jan 15;29(2):197–211.

104. Botuyan MV, Lee J, Ward IM, Kim J-E, Thompson JR, Chen J, et al. Structural basis for the methylation state-specific recognition of histone H4-K20 by

53BP1 and Crb2 in DNA repair. Cell. 2006 Dec 29;127(7):1361–73.

105. Pei H, Zhang L, Luo K, Qin Y, Chesi M, Fei F, et al. MMSET regulates histone H4K20 methylation and 53BP1 accumulation at DNA damage sites. Nature. 2011;470(7332):124–8.

106. Fradet-Turcotte A, Canny MD, Escribano-Díaz C, Orthwein A, Leung CCY, Huang H, et al. 53BP1 is a reader of the DNA-damage-induced H2A Lys 15 ubiquitin mark. Nature. 2013;499(7456):50–4.

107. Pfister SX, Ahrabi S, Zalmas L-P, Sarkar S, Aymard F, Bachrati CZ, et al. SETD2-dependent histone H3K36 trimethylation is required for homologous recombination repair and genome stability. Cell reports. 2014/06/12. 2014 Jun 26;7(6):2006–18.

108. Fnu S, Williamson EA, De Haro LP, Brenneman M, Wray J, Shaheen M, et al. Methylation of histone H3 lysine 36 enhances DNA repair by nonhomologous end-joining. Proceedings of the National Academy of Sciences of the United States of America. 2010/12/27. 2011 Jan 11;108(2):540–5.

109. Doil C, Mailand N, Bekker-Jensen S, Menard P, Larsen DH, Pepperkok R, et al. RNF168 Binds and Amplifies Ubiquitin Conjugates on Damaged Chromosomes to Allow Accumulation of Repair Proteins. Cell. 2009;136(3):435–46.

110. Thorslund T, Ripplinger A, Hoffmann S, Wild T, Uckelmann M, Villumsen B, et al. Histone H1 couples initiation and amplification of ubiquitin signalling after DNA damage. Nature. 2015;527(7578):389–93.

111. Mattiroli F, Vissers JHA, van Dijk WJ, Ikpa P, Citterio E, Vermeulen W, et al. RNF168 Ubiquitinates K13-15 on H2A/H2AX to Drive DNA Damage

Signaling. Cell. 2012;150(6):1182–95.

112. Gatti M, Pinato S, Maspero E, Soffientini P, Polo S, Penengo L. A novel ubiquitin mark at the N-terminal tail of histone H2As targeted by RNF168 ubiquitin ligase. Cell cycle (Georgetown, Tex). 2012/07/01. 2012 Jul 1;11(13):2538–44.

113. Gatti M, Pinato S, Maiolica A, Rocchio F, Prato MG, Aebersold R, et al. RNF168 Promotes Noncanonical K27 Ubiquitination to Signal DNA Damage. Cell Reports. 2015;10(2):226–38.

114. Yang G, Chen Y, Wu J, Chen S-H, Liu X, Singh AK, et al. Poly(ADP-ribosyl)ation mediates early phase histone eviction at DNA lesions. Nucleic Acids Research. 2020 Jan 22;48(6):3001–13.

115. Palazzo L, Leidecker O, Prokhorova E, Dauben H, Matic I, Ahel I. Serine is the major residue for ADP-ribosylation upon DNA damage. eLife. 2018 Feb 26;7:e34334.

116. Liszczak G, Diehl KL, Dann GP, Muir TW. Acetylation blocks DNA damage-induced chromatin ADP-ribosylation. Nature chemical biology. 2018/07/16. 2018 Sep;14(9):837–40.

117. Cheung P, Tanner KG, Cheung WL, Sassone-Corsi P, Denu JM, Allis CD. Synergistic Coupling of Histone H3 Phosphorylation and Acetylation in Response to Epidermal Growth Factor Stimulation. Molecular Cell. 2000;5(6):905–15.

118. Clayton AL, Rose S, Barratt MJ, Mahadevan LC. Phosphoacetylation of histone H3 on c-fos- and c-jun-associated nucleosomes upon gene activation. The EMBO journal. 2000 Jul 17;19(14):3714–26.

119. Lo WS, Trievel RC, Rojas JR, Duggan L, Hsu JY, Allis CD, et al. Phosphorylation of serine 10 in histone H3 is functionally linked in vitro and in vivo to Gcn5-mediated acetylation at lysine 14. Molecular Cell. 2000;5(6):917–26.

120. Winter S, Simboeck E, Fischle W, Zupkovitz G, Dohnal I, Mechtler K, et al. 14-3-3 Proteins recognize a histone code at histone H3 and are required for transcriptional activation. The EMBO Journal. 2008;27(1):88–99.

121. Pawlik TM, Keyomarsi K. Role of cell cycle in mediating sensitivity to radiotherapy. International Journal of Radiation Oncology*Biology*Physics. 2004;59(4):928–42.

122. Falk M, Lukášová E, Kozubek S. Chromatin structure influences the sensitivity of DNA to γ-radiation. Biochimica et Biophysica Acta (BBA). 2008;1783.

123. Rieder CL, Cole RW. Entry into mitosis in vertebrate somatic cells is guarded by a chromosome damage checkpoint that reverses the cell cycle when triggered during early but not late prophase. The Journal of cell biology. 1998 Aug;142(4):1013–22.

124. Kato TA, Okayasu R, Bedford JS. Comparison of the induction and disappearance of DNA double strand breaks and γ-H2AX foci after irradiation of chromosomes in G1-phase or in condensed metaphase cells. Mutation Research/Fundamental and Molecular Mechanisms of Mutagenesis. 2008;639(1):108–12.

125. Giunta S, Belotserkovskaya R, Jackson SP. DNA damage signaling in response to double-strand breaks during mitosis. The Journal of cell biology. 2010 Jul 26;190(2):197–207.

126. Nelson G, Buhmann M, von Zglinicki T. DNA damage foci in mitosis are devoid of 53BP1. Cell Cycle. 2009 Oct 15;8(20):3379–83.

127. Giunta S, Jackson SP. Give me a break, but not in mitosis: the mitotic DNA damage response marks DNA double-strand breaks with early signaling events. Cell cycle (Georgetown, Tex). 2011/04/15. 2011 Apr 15;10(8):1215–21.

128. Jullien D, Vagnarelli P, Earnshaw WC, Adachi Y. Kinetochore localisation of the DNA damage response component 53BP1 during mitosis. Journal of Cell Science. 2002 Jan 1;115(1):71 LP-79.

129. Lee D-H, Acharya SS, Kwon M, Drane P, Guan Y, Adelmant G, et al. Dephosphorylation Enables the Recruitment of 53BP1 to Double-Strand DNA Breaks. Molecular Cell. 2014;54(3):512–25.

130. Orthwein A, Fradet-Turcotte A, Noordermeer SM, Canny MD, Brun CM, Strecker J, et al. Mitosis Inhibits DNA Double-Strand Break Repair to Guard Against Telomere Fusions. Science. 2014 Apr 11;344(6180):189 LP-193.

131. Terasawa M, Shinohara A, Shinohara M. Canonical Non-Homologous End Joining in Mitosis Induces Genome Instability and Is Suppressed by M-phase-Specific Phosphorylation of XRCC4. PLOS Genetics. 2014 Aug 28;10(8):e1004563.

132. Steel GG, McMillan TJ, Peacock JH. The 5Rs of Radiobiology. International Journal of Radiation Biology. 1989 Jan 1;56(6):1045–8.

133. Barker HE, Paget JTE, Khan AA, Harrington KJ. The tumour microenvironment after radiotherapy: mechanisms of resistance and recurrence. Nature reviews Cancer. 2015 Jul;15(7):409–25.

134. Lomax ME, Folkes LK, O'Neill P. Biological Consequences of Radiation-

induced DNA Damage: Relevance to Radiotherapy. Clinical Oncology. 2013 Oct 1;25(10):578–85.

135. Weichselbaum RR, Schmit A, Little JB. Cellular repair factors influencing radiocurability of human malignant tumours. British journal of cancer. 1982 Jan;45(1):10–6.

136. Takata H, Hanafusa T, Mori T, Shimura M, Iida Y, Ishikawa K, et al. Chromatin Compaction Protects Genomic DNA from Radiation Damage. PLOS ONE. 2013 Oct 9;8(10):e75622.

137. Storch K, Eke I, Borgmann K, Krause M, Richter C, Becker K, et al. Three-Dimensional Cell Growth Confers Radioresistance by Chromatin Density Modification. Cancer Research. 2010 May 15;70(10):3925 LP-3934.

138. Wang P, Yuan D, Guo F, Chen X, Zhu L, Zhang H, et al. Chromatin remodeling modulates radiosensitivity of the daughter cells derived from cell population exposed to low- and high-LET irradiation. Oncotarget. 2017 Apr 20;8(32):52823–36.

139. Pogribny I, Koturbash I, Tryndyak V, Hudson D, Stevenson SML, Sedelnikova O, et al. Fractionated Low-Dose Radiation Exposure Leads to Accumulation of DNA Damage and Profound Alterations in DNA and Histone Methylation in the Murine Thymus. Molecular Cancer Research. 2005 Oct 1;3(10):553 LP-561.

140. Groselj B, Sharma NL, Hamdy FC, Kerr M, Kiltie AE. Histone deacetylase inhibitors as radiosensitisers: effects on DNA damage signalling and repair. British journal of cancer. 2013/01/29. 2013 Mar 5;108(4):748–54.

141. Lee J-H, Choy ML, Ngo L, Foster SS, Marks PA. Histone deacetylase inhibitor induces DNA damage, which normal but not transformed cells can repair. Proceedings of the National Academy of Sciences of the United States of America. 2010/08/02. 2010 Aug 17;107(33):14639–44.

142. Chinnaiyan P, Cerna D, Burgan WE, Beam K, Williams ES, Camphausen K, et al. Postradiation sensitization of the histone deacetylase inhibitor valproic acid. Clinical cancer research : an official journal of the American Association for Cancer Research. 2008 Sep 1;14(17):5410–5.

143. Harikrishnan KN, Karagiannis TC, Chow MZ, El-Osta A. Effect of valproic acid on radiation-induced DNA damage in euchromatic and heterochromatic compartments. Cell Cycle. 2008 Feb 15;7(4):468–76.

144. Camphausen K, Burgan W, Cerra M, Oswald KA, Trepel JB, Lee MJ, et al. Enhanced Radiation-Induced Cell Killing and Prolongation of γH2AX Foci Expression by the Histone Deacetylase Inhibitor MS-275. Cancer Research. 2004;64(1):316–21.

145. Jackman J, O'Connor PM. Methods for Synchronizing Cells at Specific Stages of the Cell Cycle. Current Protocols in Cell Biology. 1998 Oct 1;0(1):8.3.1-8.3.20.

146. Schorl C, Sedivy JM. Analysis of cell cycle phases and progression in cultured mammalian cells. Methods (San Diego, Calif). 2007 Feb;41(2):143–50.

147. Franken N a P, Rodermond HM, Stap J, Haveman J, van Bree C. Clonogenic assay of cells in vitro. Nature protocols. 2006;1(5):2315–9.

148. Shechter D, Dormann HL, Allis CD, Hake SB. Extraction, purification and analysis of histones. Nature Protocols. 2007;2(6):1445–57.

149. Laemelli UK. Cleavage of Structural Proteins during the Assembly of the Head of Bacteriophage T4. Nature. 1970;227(5259):680–5.

150. Towbin H, Staehelin T, Gordon J. Electrophoretic transfer of proteins from polyacrylamide gels to nitrocellulose sheets: procedure and some applications. Proceedings of the National Academy of Sciences of the United States of America. 1979 Sep;76(9):4350–4.

151. Batteiger B, Newhall V WJ, Jones RB. The use of tween 20 as a blocking agent in the immunological detection of proteins transferred to nitrocellulose membranes. Journal of Immunological Methods. 1982;55(3):297–307.

152. Fujiwara T, Bandi M, Nitta M, Ivanova E V, Bronson RT, Pellman D. Cytokinesis failure generating tetraploids promotes tumorigenesis in p53-null cells. Nature. 2005 Oct;437(7061):1043—1047.

153. Group) =EBCTCG (Early Breast Cancer Trialists' Collaborative, McGale P, Taylor C, Correa C, Cutter D, Duane F, et al. Effect of radiotherapy after mastectomy and axillary surgery on 10-year recurrence and 20-year breast cancer mortality: meta-analysis of individual patient data for 8135 women in 22 randomised trials. Lancet (London, England). 2014;383(9935):2127–35.

154. Ghoncheh M, Pournamdar Z, Salehiniya H. Incidence and Mortality and Epidemiology of Breast Cancer in the World. Asian Pacific journal of cancer prevention : APJCP. 2016;17(S3):43–6.

155. Jameel JKA, Rao VSR, Cawkwell L, Drew PJ. Radioresistance in carcinoma of the breast. Breast (Edinburgh, Scotland). 2004 Dec;13(6):452–60.

156. Malvia S, Bagadi SA, Dubey US, Saxena S. Epidemiology of breast cancer in Indian women. Asia-Pacific Journal of Clinical Oncology. 2017 Aug

1;13(4):289–95.

157. Kim R-K, Kaushik N, Suh Y, Yoo K-C, Cui Y-H, Kim M-J, et al. Radiation driven epithelial-mesenchymal transition is mediated by Notch signaling in breast cancer. Oncotarget. 2016 Jul 23;7(33):53430–42.

158. Yamamori T, Sasagawa T, Ichii O, Hiyoshi M, Bo T, Yasui H, et al. Analysis of the mechanism of radiation-induced upregulation of mitochondrial abundance in mouse fibroblasts. Journal of radiation research. 2016/12/14. 2017 May;58(3):292–301.

159. Leach JK, Van Tuyle G, Lin P-S, Schmidt-Ullrich R, Mikkelsen RB. Ionizing Radiation-induced, Mitochondria-dependent Generation of Reactive Oxygen/Nitrogen. Cancer Research. 2001 May 15;61(10):3894 LP-3901.

160. Shimura T, Sasatani M, Kawai H, Kamiya K, Kobayashi J, Komatsu K, et al. A comparison of radiation-induced mitochondrial damage between neural progenitor stem cells and differentiated cells. Cell cycle (Georgetown, Tex). 2017 Jan 24;16(6):565–73.

161. Lisby M, Barlow JH, Burgess RC, Rothstein R, Street W, York N, et al. Choreography of the DNA Damage Response : Spatiotemporal Relationships among Checkpoint and Repair Proteins. 2004;118:699–713.

162. Liokatis S, Stützer A, Elsässer SJ, Theillet F, Klingberg R, Rossum B Van, et al. Phosphorylation of histone H3 Ser10 establishes a hierarchy for subsequent intramolecular modification events. Nature Structural & Molecular Biology. 2012;19(8):819–23.

163. Li JI, Gorospe M, Hutter D, Barnes J, Keyse SM, Iol MOLCELLB. Transcriptional Induction of MKP-1 in Response to Stress Is Associated with

Histone H3 Phosphorylation-Acetylation. 2001;21(23):8213–24.

164. Cowell IG, Sunter NJ, Singh PB, Austin CA, Durkacz BW, Tilby MJ. γH2AX Foci Form Preferentially in Euchromatin after Ionising-Radiation. PLOS ONE. 2007 Oct 24;2(10):e1057.

165. Carlson JG. X-ray-induced prophase delay and reversion of selected cells in certain avian and mammalian tissues in culture. Radiation research. 1969 Jan;37(1):15–30.

166. Carlson JG. A detailed analysis of x-ray-induced prophase delay and reversion of grasshopper neuroblasts in culture. Radiation research. 1969 Jan;37(1):1–14.

167. Chow JPH, Siu WY, Fung TK, Chan WM, Lau A, Arooz T, et al. DNA damage during the spindle-assembly checkpoint degrades CDC25A, inhibits cyclin-CDC2 complexes, and reverses cells to interphase. Molecular biology of the cell. 2003/07/25. 2003 Oct;14(10):3989–4002.

168. Tjeertes J V, Miller KM, Jackson SP. Screen for DNA-damage-responsive histone modifications identifies H3K9Ac and H3K56Ac in human cells. The EMBO journal. 2009/04/30. 2009 Jul 8;28(13):1878–89.

169. Qu M, Xu H, Chen J, Zhang Y, Xu B, Guo L, et al. Distinct Orchestration and Dynamic Processes on γ-H2AX and p-H3 for Two Major Types of Genotoxic Chemicals Revealed by Mass Spectrometry Analysis. Chemical Research in Toxicology. 2020 Jun 2;

170. Castellano-Pozo M, Santos-Pereira JM, Rondón AG, Barroso S, Andújar E, Pérez-Alegre M, et al. R Loops Are Linked to Histone H3 S10 Phosphorylation and Chromatin Condensation. Molecular Cell. 2013;52(4):583–90.

171. Panopoulos A, Pacios-Bras C, Choi J, Yenjerla M, Sussman MA, Fotedar R, et al. Failure of cell cleavage induces senescence in tetraploid primary cells. Molecular biology of the cell. 2014/08/20. 2014 Oct 15;25(20):3105–18.

172. Uetake Y, Sluder G. Cell cycle progression after cleavage failure : mammalian somatic cells do not possess a "tetraploidy checkpoint" . Journal of Cell Biology. 2004 Jun 7;165(5):609–15.

173. Mantel C, Guo Y, Lee MR, Han M-K, Rhorabough S, Kim K-S, et al. Cells enter a unique intermediate 4N stage, not 4N-G1, after aborted mitosis. Cell Cycle. 2008 Feb 15;7(4):484–92.

174. Cimini D, Mattiuzzo M, Torosantucci L, Degrassi F. Histone hyperacetylation in mitosis prevents sister chromatid separation and produces chromosome segregation defects. Molecular biology of the cell. 2003/06/13. 2003 Sep;14(9):3821–33.

175. Murnion ME, Adams RR, Callister DM, Allis CD, Earnshaw WC, Swedlow JR. Chromatin-associated Protein Phosphatase 1 Regulates Aurora-B and Histone H3 Phosphorylation. Journal of Biological Chemistry . 2001 Jul 13;276(28):26656–65.

176. Li Y, Kao GD, Garcia BA, Shabanowitz J, Hunt DF, Qin J, et al. A novel histone deacetylase pathway regulates mitosis by modulating Aurora B kinase activity. Genes & Development . 2006 Sep 15;20(18):2566–79.

177. Qian J, Lesage B, Beullens M, Van Eynde A, Bollen M. PP1/Repo-Man Dephosphorylates Mitotic Histone H3 at T3 and Regulates Chromosomal Aurora B Targeting. Current Biology. 2011;21(9):766–73.

178. Vagnarelli P, Ribeiro S, Sennels L, Sanchez-Pulido L, de Lima Alves F,

Verheyen T, et al. Repo-Man Coordinates Chromosomal Reorganization with Nuclear Envelope Reassembly during Mitotic Exit. Developmental Cell. 2011;21(2):328–42.

179. Lieber A, Leis A, Kushmaro A, Minsky A, Medalia O. Chromatin Organization and Radio Resistance in the Bacterium emmata obscuriglobus. Journal of Bacteriology. 2009 Mar 1;191(5):1439 LP-1445.
180. Sharma K, Kumar A, Chandna S. Constitutive hyperactivity of histone deacetylases enhances radioresistance in Lepidopteran Sf9 insect cells. Biochimica et Biophysica Acta (BBA) - General Subjects. 2016;1860(6):1237–46.
181. Candas D, Li JJ. MKP1 mediates resistance to therapy in HER2-positive breast tumors. Molecular & cellular oncology. 2015 Jan 23;2(4):e997518–e997518.
182. Arrizabalaga O, Moreno-Cugnon L, Auzmendi-Iriarte J, Aldaz P, Ibanez de Caceres I, Garros-Regulez L, et al. High expression of MKP1/DUSP1 counteracts glioma stem cell activity and mediates HDAC inhibitor response. Oncogenesis. 2017;6(12):401.
183. Schrump DS. Cytotoxicity Mediated by Histone Deacetylase Inhibitors in Cancer Cells: Mechanisms and Potential Clinical Implications. Clinical Cancer Research. 2009 Jun 15;15(12):3947 LP-3957.
184. Camphausen K, Burgan W, Cerra M, Oswald KA, Trepel JB, Lee M-J, et al. Enhanced Radiation-Induced Cell Killing and Prolongation of γH2AX Foci Expression by the Histone Deacetylase Inhibitor MS-275. Cancer Research. 2004 Jan 1;64(1):316 LP-321.

185. Ceccacci E, Minucci S. Inhibition of histone deacetylases in cancer therapy: lessons from leukaemia. British journal of cancer. 2016/02/23. 2016 Mar 15;114(6):605–11.

186. Reddy D, Khade B, Pandya R, Gupta S. A novel method for isolation of histones from serum and its implications in therapeutics and prognosis of solid tumours. Clinical epigenetics. 2017 Mar 29;9:30.

Chapter 9

Appendix

APPENDIX-I

Table 9.1 Composition of MKK Lysis buffer

S.No.	Reagent	Stock	Volume (5ml)
1.	10mM Tris pH 7.4	1M	3.86 ml
2.	0.27M Sucrose	2M	0.675 ml
3.	1mM EDTA	0.5M	10 µl
4.	1mM EGTA	0.2M	25 µl
5.	1% Triton X-100	25%	200 µl
6.	10 µg/ml Leupeptin	1mg/ml	50 µl
7.	10 µg/ml Aprotinin	5mg/ml	10 µl
8.	1mM PMSF	100mM	50 µl
9.	1mM Sodium Orthovanadate	0.5M	10 µl
10.	10mM β-Glycerophosphate	1M	50 µl
11.	10mM Sodium Fluoride	1M	50 µl
Adjust final volume to 5ml with MilliQ water			

Table 9.2 Composition of 18% resolving gel

S.No	Components	Volume (10 ml)
1.	MilliQ Water	1.345 ml
2.	30% Acrylamide	6 ml
3.	1.5M Tris pH 8.8	2.5 ml
4.	10% SDS	100 µl
5.	10% APS	50 µl
6.	TEMED	5 µl

Table 9.3 Composition of 10% resolving gel

S.No	Components	Volume (10 ml)
1.	MilliQ Water	4.076 ml
2.	30% Acrylamide	3.33 ml
3.	1.5M Tris pH 8.8	2.5 ml
4.	10% SDS	100 µl
5.	10% APS	50 µl
6.	TEMED	5 µl

Table 9.4 Composition of 4% resolving gel

S.No	Components	Volume (10 ml)
1.	MilliQ Water	7.29 ml
2.	30% Acrylamide	1.3 ml
3.	1.5M Tris pH 6.8	1.25 ml
4.	10% SDS	100 µl
5.	10% APS	50 µl
6.	TEMED	10 µl

Table 9.5 Composition of Histone running buffer

S.No.	Component	Weight
1.	Glycine	14.2 g
2.	Tris	3.03 g
3.	SDS	1g
Make final volume to 1L with distilled water		

Table 9.6 Composition of 1X Transfer buffer

S.No.	Component	Weight
1.	Glycine	14.2 g
2.	Tris	3.03 g
3.	SDS	1g
4.	100% methanol	200 ml
Make final volume to 1L with distilled water and chill buffer in -20°C until use.		

Table no. 9.7 List of antibodies used in the study

S.No.	Protein/PTM	Catalogue no.	Company	Dilution	Purpose
1.	Histone H1	sc-8030	Santa Cruz	1:500	Western Blotting
2.	HP1α	2616S	CST	1:2000 1:200	Western Blotting Immuno-fluorescence (IF)
4.	H3K27ac	4729	Abcam	1:3000	Western Blotting
5.	H3K4me3	8580	Abcam	1:3000	Western Blotting
7.	H3K9me3	8898	Abcam	1:4000	Western Blotting
8.	H4K20me3	9053	Abcam	1:4000	Western Blotting
11.	H3S10pK14ac	07-181	Millipore	1:2000	Western Blotting
12.	H3K56ac	76309	Abcam	1:2000	Western Blotting
14.	PP1α	07-273	Millipore	1:4000	Western Blotting
15.	MKP-1	SC-370	Santa Cruz	1:3000	Western Blotting
16.	Msk1	99412	Abcam	1:1000	Western Blotting
17.	Msk2	99411	Abcam	1:2000	Western Blotting
18.	ERK1/2	SC-93	Santa Cruz	1:2000	Western Blotting
19.	pERK1/2	4370p	CST	1:2000	Western Blotting
20.	P38	SC-728	Santa Cruz	1:2000	Western Blotting
21.	pP38	4511p	CST	1:2000	Western Blotting
22.	Beta actin	A-5316	Sigma	1:10000	Western Blotting
23.	α-tubulin	ab-4074	Abcam	1:200	IF
24.	PKH reagent	PKH26	Sigma	4μM from	Cell membrane

				10mM stock	visualization
25.	Histone H3	05-499	Millipore	1:2000	Western Blotting
26.	H3K9ac	06-599	Millipore	1:1500 1:250	Western Blotting IF
27.	H3S28p	5169	Abcam	1:2000 1:200	Western Blotting IF
28.	H3S10p	06-570	Millipore	1:2000 1:200 1µg/100µg chromatin	Western Blotting IF Immuno-Precipitation (IP)
29.	γH2AX	05-636	Millipore	1:5000 1:50 1µg/100µg chromatin	Western Blotting IF IP
30.	Lamin A	Ab26300	Abcam	1:250	IF
31.	Cyclin B	CB-69	Laboratory produced	1:50	Western blotting
32.	p53	(DO-1) sc-126	Santa Cruz	1:1000	Western blotting

Table 9.8 Composition of MNase Digestion Buffer

S.No.	Component	Stock	Working	Volume (5ml)
1.	Sucrose	2M	250mM	625 µl
2.	Tris-Cl pH 7.4	1M	50mM	250 µl
3.	KCl	3M	25mM	42 µl
4.	$MgCl_2$	1M	5mM	23 µl
5.	Sodium Bisulfite	1M	50mM	250 µl
6.	Sodium Butyrate	1M	45mM	225 µl
7.	β-Mercaptoethanol	14.3M	10mM	3.5 µl
8.	Triton X-100	0.2%	25%	80 µl
9.	Spermine	100mM	0.15mM	15 µl
10.	Spermidine	100mM	0.5mM	50 µl
8.	PMSF	100mM	1mM	50 µl
9.	Sodium Orthovanadate	0.5M	1mM	10 µl
10.	β-Glycerophosphate	1M	10mM	50 µl
11.	Sodium Fluoride	1M	10mM	50 µl
Adjust final volume to 5 ml.				

Table no. 9.9 - Sequences of the primers used for real-time PCR.

S.No.	Gene	Forward Primer (5`-3`)	Reverse Primer (5`-3`)
1.	KLF4	CCCACCTTCTTCACCCCTAGA	CTTCCCCTCTTTGGCTTGGG
2.	LIN28A	GGAGGCACAGAATTGAGCCA	CAGTGCCAACTAGCCCCAAT
3.	MYC	TGCCCATTTGGGGACACTTC	TGCTGGTTTTCCACTACCCG
4.	NANOG	TAATAACCTTGGCTGCCGTCT	AAAGCCTCCCAATCCCAAACA
5.	SOX2	TTCATCGACGAGGCTAAGCG	AACTGTCCATGCGCTGGTT
6.	RPS13	GCTCTCCTTTCGTTGCCTGA	ACTTCAACCAAGTGGGGACG
7.	BRCA1	TTCGTATTCTGAGAGGCTGCTG	GTAATTCCCGCGCTTTTCCG
8.	ATR	TTTTGGCCTCCACACGGC	GCACTAGTCAACCACGCCAA
9.	ATM	CTAAGTCGCTGGCCATTGGT	TCTGGAGGAAGAAGCAACGC
10.	P53	TAACAGTTCCTGCATGGGCG	TGGTGAGGCTCCCCTTTCTT
11.	HDAC1	ATATCGTCTTGGCCATCCTG	TGAAGCAACCTAACCGATCC
12.	HDAC2	GGGAATACTTTCCTGGCACA	ACGGATTGTGTAGCCACCTC
13.	HDAC3	TGGCATTGACCCATAGCCTG	GCATATTGGTGGGGCTGACT
14.	HDAC4	TCGCTACTGGTACGGGAAAAC	AGAGGGAAGTCATCTTTGGCG

15.	HDAC5	ACTGTTCTCAGATGCCCAGC	TGGTGAAGAGGTGCTTGACG
16.	HDAC6	AGTGGCCGCATTATCCTTATCC	ATCTGCGATGGACTTGGATGG
17.	HDAC7	TTCCTGAGTGCAGGGGTAGT	CATCGCCAGGAGGTTGATGT
18.	HDAC8	ATAACCTTGCCAACACGGCT	CTTGGCGTGATTTCCAGCAC
19.	HDAC9	ACTGAAGCAACCAGGCAGTC	TTCACAGCCCCAACTTGTCC
20.	HDAC 10	CTGGCCTTTGAGGGGCAAAT	CAGCAGCGTCTGTACTGTCA
21.	HDAC 11	CCGGAAAATGGGGCAAAGTG	TAAGATAGCGCCTCGTGTGC
22.	AURKB	TGGACCTAAAGTTCCCCGCT	ACCCGAGTGAATGACAGGGA
23.	MSK1	TTCAGCTGTAAGCCACATGC	TGAGATTGGAAGGGAACCTG
24.	MKP-1	GAGCTGTGCAGCAAACAGTC	ACCCCTTCCTCCAGCATTCTT
25.	PPP1CA	TGCTGGAAGTGCAGGGC	GAAGGTCGTAGTACTGGCCG

APPENDIX-II

Figure 9.1

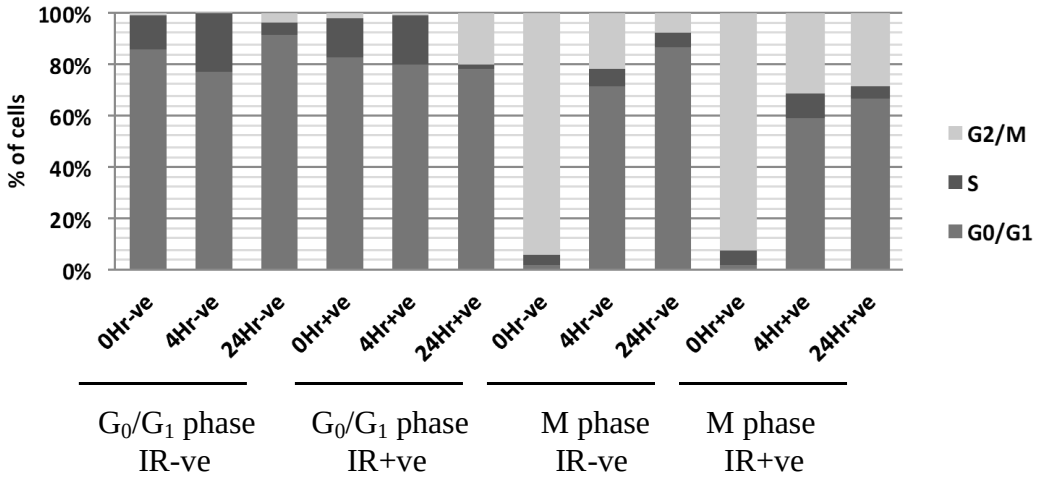

Figure 9.1 *Graph depicting cell cycle analysis of G_0/G_1 phase and mitosis synchronized cells, with and without radiation. Hr.- Hours.*

Figure 9.2

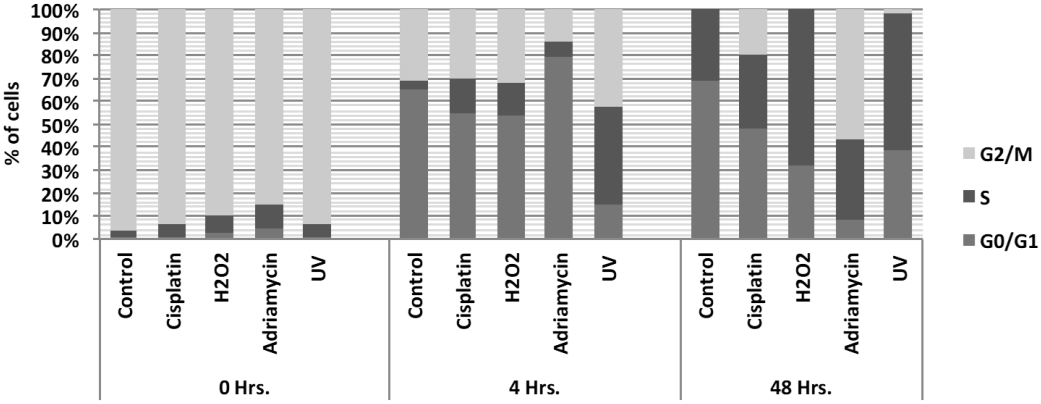

Figure 9.2 *Graph depicting cell cycle analysis mitosis synchronized cells treated with several DNA damaging agents. Hr.- Hours.*

Figure 9.3

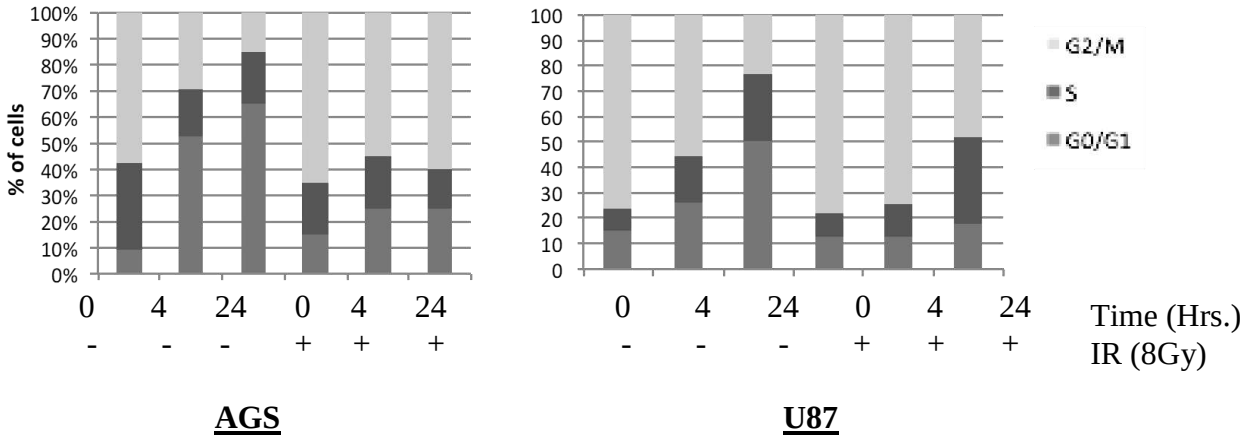

Figure 9.3 *Graphical depiction of cell cycle of mitosis synchronized AGS and U87 cells subjected to ionizing radiation. Hr.- Hours, Gy- Gray.*

Figure 9.4

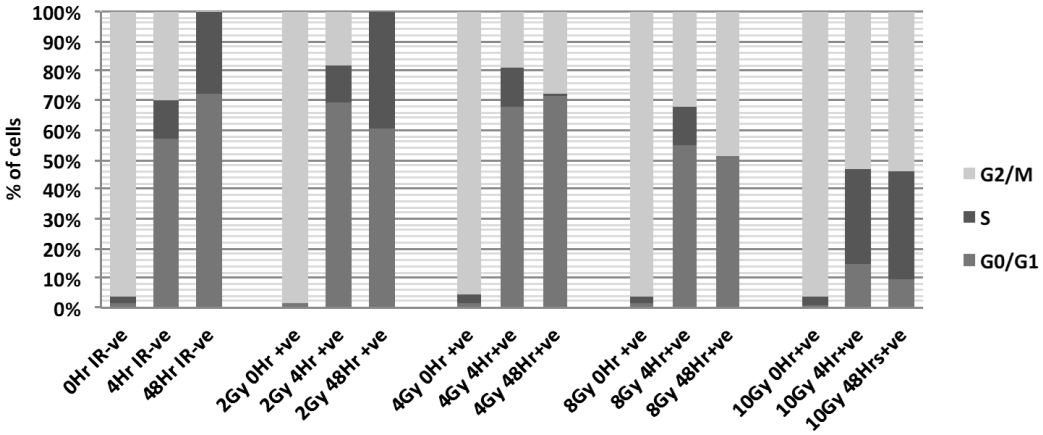

Figure 9.4 *Graphical depiction mitotic cells subjected to different doses of ionizing radiation. Hr.- Hours, Gy- Gray.*

Figure 9.5

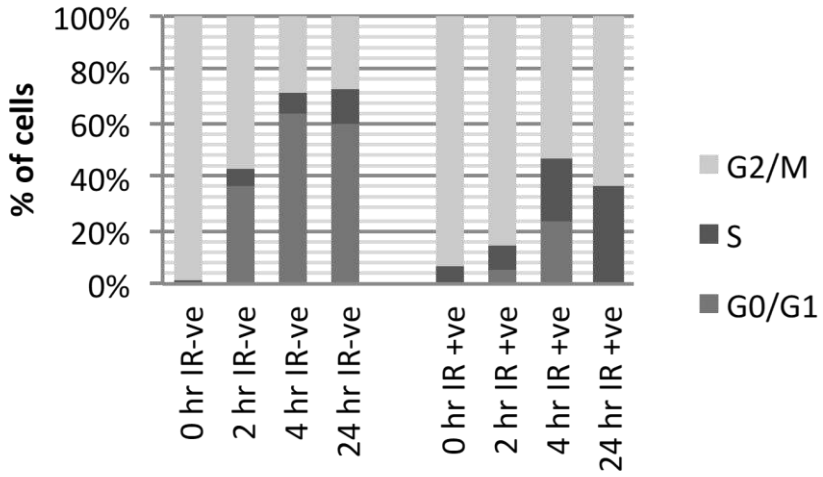

Figure 8.5 *Graph depicting cell cycle profile of MCF7 mitosis synchronized cells used for assessing transcript profile of chromatin modifying kinases and phosphatases. Hr.- Hours.*

Figure 9.6

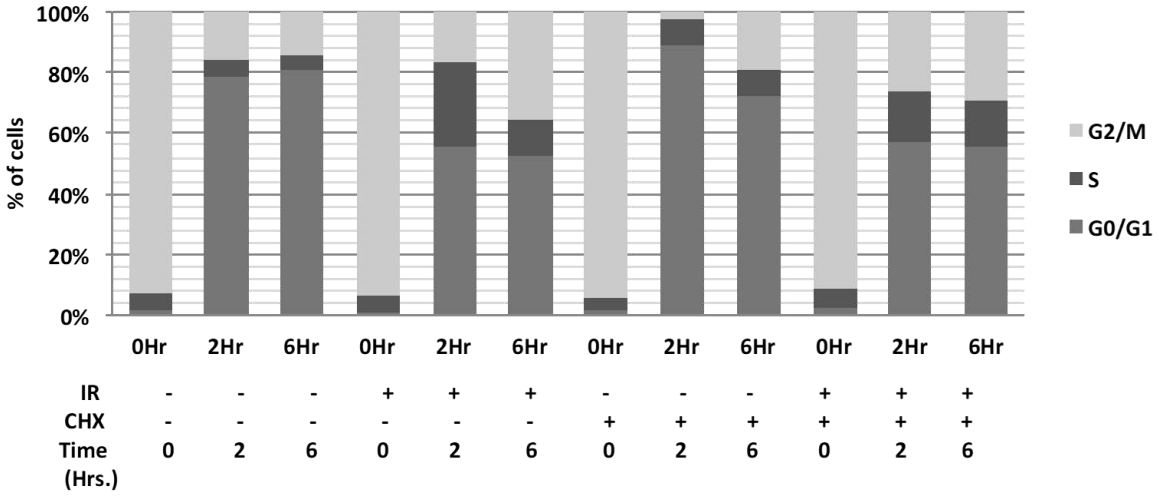

Figure 8.6 *Graph depicting cell cycle profile of MCF7 mitosis synchronized cells treated with translation inhibitor cycloheximide (CHX) and ionizing radiation (IR). Hr.- Hours.*

Figure 9.7

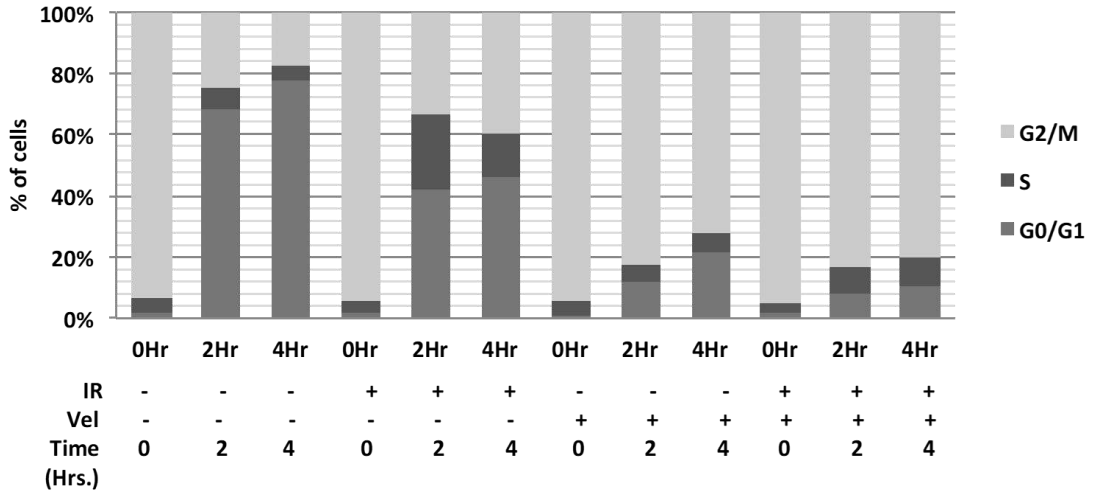

Figure 8.7 *Graph depicting cell cycle profile of MCF7 mitosis synchronized cells treated with protein degradation inhibitor velcade (Vel) and ionizing radiation (IR). Hr.- Hours.*

STATEMENT BY AUTHOR

This dissertation has been submitted in partial fulfillment of requirements for an advanced degree at Homi Bhabha National Institute (HBNI) and is deposited in the Library to be made available to borrowers under rules of the HBNI.

Brief quotations from this dissertation are allowable without special permission, provided that accurate acknowledgement of source is made. Requests for permission for extended quotation from or reproduction of this manuscript in whole or in part may be granted by the Competent Authority of HBNI when in his or her judgment the proposed use of the material is in the interests of scholarship. In all other instances, however, permission must be obtained from the author

Asmita Sharda

DECLARATION

I, hereby declare that the investigation presented in the thesis has been carried out by me. The work is original and has not been submitted earlier as a whole or in part for a degree / diploma at this or any other Institution / University.

Asmita Sharda

List of Publications arising from the thesis

Journal

1. **Asmita Sharda**[1], Mudasir Rashid, Sanket Girish Shah, Ajit Kumar Sharma, Saurav Raj Singh, Poonam Gera, Murali Krishna Chilkapati and Sanjay Gupta. Elevated HDAC activity and altered histone phospho-acetylation confers acquired radio- resistant phenotype to breast cancer cells. *Clinical Epigenetics, **(2020)** 12:4 (1-17).*
2. **Asmita Sharda**[1], Tripti Verma, Nikhil Gadewal and Sanjay Gupta. Dynamic alterations of histone H3 phospho-acetylation correlate with radiosensitivity of mitotic cells during DNA damage (Manuscript submitted)

Chapters in books and lectures notes

1. Asmita Sharda, Ramchandra Vijay Amnekar, Abhiram Natu, Sukanya, Sanjay Gupta. Histone posttranslational modifications: Potential role in diagnosis, prognosis, and therapeutics of cancer. *Prognostic Epigenetics. Vol.15, Translational Epigenetics. Academic Press, London: **(2019)**; 351-373.*

2. Asmita Sharda and S. Gupta. Chromatin Landscape – Reshaping Radiation Biology and Oncology. *Journal of Radiation and Cancer Research. **(2017)**; 8: 121-2.*

Conferences

1. 16th Asian Forum of Chromosome and Chromatin Biology, CCMB Hyderabad, 2017. Poster presented entitled " Cell cycle specific histone modifications during ionizing radiation induced DNA damage response and radio-resistance" *****
2. International Conference on Radiation Research (ICRR)- Impact on Human Health and Environment (HHE), University of Hyderabad, Hyderabad, 2018. Oral presentation "Epigenetic basis of cell cycle phase specific radio-resistance: role of histone PTMs and modifying enzymes". *****
3. Indo-Japan Conference on Epigenetics and Human Disease, Bose Institute, Kolkata, 2018. Oral presentation " Role of histone PTMs in determining the epigenetic basis of cell cycle phase specific radio-resistance".
4. 4th Annual Conference of Environmental Mutagen Society of India, BARC, Mumbai, 2018. Poster presented entitled "Histone Modifications and their importance in cell cycle phase specific radio-resistance". *****

5. "Chromatin Dynamics and Nuclear Organization in Genome Maintenance", EMBO Workshop, Illkirch, France in 2018. Poster presented entitled "Histone H3 Serine 10 phosphorylation and cell cycle phase specific radio-resistance: an epigenetic connection". **
6. 14th Indo-Australian Biotechnology Conference "Emerging modalities to improve cancer outcome", ACTREC, Mumbai, 2018. Poster presented entitled " Histone H3 Serine 10 phosphorylation and cell cycle phase specific radio-resistance: an epigenetic connection".
7. 17th Asian Forum of Chromatin and Chromosome Biology, JNCASR Bangalore, 2018. Poster presented entitled " Histone H3 Serine 10 phosphorylation and cell cycle phase specific radio-resistance: an epigenetic connection". *

(*Received award; ** Received EMBO travel grant)

Others

1. Ajit Kumar Sharma, Shafqat Ali Khan, Asmita Sharda, Divya Velga Reddy and Sanjay Gupta. MKP-1 phosphatase mediates G1-specific dephosphorylation of H3Serine10P in response to DNA Damage. *Mutation Research 778; **(2015)**; 71-79.*
2. Saikat Bhattacharya, Divya Reddy, Raja Reddy, Asmita Sharda, Kakoli Bose and Sanjay Gupta. Incorporation of a tag helps to

overcome expression variability in a recombinant host. *Biotechnology Reports 11:* ***(2016)****; 62-69.*

3. Tanushree Pal, Asmita Sharda, Bharat Khade, C.S. Ramaa and Sanjay Gupta. Re-positioning of difluorinated propanediones as inhibitors of histone methyltransferases and their biological evaluation in human leukemic cell lines. *Anti-Cancer Agents in Medicinal Chemistry 18(13),* ***(2018)****; 1892-1899.*

This thesis is dedicated to my parents and my brother for their unconditional love, support and belief in me.

This thesis is also dedicated to all the dogs at ACTREC, who were my best friends throughout this long journey.

ACKNOWLEDGEMENTS

As John Donne put it aptly, no man is an island unto himself. So as I inch towards the culmination of this phase of my life, I would like to express my gratitude towards everyone who has helped me sail through this journey. I would like to begin by thanking my mentor, Dr. Sanjay Gupta, for providing me an opportunity to work with him. I acknowledge him for his unending belief and support that had always motivated me to give my best. I will always remember him for his zeal, resourceful nature, infectious enthusiasm and his never give up spirit. One of the most important things that I have learned from him is to appreciate negative criticism and use it to amp up your performance. I would like to thank him for never ever pressurizing me, neither professionally for the progress of my project nor personally for dog-feeding activities. I will lifelong carry the values I have learned from him and not just be a good scientist, but become a better human first.

I would like to thank Dr. Sudeep Gupta (Director, ACTREC), Dr. Rajiv Sarin and Dr. S.V. Chiplunkar (Ex-Directors, ACTREC) for providing us excellent research and academic infrastructure. I would like to thank Dr. Prasanna Venkatraman (Deputy-Director, CRI) for her caring and supportive nature towards students. I also thank UCG and DBT India, for providing financial assistance. I would like to acknowledge my doctoral committee members, Dr. Sorab N. Dalal (Chairperson), Dr. B.N. Pandey and Dr. Sanjeev Waghmare for their intellectual insights and guidance. I would like to thank Sorab, for he always genuinely cared for me as if I were one of his own students. I am really going to miss his smile and our daily banter over coffee.

This research work would not have been possible without the help and expertise of so many people. I would like to thank Mr. Uday Dandekar and all the CIR staff members. I also thank all members of the workshop, especially Mr. Panchal, for repairing any broken equipment. I thank Dr. Tejpal Gupta, Dr. Jayant Sastry, the technicians- Mr. Anil, Mr. Santosh, Mr. Kamlesh, Ms. Puspha, Ms. Jyotsana, Ms. Poonam and the physicists- Ms. Reena, Ms.Siji, Mr. Kishore and Mr. Shubhajeet from the Department

of Radiation Oncology, ACTREC. I would also like to thank Ms. Rekha, Ms. Shyamal, Mr. Ravi and Mr. Prashant (Flow Cytometry), Ms. Vaishali, Ms. Tanuja, Mr. Jayaraj and Mr. Mithilesh (Microscopy), Ms. Sharda (DNA sequencing), Ms. Sharda Sawant and Ms. Siddhi (Electron Microscopy) for their expertise and assistance. I would also like to thank Dr. A. Ingle, Mr. Rahul Thorat and all the personnel of the Laboratory Animal Facility for their help. A personal and heartfelt thanks to Dr. Pradip Chaudhari and Dr. Kiran Bendale for treating my dogs whenever they were ill. I also thank Mr. Anand (IT facility), Mr. Munnoli, Ms. Swati and Ms. Mughda (Library), Ms. Aparna Bagwe, Ms. Ojaswini and Ms. Prema (SCOPE) for their assistance.

I think whatever I have learned throughout Ph.D, I have learned the most from my seniors. My heartfelt thanks to Dr. Ajit, Dr. Monica, Dr. Shafqat, Dr. Saikat and Dr. Divya for nurturing, helping, supporting, teaching, criticizing and appreciating me. A special thanks to Ajit, whose intense hard work laid the foundation for this project. I would like to thank Mr. Bharat, Mr. Arun and Mr. Santosh for their day-to-day assistance and impeccable performance of their duties. I would like to thank all the sincere and hardworking girls who worked with me- Poornima, Juilee, Akanksha, Sneha, Namrata, Kajal, Dr. Shashi and Soumita. I hope they keep working hard and achieve success in life. I fall short of words for my batch mate and lab member Mr. Ramchandra Amnekar, who has been a friend like no other and my rock solid support. I also thank all the present lab members Mr. Sanket, Mr. Mudasir, Ms. Tripti, Mr. Abhiram, Ms. Sukanya and Ms. Anjali for all their help and support. I hope they work hard and achieve success.

I would like to thank the entire student community of ACTREC for their help and support. I am thankful for my first friends at ACTREC, the entire batch of 2013. They are the coolest group I have met and we all will always be together. I wish all of them achieve great heights of happiness and success. Words won't do justice to express my gratitude towards Burhan, whom I have troubled the most, but still he always lovingly made tea for me. I feel so happy to be his friend and hope to stay buddies for life. I share so many fond memories with all the members of Sorab lab, who always made

me feel a part of their own lab. In Arunabha and Sonali, I have found my closest friends with whom I can discuss anything without the fear of judgment. Sarika and Monica have been my dog-lover buddies and Amol, my politics discussion buddy. My first friend and roomate in ACTREC, Dr. Priyanka, helped me develop a close bond with Mahimkar lab members. I am really thankful to Usha and Mayuri for their love and support. I am thankful to all members of Sorab and Mahimkar lab for always showering me with love and lots of food. Finally, I feel so lucky that I met a nutcase named Sayoni (Waghmare Lab), who never failed to make me smile, even if we met for a fleeting moment. She is the most helpful, kind and understanding person I met at ACTREC. I wish her the best for all future endeavors. As genuine people like her are so hard to come by, they must be treasured for a lifetime.

My feelings of gratitude for my mother and father cannot be penned down easily. Hence, I thank them for being the wind beneath my wings. I thank my brother for being my biggest supporter since childhood and my best friend forever. I would like to thank the Almighty, who gave me the strength to bear the tribulations during Ph.D. Most importantly, I would like to thank my best friends, my ACTREC dogs, for keeping me mentally sane. If it would not had been for them, I would have knocked off my mental balance like an imbalanced centrifuge. So cheers to you Tinny, Gajjo, Awooooo, Whitey, Smarty, Nibow, Girl, Teeki, Cheeki, White-Brown, Pappu, Gogo, Gajji, and White-Black. I so wish you all could read this and wag your tail with happiness!!

INDEX